The Dissertation Committee for Corri Beth Levine Certifies that this is the approved version of the following dissertation:

Bundibugyo Versus Zaire Ebolaviruses: Examination of the Polymerase Complex as a Therapeutic Target

Committee:

Thomas W. Geisbert, PhD,
Mentor

Susan McLellan, MD, MPH
Clinical Co-Mentor

Chad E. Mire, PhD

Scott Weaver, PhD

Elke Muhlberger, PhD

Bundibugyo Versus Zaire Ebolaviruses: Examination of the Polymerase Complex as a Therapeutic Target

by

Corri Beth Levine, BS, MS, MPH

Dissertation

Presented to the Faculty of the Graduate School of

The University of Texas Medical Branch

in Partial Fulfillment

of the Requirements

for the Degree of

Doctor of Philosophy in Human Pathophysiology and Translational Medicine

The University of Texas Medical Branch

December, 2021

Dedication

To my Zayde and Poppy: I wish you could have been here to see this day, but I know you are proud of my endeavor to become a PhD.

Zayde, you fostered my love of science with our regular trips to the Rochester Museum and Science Center and you taught me to never stop asking questions. You were always full of fun and random facts that I never would have learned without you. I remember when I told you I was heading to school in Galveston you asked if I knew who the island was named after, to which you promptly informed me: “Mr. Galvez!” and then proceeded to tell me about the colonization of the island. I love you and miss you.

Poppy, you were always there to drive me to every activity I wanted to do, even the ones I had no hopes of being good at. Fortunately, I did find one activity to excel at, crew, and was glad to keep this family tradition alive. When I got into graduate school you were quick to point that I’d be the first doctor in our family. That on its own has motivated me even through the hardest days. I love you and miss you.

Acknowledgements

There are so many people to acknowledge who have helped me get to this point. First, I would not be here without the love and support of my parents Nancy and Stephen Levine. You gave me the freedom to explore whatever most interested me at any given time and made sure I had every science "toy" I could want, from a microscope set to anatomy models to a copy of Gray's Anatomy. Thank you for always pushing me just the right amount, believing in my dreams, and helping me find a way to achieve them. There aren't enough words or space to express how grateful I am for you.

To my husband Ben Perry, thank you for staying by my side through 4 degrees and moving across the country so I could pursue my dream. At this point you probably know as much about this dissertation as I do. Thank you for listening to my ramblings and at least pretending to stay interested. I promise that I will now get a job and stop being a professional student.

To my best friend Mandy Ellis, we've known each other nearly three decades and still remain as close as ever. I'm so happy that your job and my schooling brought us back within driving distance, visiting you was always the vacation I needed when life got stressful. Our weekly phone calls are the perfect end to every week, recapping successes and failures and planning how to move forward. Thank you for always being there for me.

Thank you to my entire committee: Dr. Tom Geisbert, thank you for supporting my projects and helping me navigate this process, the experiences I've had would not have been possible without you. Dr. Susan McLellan, you have given me so many amazing opportunities and helped me find a home in the clinic. Dr. Chad Mire, you stuck with me and somehow knew exactly what I needed every step of the way, thank you for guiding me to this point and shaping my career path. Dr. Scott Weaver, I really appreciate

your expertise and support on this project and others. Dr. Elke Muhlberger, your research was the backbone of this dissertation, thank you for your guidance along the way and the push to publish.

To all the members of the Geisbert lab, past and present: Thank you! Drs. Tera Sorvillo and Sergio Rodriguez, your experience and insight made graduate school a little less stressful. Dr. Kevin Melody, days in the lab were made better with you there to lighten the mood, thank you also for taking the time to read and edit this dissertation, it would not have been completed without your help. Dr. Vika Borisevich, thank you for keeping me on track and constantly reminding me of my goals, you are one of the best motivators I know! Dr. Karla Fenton, I truly appreciate you taking the time to teach me gross and microscopic pathology, our sessions in your office have helped me link together disease processes and formulate a better understanding of Ebola. Dr. Courtney Woolsey, Dr. Bob Cross, Dr. Abhi Prasad, Dr. Liana Medina, Dr. Dylan Johnson, Stephanie Foster, Joan Geisbert, Krystle Agans, Dan Deer, Natalie Dobias, Kira Zapalac, and Brittany Fransaw, thank you for your support, answering my questions, and helping in my quest to become a virologist.

I would also like to acknowledge and thank Tori Morris, Dr. Andrew Routh, and the rest of the Routh lab for their assistance in preparing, running, and analyzing the click-seq data. Tori, thank you for taking the time to teach me how click-seq works and being so responsive every time I asked how the analysis was coming along.

Finally, Stephanie Foster and Megan Mears, I would not have made it through without you two. Whether it was a lunch, hallway chat, text, or standing around the garage parking lot you both have been there for me every step of the way. Thank you for being there for the highs and the lows, listening to me working through some data and telling me when to take a break. There is a light at the end of the tunnel and I’m glad I was riding this train with you both.

Bundibugyo Versus Zaire Ebolaviruses: Examination of the Polymerase Complex as a Therapeutic Target

Publication No._____

Corri B. Levine, PhD

The University of Texas Medical Branch, 2021

Supervisor: Thomas W. Geisbert

Ebolaviruses, of the family *Filoviridae*, are the causative agents of outbreaks of hemorrhagic fever throughout Africa. In eastern Africa, three outbreak causing species of ebolavirus overlap in geographic distribution: *Zaire ebolavirus* (EBOV), *Sudan ebolavirus* (SUDV), and *Bundibugyo ebolavirus* (BDBV). EBOV and BDBV are distinctly different in case-fatality rate, disease course, and clinical presentation in both humans and non-human primates, but the reasons for these differences are unknown. Examination of the growth kinetics indicate that variations in the polymerase complex may be a factor in the differing pathogenicity. The rate of growth for infectious virions, genomic copies, and transcripts was slower for BDBV compared to EBOV. In addition to lower peak viral titers, BDBV infection also resulted in fewer viral transcripts being produced per genome compared to EBOV. An artificial transcription and replication system utilizing a 'minigenome' reporter was constructed for the study of BDBV. The minigenome system was used to compare the polymerase complex efficiency with that of EBOV and to screen potential therapeutics. Through the exchange of polymerase complex proteins, it was found that EBOV could more readily accept proteins from another viral species than BDBV. In fact, use of the BDBV NP enhanced transcription of the EBOV minigenome, while the

inverse resulted in significantly decreased minigenome expression. The utility of the minigenome system was further shown by screening of small molecule inhibitors, of which the nucleoside analog remdesivir emerged as a lead candidate. Remdesivir was found to be highly effective at inhibiting primary transcription, and delayed treatment required a significantly higher concentration. Use of remdesivir was more effective at inhibiting BDBV than EBOV, likely due to the slower and diminished amount of viral transcription occurring over the course of BDBV infection. Targeting the polymerase complex of ebolaviruses is a viable strategy for therapy but efficacy will be highly dependent on timing and concentration. Future studies should examine modified treatment schedules and doses when care is delayed to overcome the increased polymerase activity that occurs later in infection.

This dissertation is based in part on the previously published manuscript listed below. I have permission from my co-authors and publishers to use the work listed below in this dissertation. Figures and tables from the listed manuscript which have been used in full or part in this dissertation include a citation within the text. Dissertation sections which have been based on the work listed below include:

Chapter 2: Results – Growth Kinetics

Chapter 2: Results – Production and Release of Viral Genomes

Chapter 3

Chapter 4

Chapter 5: Results – Titration of Remdesivir against Full-Length Virus

Chapter 5: Results – Continuous Treatment Effect on Viral Replication & Growth

125. Levine, C. B., Mire, C. E. & Geisbert, T. W. Comparison of Zaire and Bundibugyo Ebolavirus Polymerase Complexes and Susceptibility to Antivirals through a Newly Developed Bundibugyo Minigenome System. *J Virol* **95**, e0064321, doi:10.1128/JVI.00643-21 (2021).

TABLE OF CONTENTS

List of Tables

List of Figures

List of Abbreviations

BDBV	Bundibugyo ebolavirus
BVD	Bundibugyo virus disease
CFR	Case fatality rate
DRC	Democratic Republic of the Congo
EBOV	Zaire ebolavirus
EVD	Ebolavirus disease
GE	Genome Equivalent
hpi	Hours post-infection
hpt	Hours post-transfection
LLOV	Lloviu virus
MARV	Marburg virus
MOI	Multiplicity of Infection
mRNA	Messenger RNA
NPBP	NP Binding Peptide
RESTV	Reston ebolavirus
SUDV	Sudan ebolavirus
SVD	Sudan virus disease
RT-qPCR	Quantitative reverse transcription polymerase chain reaction
RdRp	RNA-dependent RNA polymerase
vRNA	Viral genomic RNA

Chapter 1: Introduction – Ebola: The Virus and the Disease

EBOLAVIRUS EPIDEMIOLOGY

Ebola disease, the disease caused by any member of the genus *Ebolavirus*, was first documented in 1976 during simultaneous outbreaks in the Democratic Republic of the Congo (DRC; formerly Zaire) and South Sudan (formerly Sudan).[1,2] The outbreaks were caused by two different ebolavirus species, each named for the region of origin: *Zaire ebolavirus* (EBOV) and *Sudan ebolavirus* (SUDV). The establishment of two separate species was determined by the fact that the full-length genome differed by greater than 30% while still maintaining similar characteristics.[3] Since the 1976 outbreaks, 19 more outbreaks of Ebola virus disease (EVD) and 6 outbreaks of Sudan virus disease (SVD) have occurred (Table 1.1).[4]

The reservoir host of ebolaviruses is still to be determined; although, bats of the family *Pteropodidae* are a suspected source. Anti-ebolavirus antibodies have been detected in these bats, and although small RNA fragments aligning with the EBOV genome have been detected in organ tissue, no live virus has been collected from any bat.[5,6] This is also the case for the ebolavirus species *Bombali ebolavirus* (BOMV), which was discovered during surveillance of wildlife populations in Sierra Leone and Kenya.[7,8] Viral RNA was detected in four bats and the genome was determined using high-throughput sequencing. In comparison, bats are considered the reservoir host for another filovirus, Marburg virus (MARV), which has been isolated from *Rousettus aegyptiacus* bats.[9] If bats are the reservoir host for ebolaviruses, it is thought that transmission occurs via secretions, either via direct contact with saliva or feces or through contamination of fruits and other food products.[5] The other likely route for infection is through ingestion of meat from either butchered or scavenged animals such as chimpanzees, gorillas, or duikers.[6] These animals succumb to infection and are therefore not suspected to be reservoir hosts, but instead

acquire the virus from another source as is the case with humans. This is exemplified by the speicies *Tai Forest ebolavirus* (TAFV) and *Reston ebolavirus* (RESTV). TAFV has caused two outbreaks in a troop of chimpanzees in the Taï Forest National Park in Côte d'Ivoire. A single human case of TAFV infection has been documented, a woman who was infected while performing necropsies on the affected animals and survived.[10] RESTV was discovered when a number of cynomolgus macaques at a laboratory facility began to show signs of a hemorrhagic disease and subsequently died.[11,12] No human cases of RESTV infection have been documented although several individuals who had contact with infected macaques were subsequently found to have seroconverted.[13,14] In the case of EBOV and SUDV outbreaks, many have been linked to hunters or those who are involved with butchering and preparing meat; although, several outbreaks still have no known source of introduction.[15]

After an introduction into the human population, the transmission chain of Ebola disease is maintained by direct human-to-human contact via contact with bodily fluids including blood, vomit, urine, and stool.[16] As family members are usually the first to care for an infected individual, they often account for secondary and tertiary cases.[16-18] Healthcare workers are also at risk of infection if proper personal protective equipment is unavailable or insufficient.[17] This is most likely to occur at the start of an outbreak as Ebola disease initially presents with non-specific symptoms and cases may be misdiagnosed as malaria, influenza, or typhoid fever and so the precautions necessary to protect against ebolavirus infection may not be used. In addition, the virus can still be transmitted even after death so additional care must be taken in performing burial rituals.[16,18] As with any highly communicable and severe disease, rapid contact tracing and isolation is crucial to control spread. Increased education of the public and healthcare workers living in the border region of the DRC, Uganda, and South Sudan has helped to limit the spread, but external factors such as civil unrest and a lack of access to care means that cases can slip

past detection and reignite a waning outbreak in this region and recently there has been evidence of chronic infections leading to reemergence.[19,20]

At the turn of the 21st century, ebolavirus outbreaks have increased in frequency and have emerged almost annually (Table 1.1).[4,21,22] Ebolavirus outbreaks in humans have been contained to the continent of Africa, although isolated cases have been documented elsewhere and linked to travel, repatriation, or close-contact with a traveler.[23,24] With the exception of the single case of TAFV infection originating in the Taï Forest in Côte d'Ivoire, all outbreaks up until December 2013 were localized to Central and Eastern Africa, and ranged from 8-425 cases, with case fatality rates (CFR) ranging from 36-90%.[4,10,21,25]

In the border region between the DRC, Uganda, and South Sudan, three different ebolaviruses species have caused outbreaks: EBOV, SUDV, and *Bundibugyo ebolavirus* (BDBV).[4] Outbreaks are regularly detected in this region including the second largest and second longest outbreak to date occurring in Uganda from August 2018 through June 2020 resulting in nearly 3,500 infections and over 2,000 deaths.[4] In 2013, EVD emerged on the West coast of Africa, causing an epidemic lasting 3 years, infecting over 30,000 people and killing over 11,000.[4] In 2021, another outbreak was detected in Guinea and found by sequence analysis to be linked to the previous outbreak ending in 2016, indicating that the geographic range of ebolaviruses have now expanded. Taking into account all outbreaks through June 2021, the average case fatality rate is 65% for EBOV and 50% for SUDV.[4,22]

For 30 years, EBOV and SUDV were the only two ebolaviruses known to cause outbreaks. In 2007, a new species was discovered, BDBV, when an outbreak was declared in the Bundibugyo district of Uganda.[26,27] On 2 August 2007, two cases of febrile illness were reported in Uganda.[27] Laboratory testing was unable to confirm the etiology of the disease; however, three months later, on 5 November 2007, 20 deaths due to a febrile hemorrhagic disease were reported to the Ugandan Ministry of Health.[27] Samples were shipped to the U.S. Centers for Disease Control and Prevention for testing, and by the end

of the month it was confirmed that an ebolavirus was the culprit of the disease.[28] An outbreak was officially declared on 29 November 2007 and outbreak response teams began to set up isolation wards and educate health care workers and civilians about the illness and proper infection control hygiene.[27] The index case was suspected to be a 26-year-old woman who was linked to nine other cases.[27] It is believed that she came in contact with blood or secretions from a hunted animal, although this was never confirmed. By February 2008 the outbreak had subsided with 116 confirmed or probable cases resulting in a CFR of 34%.[27,29] When suspect cases were included in this calculation, the overall CFR was 25%. This seemingly lower CFR was initially attributed to improved healthcare infrastructure including a rapid response, increased education and awareness, and prior familiarity with the disease by healthcare workers.[27,30]

Four years after the first appearance of BDBV, a second outbreak was declared, this time in Isiro, the capital of the Haut-Uele District in the DRC. Notification of the first two cases was made on 2 August 2012 and an epidemic was declared two weeks later on 17 August 2012.[31,32] By 26 November 2012 the epidemic was declared over with a total of 62 cases, including 5 suspect cases, and a CFR of nearly 55%.[31] When looking solely at laboratory-confirmed cases the CFR is comparable to the previous outbreak at 36%.[4] As with the first outbreak, the response was quite rapid with a mobile laboratory and treatment center available before confirmation of the disease was even complete.[31]

Compared to other recorded ebolavirus outbreaks, the one in Bundibugyo, Uganda was moderate in size and had a substantially lower CFR. The BDBV outbreak in Isiro had case counts similar to other small outbreaks in the region, and the CFR was lower than what had been previously observed by EBOV outbreaks in the area. The average CFR from the two BDBV outbreaks is 34 - 40%, substantially lower than that for EBOV and SUDV outbreaks that had occurred through 2012 (73% and 50%, respectively).[4,22] This is an interesting finding when considering the overlapping geography of the BDBV outbreaks with previous outbreaks caused by the other ebolavirus species. The seemingly lower CFR

of BDBV suggests that BDBV is less pathogenic than the other outbreak causing species EBOV and SUDV. However, the reason for this difference is unknown and several hypotheses have been suggested including both social and biological factors.

Zaire ebolavirus				
Year	Country	Cases	Deaths	Case Fatality Rate
1976	Zaire (present day DRC)	318	280	88%
1994	Gabon	52	31	60%
1995	Zaire (present day DRC)	315	250	79%
1996	Gabon	60	45	75%
1996	Gabon	37	21	57%
2001	Republic of Congo	57	43	75%
2001	Gabon	65	53	82%
2002	Republic of Congo	143	128	90%
2003	Republic of Congo	35	29	83%
2007	DRC	264	187	71%
2008	DRC	32	15	47%
2014	DRC	66	49	74%
2014-2016	West Africa (multiple countries)	28,646	11,323	40%
2017	DRC	8	4	50%
2018-2020	DRC	54	33	61%
2018	DRC, Uganda	3,470	2,287	66%
2020	DRC	130	55	42%
2021	Guinea	23	12	52%
2021	DRC	12	6	50%
			Average Case Fatality Rate	65%

Sudan ebolavirus				
Year	Country	Cases	Deaths	Case Fatality Rate
1976	Sudan (present day South Sudan)	284	151	53%
1979	Sudan (present day South Sudan)	34	22	65%
2000	Uganda	425	224	53%
2004	Sudan (present day South Sudan)	17	7	41%
2012	Uganda	6*	3*	50%*
2012	Uganda	11*	4*	36%*
			Average Case Fatality Rate	50%

Bundibugyo ebolavirus				
Year	Country	Cases	Deaths	Case Fatality Rate
2007	Uganda	149	37	25%
2012	DRC	36*	13*	36%*
			Average Case Fatality Rate	30%

Table 1.1 Ebolavirus outbreaks in Africa

Chronological listing of outbreaks by ebolavirus species *Zaire ebolavirus*, *Sudan ebolavirus*, and *Bundibugyo ebolavirus*. Single case outbreaks are not included.
* Indicates that only laboratory-confirmed cases are listed. DRC Democratic Republic of the Congo. Data compiled from
https://www.cdc.gov/vhf/ebola/history/distribution-map.html

FAMILY FILOVIRIDAE & VIRAL LIFECYCLE

The genus *Ebolavirus* is included in the family *Filoviridae* in the order *Mononegavirales*. Within the *Filoviridae* family are six genera: *Ebolavirus*, *Marburgvirus*, *Cuevavirus*, *Dianlovirus*, *Striavirus*, and *Thamnovirus*.[33] Viruses of the genera *Ebolavirus* and *Marburgvirus* cause lethal disease in humans.[34] As with all viruses within the order *Mononegavirales*, ebolaviruses are single stranded, negative-sense, RNA viruses. There are six species included in the *Ebolavirus* genus: *Zaire ebolavirus*, *Sudan ebolavirus*, *Bundibugyo ebolavirus*, *Tai Forest ebolavirus*, *Reston ebolavirus*, and *Bombali ebolavirus*.

Ebolavirus genomes are approximately 19 kb long and encode seven genes in genomic order: the nucleoprotein (NP), viral protein (VP) 35 (VP35), VP40, glycoprotein (GP), VP30, VP24, and the large gene (L) (Figure 1.1). These seven genes produce eight viral proteins which facilitate a complete replication cycle including transcription, replication, packaging, budding, and immune evasion (Figure 1.1). GP is the only gene that encodes for more than one protein, and it encodes two variations of the glycoprotein: membrane bound GP and soluble GP (sGP).[35] With a limited number of proteins, each must carry out multiple functions. For example, VP35 acts as both an innate immune antagonist and as the polymerase co-factor.[36] VP24 acts as an immune antagonist as well and has another function as the minor matrix protein.[36] The major matrix protein VP40 plays a critical role in virion formation and budding from the cell membrane. The presence of VP40 alone is sufficient to produce viral-like particles, although the addition of NP greatly enhances particle production.[37] The proteins NP, VP35, VP30 and L make up the functional polymerase complex for RNA synthesis of gene transcripts and genome copies.[38] NP binds and encapsulates viral RNA strands and binds to the polymerase components to direct transcription and replication.[39-44] L is the catalytic subunit and VP35 is the polymerase co-factor.[45,46] VP30 is the final protein of this complex, and it functions to mediate the switch from transcription to replication based on phosphorylation status.[47-50] New roles for these

proteins are still emerging and it is clear that each protein contributes to multiple stages of the viral life cycle.[51]

The first target cells are those of the immune system, specifically monocytes, macrophages, and dendritic cells.[34,36,52] Virions associate with the cell surface using a variety of receptors including C-type lectins, glycosaminoglycans, or phosphatidylserine, and are taken up by cells through micropinocytosis and clatherin-mediated endocytosis.[53,54] The binding receptor for ebolaviruses Niemann-Pick 1 (NPC1) is found on the membrane of endosomes and lysosomes.[55,56] The receptor binding site on the virions is masked until enzymatic cleavage of GP occurs within the endosome.[15] After GP cleavage, acidification of the endosome results in a conformational change of GP resulting in fusion between the virion envelope and the endosomal membrane and subsequent release of the ribonucleoprotein complex into the cell cytoplasm.[15,34] The ribonucleoprotein complex is made of up viral RNA encapsulated by NP and bound by the polymerase complex proteins VP35 and L along with the transcriptional activator VP30.[38,57] Upon release, the complete ribonucleoprotein complex can immediately begin transcription of viral genes. Genes are transcribed in a polar fashion, that is, the first gene, NP is the most abundant and subsequent genes are produced in lesser quantities with the final gene, L, being the least abundant.[58]

During transcription, the viral polymerase complex creates mRNAs that are recognized by host cell ribosomes, complete with a 5'-cap and a 3'-poly-A tail.[59] The 5'-cap is added by the capping domain (regions IV and V) of the L protein, and the 3'-poly-A tail is added by polymerase stuttering in the gene end regions.[59] After transcription by the viral polymerase complex, the host cell machinery takes over and produces viral proteins. These proteins form new polymerase complexes and continue the cycle of gene transcription. Phosphorylation of VP30, the transcriptional activator, controls the switch from transcription to replication, but the exact mechanism triggering this event is still to be determined.[48,50,60] Genome replication occurs by continued read through across the genome boarders to produce an intermediate RNA species termed the anti-genome. The anti-

genome is a complement to the viral genome and is used as a template to create new genome copies. The anti-genome is also encapsulated by NP to prevent RNA degradation and detection from host immune sensors. The newly produced viral genomes serve three purposes: new templates for gene transcription, new templates for replication, and material for packaging of new virions. When sufficient concentrations of viral proteins and viral RNA are reached, packaging and release can occur. GP is shuttled to the host cell membrane and stabilized by the matrix proteins VP40 and VP24. These two proteins interact with the NP encased RNA that is also associated with a complete polymerase complex, and new virions are released by budding.[37] These mechanisms of gene transcription and genome replication appear to be fairly conserved across the ebolavirus species, but whether genomic variations between species result in noticeable differences in virion production has yet to be fully examined.

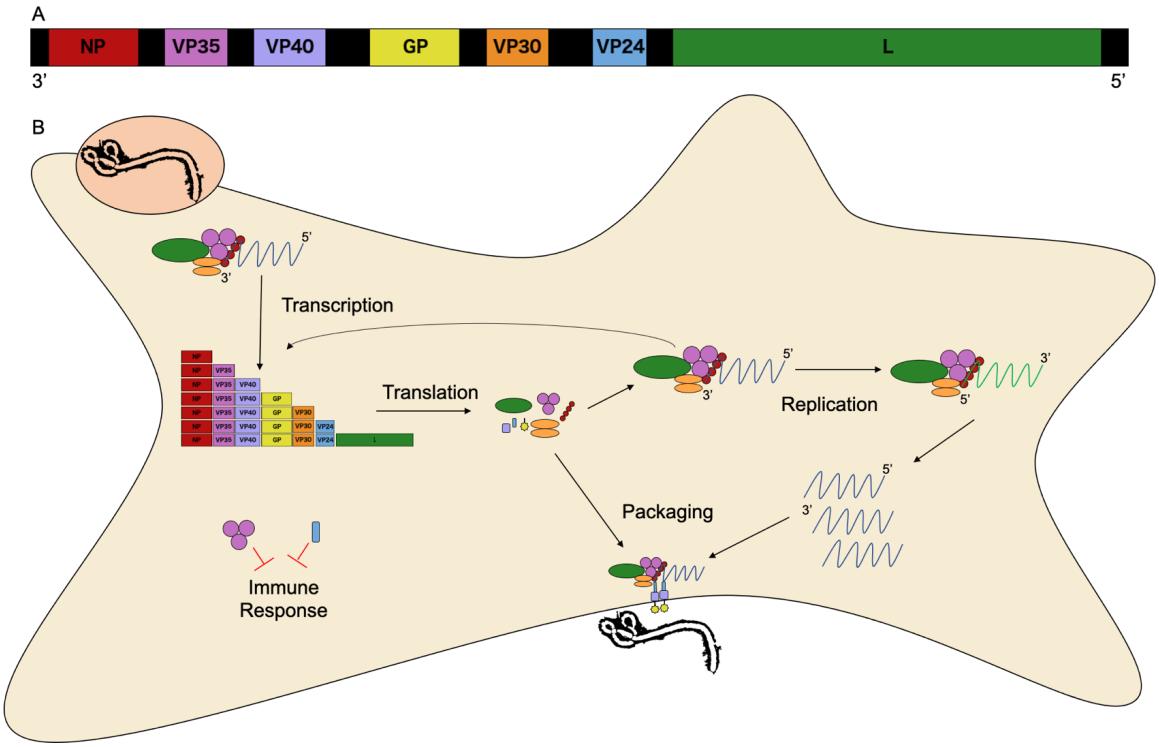

Figure 1.1 Ebolavirus genome and life cycle

(A) Genome organization of ebolaviruses in 3'→5' orientation. (B) Lifecycle of ebolaviruses starting at viral entry, transcription of viral mRNA, translation of viral proteins, genome (blue) replication through an antigenomic (green) state, viral packaging, virion release, and innate immune evasion. Image created by Corri B. Levine using Microsoft PowerPoint.

CLINICAL MANIFESTATIONS & PATHOGENESIS OF EBOLA DISEASE

Ebola disease, like many viral infections, first presents as a non-specific flu-like illness consisting of fever, myalgia, and malaise. These symptoms occur after an incubation period ranging from 2 - 21 days (mean of 6.22 days), and subsequent disease progression often occurs rapidly over an average of 10 days.[61] Symptoms worsen over the disease course with headache, muscle and joint pain, severe weakness and fatigue, a loss of appetite, nausea, and vomiting.[17,34] In about 50% of cases, hemorrhaging can be observed but this clinical manifestation is not necessarily linked with survival outcome.[30,62-65] When hemorrhaging occurs, it typically presents as a petechial rash, epistaxis, bloody stool, or bleeding from venipuncture sites.[65] Spontaneous abortions and vaginal bleeding have also been observed in women.[66] Neurological signs and symptoms can occur but it is unclear if this is due to direct viral damage or linked to widespread inflammation and multi-organ failure.[17,34,67,68] After 5-15 days of acute illness patients either recover or succumb to the disease.[61] The biomarkers to determine clinical outcome are yet to be fully determined, but high viral load in the blood is often indicative of a fatal outcome.[17,69]

Most of the information about Ebola disease comes from clinical management of EBOV infection or animal models of EBOV. Infection with EBOV leads to a dysregulation of the immune response and a rapid exhaustion of biological resources. Initial infection of immune cells prevents early innate immune responses, and these cells are used to disseminate virus throughout the body to secondary target organs including the liver, spleen, kidney, and adrenal glands.[34,36,52] Infection of immune cells results in a characteristic 'cytokine storm' in which there is a large release of pro-inflammatory cytokines that increases vascular permeability, thus leading to loss of fluid into extravascular spaces. In addition, these pro-inflammatory cytokines cause excessive T-cell activation resulting in T-cell exhaustion and apoptosis.[34] Clinical hematology can track disease progression through lymphopenia and thrombocytopenia as lymphocytes undergo

apoptosis and platelets are rapidly used up.[36,66] Clotting factors are quickly consumed in response to the increased vascular permeability and damage by viral replication prevents the liver from replenishing the supply. Damage to the liver can be seen on clinical testing where liver enzymes such as alanine aminotransferase (ALT) and aspartate aminotransferase (AST) are elevated. Impaired renal function is observed over the course of disease and blood urea nitrogen (BUN) and creatinine levels are elevated.[66,70] While clinical hematology and chemistry results can be informative regarding disease course, they are not necessarily indicative of outcome, especially if critical care is available to correct for the damage and imbalances.[65] Maintenance of blood volume and electrolyte balance is necessary to prevent the eventual hypovolemic shock and multi-organ failure that results in disease fatalities.[65]

In the case of BDBV infection, analysis of the 2012 outbreak offered a glimpse into the clinical manifestations of this specific ebolavirus species since most cases were managed at a single clinic and retrospective analysis of patient charts and disease management protocols were easily completed.[31] All initial suspected cases were diagnosed based on symptoms similar to those used during other ebolavirus outbreaks including non-specific flu-like symptoms (fever, myalgia, malaise) or fever with reported contact to a suspected case. BDBV was confirmed by laboratory testing in 36 of the 62 presumed cases.[31] More common symptoms during hospitalization included weakness, muscle and joint pain, anorexia, nausea, vomiting, diarrhea, and difficulty swallowing, similar to EVD.[31] Another study looking at the clinical manifestations observed in 26 patients from the 2007 outbreak, reported a similar set of symptoms.[29] Fever was self-reported in 73% of patients but only 52% had a clinically observed fever. Headache, weakness, muscle pain, anorexia, nausea/vomiting, and diarrhea were commonly observed symptoms.[29] The clinical course of disease was found to be quite varied with no accurate way to determine prognosis. Examination of four patients, two survivors and two non-survivors found that for each outcome, there was one patient who presented with severe symptoms for an

extended duration and one patient with a short disease course.[31] The lack of a clear clinical course complicates treatment protocols and resource management.

Long-term sequelae from EVD have been documented, but the size of the 2013 West African epidemic revealed the extent of such outcomes. Survivors have reported arthralgia, vision loss, and hearing loss.[62,71] In addition, there have been reports of live virus persisting in immune privileged sites such as the eyes, testes (seminal fluid), and cerebral spinal fluid.[72-74] This leads to the possibility of sustained transmission or future recurrence of an outbreak, as is suspected for the 2021 Guinea outbreak. Due to the limited number of BDBV cases, it is unclear if sequalae and sustained infection are possible with this and other lesser studied ebolavirus species, but it is possible.

There are still many questions surrounding the pathogenesis and clinical course of BDBV, especially since only two outbreaks have been recorded to date. Even with the availability of animal models, research into this species is limited and most studies have focused on EBOV infection, and to some extent SUDV. Understanding the mechanisms behind the different disease course and clinical findings could lead to new targets for antivirals or a better understanding of what immune response is needed to provide protection from disease.

HYPOTHESIS & SPECIFIC AIMS

Given the recorded differences in CFR and clinical course between EBOV and BDBV, it is believed that a molecular mechanism may contribute to these variations. This dissertation sets out to examine this hypothesis: *the EBOV polymerase complex is more efficient than the BDBV polymerase complex resulting in the observed differences in disease course and lethality*. Insights into the molecular mechanism(s) that results in differential disease severity will provide potential targets for antiviral therapeutics as well as provide a better understanding of the sequence of events leading to Ebola disease. The hypothesis will be addressed using three aims:

Aim 1: Measure and compare the growth kinetics, transcription, and replication of EBOV and BDBV in target cells

We hypothesized that transcriptional activity is diminished in BDBV infection compared to EBOV resulting in reduced production of new virions. A direct comparison of the viral growth kinetics was assessed between EBOV and BDBV in known target cells: macrophages and hepatocytes. Growth kinetics were assessed by looking at viral titers, gene transcription, and genome production. Examination of individual gene transcription and viral genome replication was used to assess which stage of RNA synthesis was most variable between these species.

Aim 2: Evaluate the fitness of the BDBV replication machinery in relation to EBOV

We hypothesized that minigenome transcription and replication would be diminished when the BDBV proteins were used compared to the EBOV proteins. An artificial minigenome replication system was developed for BDBV to examine the polymerase complex in isolation. Using this minigenome system, the polymerase complex proteins (NP, VP35, VP30, and L) from BDBV and EBOV were exchanged to compare replicative capacities. Differences in the ability of the polymerase complexes to synthesize RNA could explain the variations in fatality rate observed during outbreaks of BDBV compared to outbreaks of EBOV.

Aim 3: Evaluate the efficacy of small-molecule inhibitors targeting components of the polymerase complex and determine the effects on minigenome expression and viral replication *in vitro*

We hypothesized that small-molecule inhibitors would have a greater effect on the BDBV polymerase complex compared to EBOV. Several small molecules were identified that either bind to proteins of the EBOV polymerase complex or have been shown to directly inhibit EBOV RNA synthesis. Testing of these compounds has been limited to EBOV or EBOV replication systems and it is unknown if they are efficacious against other species such as BDBV.

Chapter 2: Comparison of Viral Replication Capacities Between Bundibugyo and Zaire ebolaviruses

INTRODUCTION

Most *in vitro* and *in vivo* studies, as well as clinical data collection, have been focused on EBOV. Minimal experimental data has been collected on BDBV and clinical data are limited to the two recorded outbreaks in 2007 and 2012. Interestingly, the clinical observations as well as the few *in vitro* and *in vivo* studies suggest a clear difference in the fatality and pathogenesis between BDBV and EBOV. These differences include variations in the overall clinical course both in timing and severity, differences in various cytokine profiles and immune responses, and differences in *in vitro* growth kinetics.

Comparing clinical data from the various EBOV outbreaks with the two BDBV outbreaks show a stark difference in the overall CFRs.[21] This difference holds true in non-human primate models of disease where EBOV is uniformly lethal, while BDBV infection results in a 60 - 75% mortality rate in the non-human primate model.[75-78] The immune response profiles, both clinically and in animal models, show a different response indicating a longer period of replication and dissemination for BDBV compared to EBOV.[29,79] This is further exemplified by the presence of both an IgM and IgG antibody response in the acute period of BDBV infection, whereas those infected with EBOV only generate an IgG response if they survive the acute phase.[79] In addition, while EBOV infection results in a strong pro-inflammatory response, BDBV infection results in a marked anti-inflammatory response as the acute phase progresses, perhaps indicating an

attempt to maintain homeostasis.[79] There are several mechanisms that could explain these differences between EBOV and BDBV including variations in immune evasion capabilities and diminished growth efficiency of the virus itself.

Previous research examined whether these differences could be explained by a decreased ability of the BDBV viral immune modulating proteins VP35 and VP24 to inhibit the innate immune response. VP35 immune inhibition acts on the interferon (IFN) induction pathway.[80-82] One of the major mechanisms of immune evasion is in the inhibition of retinoic inducible gene I (RIG-I), a dsRNA recognition molecule that initiates a signaling cascade for production of IFN-α/β.[83] EBOV VP35 blocks this recognition by binding to the ends of viral dsRNA as well as by binding to PKR activator (PACT), preventing its interaction with RIG-I.[83,84] In addition, VP35 can block the induction of interferon through interaction with IFN-regulatory factor 3 (IRF-3), IFN-β promoter stimulator 1 (IPS-1), TANK-binding kinase 1 (TBK-1), and IκB kinase epsilon (IKKε).[85] VP24, works downstream in the IFN pathway, inhibiting the cellular response to IFN.[86,87] It does so by binding to karyopherin α1 (KPNA) and preventing it from binding to signal transducer and activator of transcription 1 (STAT1), a necessary step for STAT translocation to the nucleus and subsequent initiation of transcription of IFN-stimulated genes.[86]

One study examining the ability of BDBV VP35 to inhibit IFN production found that there was no difference compared to EBOV VP35.[88] Additional data showed that replication of BDBV or EBOV was not influenced in cell lines with either RIG-I or STAT2 knocked out indicating both viruses were able to inhibit these pathways and that signaling through these pathways did not dampen viral growth (Versteeg, unpublished).

Although the inhibitory capabilities were not different between species, any differences in the amount of viral proteins present could affect immune inhibition. A reason for variations in protein concentrations during infection could be a deficiency in the ability to produce viral gene transcripts and subsequent translation of viral proteins. It was therefore of interest to determine if there was a difference in viral genome transcription or replication that would indicate a mechanism responsible for the observed differences in clinical outcomes.

Since limited side-by-side comparisons exist, we set out to compare the growth kinetics of BDBV and EBOV in both primary and secondary target cell types. While viral growth kinetics offer an overarching view of variations in viral replication capacities, differences can be attributed to various points in the viral life cycle. These include viral entry, genome replication, transcription of viral genes, translation of viral proteins, virion assembly, and release of new virions. This chapter will look specifically at virion release, viral gene transcription, and viral genome production. We hypothesize that BDBV produces fewer transcripts and genome copies over time compared to EBOV resulting in fewer infectious viral particles.

METHODS

Cell Culture

The THP-1 human protomonocytic cell line was used to derive macrophage-like cells in accordance with a previously published protocol.[89] Cells were maintained in complete Roswell Park Memorial Insitute medium (cRPMI: 10% FBS + 1% Penicillin/Streptomycin) in an upright T-75 flask at 37°C in 5% CO_2. For differentiation

of macrophage-like cells, 24-well plates were seeded with 2 x 10^5 cells per well in cRPMI with 200nM phorbol 12-myristate 13-acetate (PMA). Three days after plating, cells were observed for adherence and the media was removed and replaced with fresh cRPMI. Two days after the media change cells were transferred into the BSL-4 for inoculation.

The HepG2 cell line, derived from the liver tissue of a case of hepatocellular carcinoma, was maintained in complete Eagle's Minimum Essential Medium (cEMEM: 10% FBS + 1% Penicillin/Streptomycin) in T-150 flasks at 37°C in 5% CO_2. For experiments, cells were plated on a 24-well plate at a density of 5 x 10^5 cells per well. Once a confluent monolayer was reached, cells were transferred into the BSL-4 for inoculation.

Vero E6 cells were used for titering of all samples. Cells were maintained in cEMEM in T-150 flasks at 37°C in 5% CO_2. For titering, cells were plated on 6-well plates and, once a confluent monolayer was reached, cells were transferred into the BSL-4 for titrations.

Virus Isolates

A laboratory seed stock of *Zaire ebolavirus* strain Mayinga was grown from the serum of a fatal human case in 1976 in the Democratic Republic of the Congo (Zaire ebolavirus/H.sapiens-tc/COD/1976/Yambuku-Mayinga, accession number NC_002549) and passaged twice in authenticated Vero E6 cells.[90,91]

A laboratory seed stock of *Bundibugyo ebolavirus* was grown from the serum of a 2007 fatal human case in Uganda (Bundibugyo virus/H. Sapiens-tc-UGA/2007/Bundibugyo-200706291, accession number KU182911) and passaged twice in authenticated Vero E6 cells.[28,76,92]

Viral Infection

A multiplicity of infection (MOI) of 1 was used for measuring growth kinetics and viral RNAs. For inoculations, media was removed from all wells and 150 μL inoculum in serum free media was added to each well. Plates were kept at 37°C in 5% CO_2 for 1 h with gentle rocking every 15 m. After 1 h, wells were washed five times with complete media to ensure removal of unattached virions. After the final wash, 500 μL complete media was added.

Sample Collection

Samples for titering and RNA extraction were collected at 1, 6, 24, 48, 72, and 96 hours post-infection (hpi). A mock infected plate was collected for titering and RNA experiments at 1 hpi. At each collection timepoint, the supernatant was removed and centrifuged at 14,000 x *g* for 10 m at room temperature to clarify. The clarified supernatant was divided in half: half was saved for titering and half was added to TRIzol LS for RNA extraction. Cell monolayers were treated with TRIzol for RNA extraction. Following approved inactivation procedures, TRIzol samples were removed from BSL-4 for RNA extraction.

RNA Extraction and Calculation of Genome Equivalents

Seed stock and sample RNA was extracted from TRIzol samples using the Direct-zol RNA kit (Zymo Research, Irvine, CA) following manufacturer instructions. Samples were eluted in DNase/RNase-free water and the concentration was determined by spectrometry using the Cytation 5 multi-mode reader (BioTek, Winooski, VT). Genome

equivalents were calculated by determining the mass of one molecule of EBOV or BDBV using the formula:[93]

$$m = n \frac{M}{Na}$$

m = mass
n = bases (18,959 for EBOV; 11,161 for BDBV)
M = mass per mole of RNA base (339 g/mol)
Na = 6.02 x 10^{23} base pairs/mol

Samples were diluted to a concentration of 1x10^9 genome equivalents (GE) per 2 μL and used for cDNA synthesis.

Titration

Clarified supernatants were diluted 1:10 in serum free EMEM and 200 μL inoculum was added to the Vero E6 cell monolayer in each well of a 6-well plate in duplicate. Plates were kept at 37°C in 5% CO_2 for 1h with gentle rocking every 15 m. After 1 h, 0.8% agarose in 2X MEM was overlayed and allowed to form a semi-solid layer. Plates were incubated at 37°C in 5% CO_2 until staining. Plates were stained with 5% neutral red in phosphate-buffered saline (PBS) 5 days later for EBOV or 7 days for BDBV. Plaques were counted 24 h after staining.

Quantitative Reverse Transcription PCR

Quantitative reverse transcription polymerase chain reaction (RT-qPCR) was used to quantify the amount of RNA of various types including viral genomic RNA (vRNA) and messenger RNA (mRNA). The SuperScript IV first-strand RNA synthesis kit (Invitrogen, Waltham, MA) was used for reverse transcription. An oligo-dT primer was used for

detection of mRNA. A strand specific primer was designed against the sequence of the trailer region for the genomic strand to distinguish it from the anti-genomic strand. A primer binding site in the trailer region was chosen to ensure only complete genome copies were detected.

The primer-probe set for detection of viral genomic RNA (vRNA) was manually designed using the recommended parameters for TaqMan assays (Table 2.1). Primer-probe sets for each gene of interest were designed using TaqMan custom design software (Invitrogen) (Table 2.1). After first-strand reverse transcription, qPCR was performed using TaqMan Fast Advanced Master Mix (Invitrogen) per manufacturer's protocol. To generate a standard curve for vRNA, genome equivalents were calculated based on the concentration of RNA extracted from the viral stocks. For each gene of interest, a known concentration of plasmid encoding the viral gene of interest was used to create a standard curve to determine the number of copies detected in each sample. For detection of vRNA in the supernatant, equal volumes (μL) of extracted RNA were analyzed and normalized to copies per mL. vRNA in supernatant is reported as raw values of GE and as fold-change compared to the sample taken 1 hpi. For detection of vRNA and mRNA in cells, equal amounts (ng) of cellular RNA were analyzed and normalized to copies per ng. mRNA was then further standardized as transcripts per GE.

Primer Name	Sequence
BDBV-Genome-Forward	GGCCGTCATGGTGGCGAAT
BDBV-Genome-Reverse	AGGTTTGAATAGCCTCAACTCATACTG
BDBV-Genome-Probe	AGTCTCAGTTGTTGGTTGTTGAGTTGT
BDBV-VP35-Forward	GCATACTGGGCAGAACATGGA
BDBV-VP35-Reverse	GGTACCATATCCCCTTGTTTTCCAA
BDBV-VP35-Probe	CCTGATTGCATCCTCC
BDBV-VP30-Forward	GCTTTTGCTGATTGCACGGAAA
BDBV-VP30-Reverse	GGAGCAGTGATGTTCAATTGTTGTT
BDBV-VP30-Probe	CCTGCGGCTCCCTTG
BDBV-L-Forward	GTCTCGAACAGAGGACAAGATTGG
BDBV-L-Reverse	GCAGCAGAGGGACACTTAGG
BDBV-L-Probe	CAGCCAGCAATCAAG
EBOV-Genome-Forward	GGCCGTCATGGTGGCGAAT
EBOV-Genome-Reverse	TCACGCAGGGAGAGAGGC
EBOV-Genome-Probe	CTCATACATCATATTGATCTAATCTCA
EBOV-VP35-Forward	CCGCTGCGGCAACTG
EBOV-VP35-Reverse	GGTCCAGGTGGTGGTTGAC
EBOV-VP35-Probe	TCGGCCCAATAAGCCT
EBOV-VP30-Forward	GCAAGAGGAAGGTCCAAAAATTACC
EBOV-VP30-Reverse	TGCTCTTAATTTTGAATCCTCTATGGTTCTG
EBOV-VP30-Probe	CAAGACGGCAGAACAC
EBOV-L-Forward	GAATTGGCGTCCCGTTTAACAT
EBOV-L-Reverse	TGGTTTTATTAGCAAGTCACTGTTCGA
EBOV-L-Probe	CTGCCTTGAGTTACCC

Table 2.1 Taqman primer/probe sets for RT-qPCR

Primers and probes designed using TaqMan Custom Design Software (Invitrogen). Genome primer/probe sets align to the genomic trailer (5'-end). All probes contain a FAM reporter.

RESULTS

Growth Kinetics

Previous work found that in a mixed peripheral blood mononuclear cell (PBMC) population, BDBV grew slower and to lower peak titers than EBOV.[94] To confirm and further examine these results, the growth kinetics of BDBV and EBOV were measured in cell types representing the primary and secondary target cells of ebolavirus infection. The primary target cell types are monocytes, macrophages, and dendritic cells and a secondary target cell type is hepatocytes.[34,36,52] For macrophages, the THP-1 protomonocytic cell line was used to derive macrophage-like cells; for hepatocytes, the HepG2 hepatocyte-derived cell line was used. Cells were infected with an MOI = 1.0 to simulate a single round of infection. Although an MOI of 1 does not guarantee all cells will be infected, this was the highest MOI that could be reached using the BDBV seed stocks.

Growth kinetics of BDBV and EBOV in the two target cell types are shown in Figure 2.1A,B**.** In both cell types, EBOV grew to higher titers than BDBV. In THP-1 macrophages, EBOV reached a peak titer of 6.4×10^5 PFU/mL by 72 hours post-infection (hpi) while BDBV reached a peak titer of 3.3×10^4 PFU/mL by 96 hpi. In the HepG2 cells, EBOV reached a titer of 1.2×10^7 PFU/mL at 48 hpi with a slight increase to 1.5×10^7 PFU/mL by 72 hpi, while BDBV reached a peak titer of 1.6×10^6 PFU/mL by 72 hpi. At timepoints 24, 48, 72, and 96 hpi EBOV titers were consistently at least a half log higher than BDBV, and in most cases more than a log higher, and were significantly different at timepoints 24 and h8 hpi in THP-1 cells and at timepoints 48 and 72 hpi in HepG2 cells. Interestingly, the rate of growth, measured as fold-change from baseline, did not reach

statistical significance between viral species at any timepoint; however, EBOV consistently showed a greater increase from baseline than BDBV in HepG2 cells (Figure 2.1 C,D). These results, coupled with previously published data, indicate that there is a mechanism in place that is limiting BDBV from reaching titers as high as EBOV.[94]

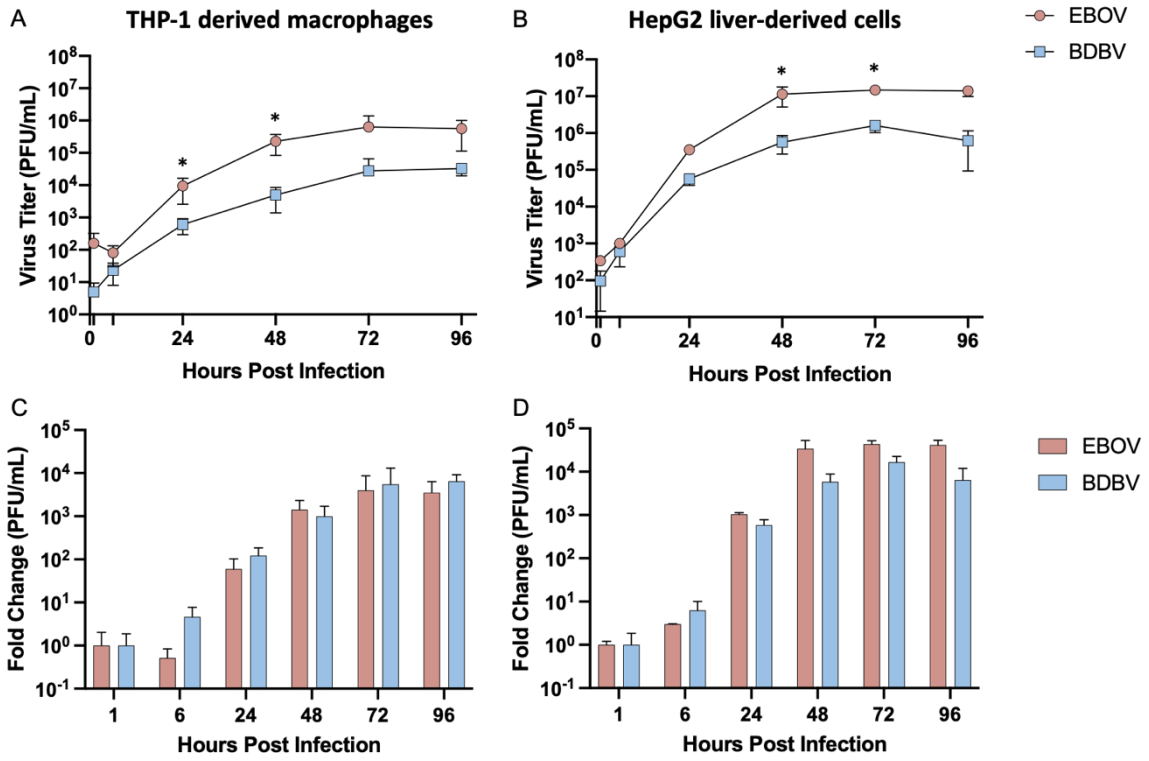

Figure 2.1 Growth kinetics of EBOV and BDBV in target cells

THP-1 macrophages (A,C) and HepG2 cells (B,D) were infected with EBOV or BDBV. Supernatant samples were collected at the indicated times post-infection and titered to quantify plaque forming units (PFU). Viral titers in PFU/mL are shown as mean ± standard deviation of three replicates (A, B). Change in titers compared to the 1 hpi sample are shown as mean mean ± standard deviation of three replicates (C,D). Reproduced from Levine, et al 2021 with permission.[125]

Production and Release of Viral Genomes

Next, we looked at the number of genome copies in the supernatant to compare this to the titration data. Equal volumes of extracted RNA were reverse-transcribed and analyzed by qPCR and the number of GEs was determined. The raw values indicate that at early timepoints after infection (1 and 6 hpi) there were slightly more BDBV GE in the supernatant, but by 24 hpi this difference disappears and there are roughly equivalent amounts of GE in the supernatant (Figure 2.2 A,B). When examined in relation to the baseline number of GE, EBOV infection results in a larger increase in the production and release of GE starting 24 hpi for both cell types (Figure 2.2 C,D). This is more pronounced in the THP-1 macrophages where there is an order of magnitude difference in fold-change for GE released which was significant at timepoints 24, 48, 72, and 96 hpi. In HepG2 cells, the difference in fold-change is smaller, but still shows a significantly greater increase in EBOV GE released compared to BDBV at timepoints 24, 48, 72, and 96 hpi. These results indicate that over time, more viral genomic RNA is being released from cells infected with EBOV than BDBV. This could be due to either an increase in the number of virions produced or due to cellular lysis resulting in not yet packaged viral genomes being released.

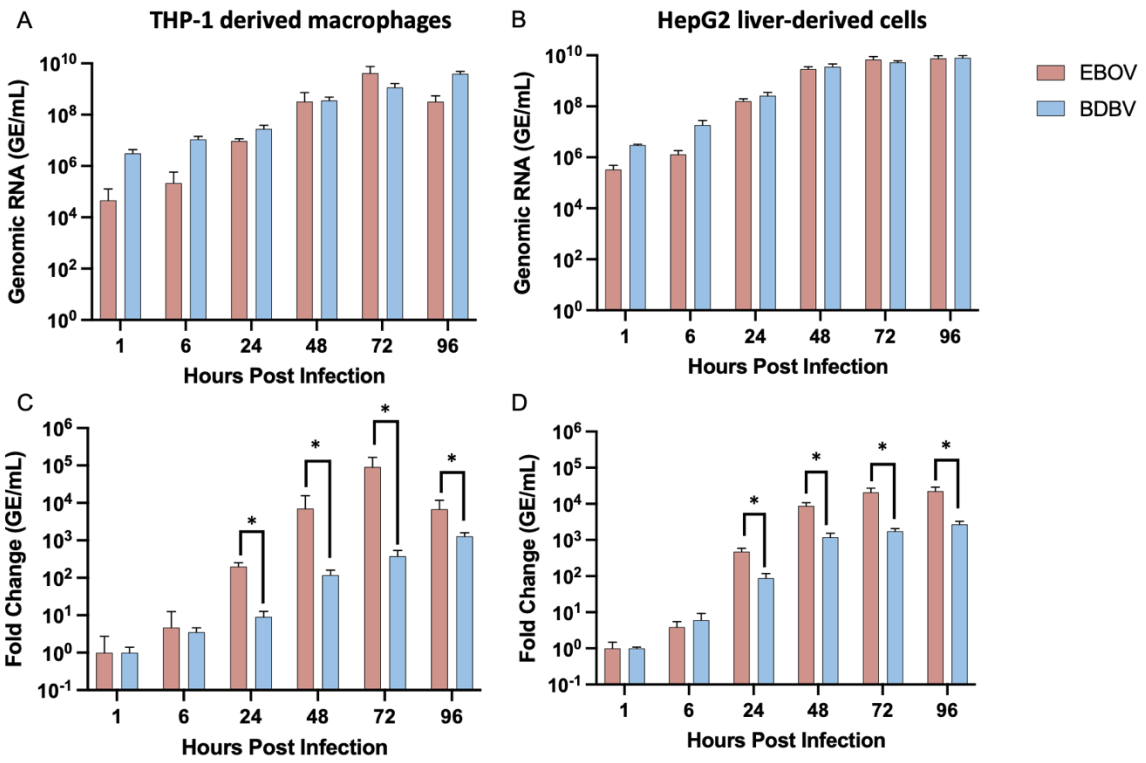

Figure 2.2 Genome equivalents of EBOV and BDBV released in supernatant

RNA was extracted from supernatant samples at the indicated timepoints post-infection and genome equivalents were quantified from THP-1 macrophages (A,C) and HepG2 cells (B,D). Genome equivalents per mL are shown as mean ± standard deviation of three replicates (A, B). Change in genome equivalents compared to the 1 hpi sample are shown as mean mean ± standard deviation of three replicates (C,D). Reproduced from Levine, et al 2021 with permission.[125]

When measuring intracellular copies of genomes, there is a similar trend to what was seen in the supernatant samples. There is a slight increase in the number of EBOV GE within cells compared to BDBV at time points after 24 hpi, especially in THP-1 cells which is significantly different by 96 hpi (Figure 2.3 A,B). Notably, there are significantly more copies of genomic RNA in BDBV infected HepG2 cells at 1 and 6 hpi compared to EBOV infected cells. This could be due to multiple virions infecting the same cell or to more copies of genomic RNA packaged within each BDBV virion. When examined in relation to baseline copies at 1 hpi, EBOV infection results in a greater change in GE within cells (Figure 2.3 C,D). In THP-1 cells, the change over time slows for EBOV infection, plateauing at 48 hpi, while the change in BDBV GE in cells continues to increase through 96 hpi. In HepG2 cells, the production of EBOV GE continues to rise through 72 hpi and then plateaus, while BDBV continues to show an increase in GE over the time course. The difference in fold change is significantly different at the later timepoints, 96 hpi for THP-1 cells and 72 and 96 hpi for the HepG2 cells. The rapid accumulation of EBOV GE from 24 to 48 hpi for THP-1 cells and 24 to 72 hpi for HepG2 cells likely points to the period when replication of genomes is the central activity of the polymerase complex, rather than transcription. This would coincide with the continued release of virions and genomic copies into the supernatant.

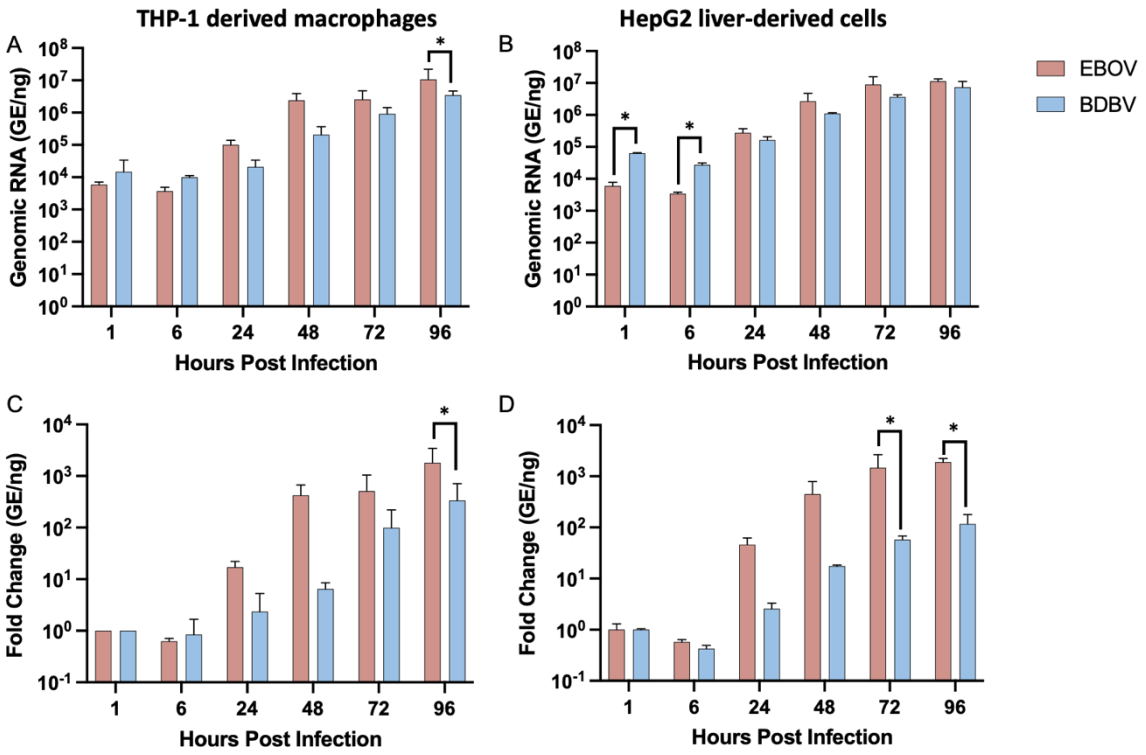

Figure 2.3 Intracellular genome equivalents of EBOV and BDBV

RNA was extracted from lysed cell monolayers at the indicated timepoints post-infection and genome equivalents were quantified from THP-1 macrophages (A,C) and HepG2 cells (B,D). Genome equivalents per ng RNA are shown as mean ± standard deviation of three replicates (A, B). Change in genome equivalents compared to the 1 hpi sample are shown as mean ± standard deviation of three replicates (C,D).

Transcription

To examine genome transcription, RT-qPCR was used to look at mRNA copies produced throughout the course of infection. Copies of VP35, VP30, and L mRNA were selectively measured by performing reverse transcription using oligo-dT primers. Gene specific TaqMan primer-probe sets were used to amplify and quantify transcripts over a 96-h infection period in both THP-1 derived macrophages and HepG2 cells. For cells infected with either EBOV or BDBV, it was found that transcription was most abundant in the first 24 h after infection (Figure 2.4) and a dramatic increase was observed during the first 24 h period. For individual transcripts there was a 100 - 1,000-fold increase in the number of copies of EBOV mRNA from 1 hpi to 24 hpi (Figure 2.4). For BDBV, the increase was not as large, ranging on average from 10 - 100-fold increase from 1 hpi to 24 hpi (Figure 2.4). This rapid increase correlates to the first round of transcription which is carried out by polymerase complexes packaged within each virion, and the addition of secondary transcription by newly formed polymerase complexes.

To further analyze transcription, mRNA transcripts were normalized per GE. As would be expected, VP35, the second gene to be encoded, was produced at levels substantially greater than VP30 and L which are encoded later in the genome (Figure 2.5). This fits with the known mechanism of polar transcription for ebolaviruses. For all three genes, the amount of transcript per GE was highest at 24 hpi and then decreased across all the later timepoints. The starkest difference between EBOV and BDBV was in the amount of VP35 transcript produced per GE. EBOV infection resulted in 2 and 2.4 VP35 transcripts produced per GE in THP-1 and HepG2 cells, respectively (Figure 2.5). BDBV infection resulted in 0.4 and 0.7 VP35 transcripts per GE for THP-1 and HepG2, respectively (Figure 2.5). This difference was observed at 1, 6, and 24 hpi and then transcripts became equivalent for later timepoints, with a significant difference observed at 6 and 24 hpi in both cell types. The amount of VP30 transcripts per GE were roughly equivalent at all

timepoints for both viruses. In the case of the L gene, there were more transcripts per GE produced for EBOV compared to BDBV in both cell types at 24 hpi, while all other timepoints showed nearly equivalent amounts of transcripts per GE. This difference was significant in the HepG2 cell line. These results point to a mechanism in which EBOV can more efficiently transcribe specific genes compared to BDBV.

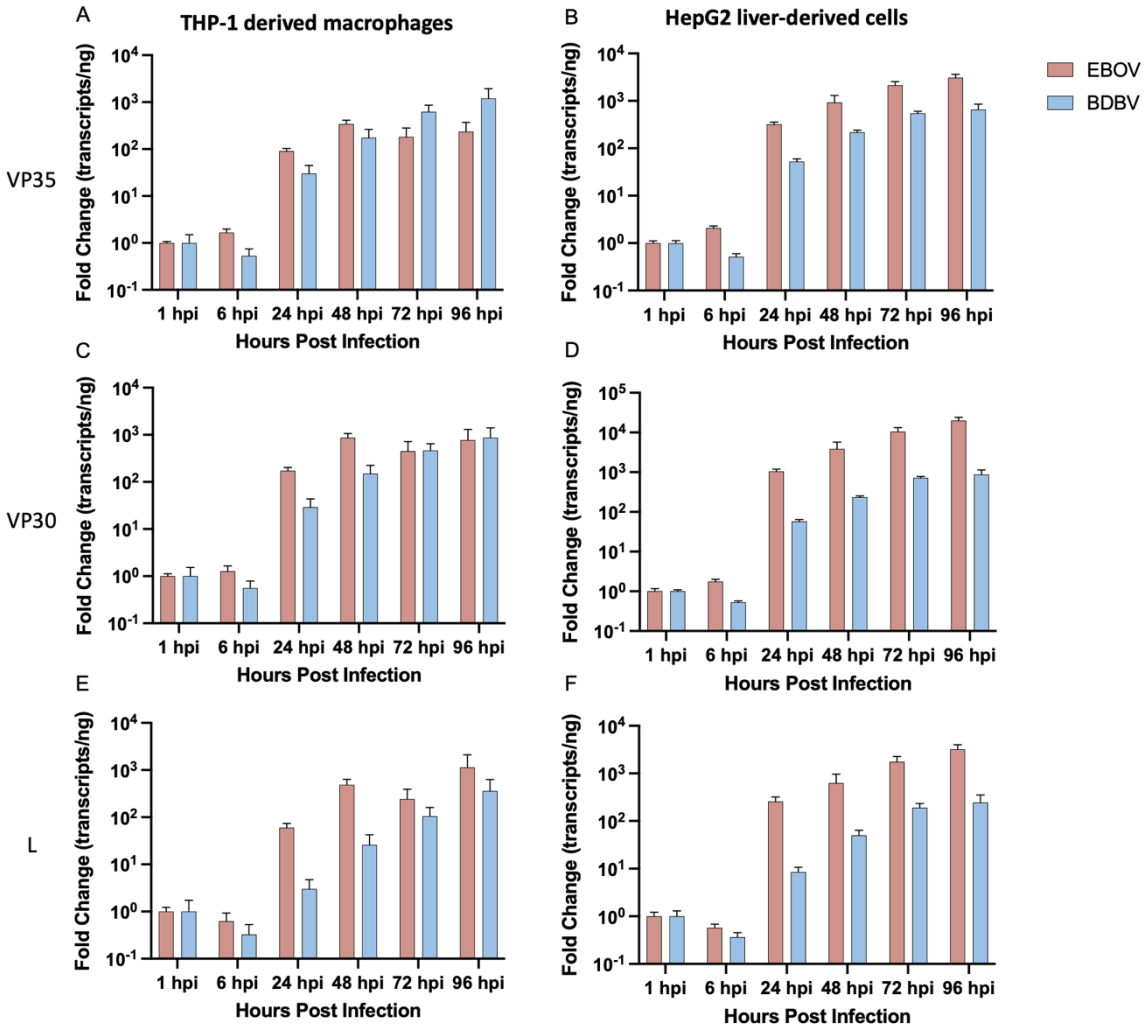

Figure 2.4 Fold change in viral transcripts during EBOV and BDBV infection

RNA was extracted from lysed cell monolayers at the indicated timepoints post-infection and mRNA transcripts were quantified from THP-1 macrophages (A,C,E) and HepG2 cells (B,D,F). Transcripts measured were VP35 (A,B), VP30 (C,D), and L (E,F). Change in viral transcripts over time were compared to the 1 hpi sample are shown as mean ± standard deviation of three replicates.

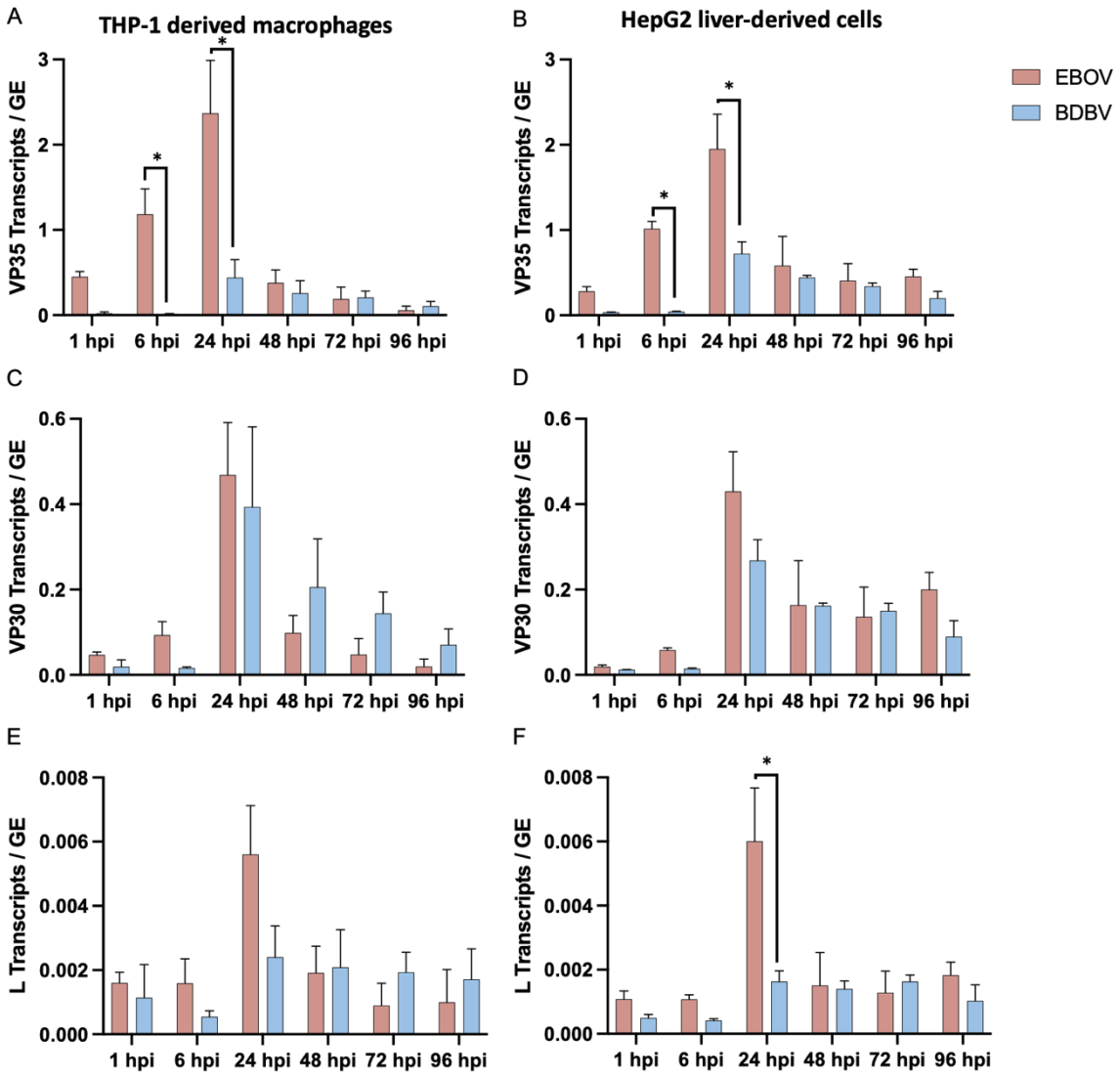

Figure 2.5 Transcripts per genome during infection with EBOV and BDBV

RNA was extracted from lysed cell monolayers at the indicated timepoints post-infection and mRNA transcripts were quantified from THP-1 macrophages (A,C,E) and HepG2 cells (B,D,F). Transcripts were normalized per GE at each timepoint and are shown as mean ± standard error of the mean of three replicates.

DISCUSSION

Clinical and *in vivo* data have shown that BDBV is less lethal than EBOV but the underlying reason for this observation has yet to be determined. While some have suggested the difference in clinical CFR is due to improved medical infrastructure in the regions where BDBV has emerged, this cannot be adequately assessed due to the limited number of outbreaks. Animal models of BDBV point to a viral mechanism for the lower fatality rate. Both NHP and ferret models of infection show a delayed time to death when compared to both EBOV and SUDV.[77,78,95-97] It is still unknown whether this delayed disease course is due to differential immune responses, viral growth kinetics, or a combination of both. The experiments presented in this chapter set out to directly compare the growth kinetics, viral genome production, and transcription patterns of EBOV and BDBV. By performing this side-by-side comparison we were able to distinguish what portions of the viral replication process differ between these two species.

One study which looked at the replication kinetics of BDBV compared to EBOV, found a marked difference in the viral titers and the rate of growth of these viruses in a mixed PBMC population.[94] The results presented in this chapter show a similar trend in which BDBV grows to lower peak titers when compared to EBOV in both THP-1 derived macrophages and HepG2 hepatocytes. In both these experiments and those previously published the difference in peak titers were half to one log different between species. In contrast to the published data using a mixed PBMC population, the growth curves in THP-1 macrophages and HepG2 cells proceeded at approximately the same rate, with EBOV titers increasing at a slightly higher rate than BDBV titers at later timepoints in the HepG2 cells. The reason for this difference in results could be due to the cell types used, the MOI used (1.0 versus 2.0), the method for quantification (plaque assay versus immunofluorescent staining), or a combination of these factors. Regardless of these

differences, both sets of experiments show that BDBV grows to lower titers than EBOV and that the time to reach peak titers is delayed for BDBV.

To confirm our titration results, we also looked at the number of genome copies within the supernatant. The trend was similar, although it is interesting to note that at 1 and 6 hpi there were more copies of BDBV genomic RNA in the supernatant than EBOV. Considering that the number of genomic copies was roughly equivalent between species while the titers were lower for BDBV, this equates to a higher ratio of viral genomes per PFU for BDBV compared to EBOV. This is surprising and deserves further examination. One reason for this finding is that BDBV may be producing defective interfering (DI) particles which are incapable of infecting cells. These DI particles would still contain genomic material but may not be capable of infecting naïve cells or replicating once internalized.[98,99] It would be interesting to examine the population of RNA genomes in the supernatant from BDBV infection to determine if any deletions or mutations are found that would inhibit further infection and viral replication.

In addition to the number of infectious particles, the amount of individual viral proteins produced could have an impact on the replicative capacity of each virus. While it appears that there is no difference in the direct ability of the immune antagonists VP35 and VP24, a decreased amount of either protein would result in a lower ability to evade cellular immune sensors. In addition, the proteins of the polymerase complex must be produced early after infection to create new complexes and carry out secondary transcription and replication. This hypothesis was examined by measuring viral gene transcripts by RT-qPCR over the course of infection in both primary and secondary target cells. Three genes were selected across the genome to account for the polar transcription which takes place. The rate of production for all three transcripts was higher for EBOV than for BDBV indicating that more transcription was taking place. The most substantial increase was seen between 6 and 24 h which would align with when the viral polymerase complex is carrying out transcription rather than genome replication. One mathematical model of ebolavirus

replication estimates that approximately 30 h pass before new virions are released and this matches what was observed here.[100] It would be interesting in future studies to collect multiple samples within the first 24 h of infection to further narrow down when the polymerase complex switches from transcription to replication. RT-qPCR or RNAseq data could be coupled with western blotting to probe for hyperphosphorylated VP30 which is necessary to promote genome replication.[60]

The rate of production for viral transcripts plateaued for EBOV in THP-1 macrophages after 48 h. This could indicate transcription had reached a steady state either due to the process of replication competing for template genomic RNA or due to a lack of production of more polymerase complexes. In contrast, EBOV transcription continued in HepG2 cells throughout the infection time course, although it appeared to slow over time. The same was true for BDBV infection in both THP-1 macrophages and HepG2 cells. These results suggest that macrophages are highly amenable to EBOV infection resulting in rapid transcription and replication while BDBV replication is more limited in this cell type.

The most telling result was in examination of transcription in the context of viral genome production. There was a substantial increase in the number of EBOV VP35 transcripts produced per viral genome, 2.4 and 2.0 transcripts per genome for THP-1 and HepG2, respectively. This was not the case for BDBV in which there were fewer than 1 transcript produced per genome. This could account for twice as much VP35 present during EBOV infection compared to BDBV infection. Since VP35 has carries out two important functions during infection, inhibition of the RIG-I pathway and RNA synthesis, this increase in protein concentration could account for the increased production of infectious virions. Similar to what was seen with VP35, there was a three-fold difference in the ratio of L transcripts per genome at 24 hpi with EBOV infection resulting in more transcripts than BDBV. This is to be expected as VP35 and L interact in the polymerase complex and a proper ratio of these two proteins must be maintained.[38] As with VP35, an increase in the

production of the L protein could result in the formation of more polymerase complexes, thus resulting in more transcription and genome replication. Future experiments should verify these results by RNA sequencing and measurement of viral protein concentrations over the course of infection either by western blot or quantitative mass spectrometry.

The results presented here indicate a possible mechanism for the variations in viral growth kinetics, disease course, and case fatality rate between EBOV and BDBV. It appears that EBOV infection results in increased transcription of viral genes compared to BDBV. This would result in a cascading effect in which EBOV produces more immune inhibitory proteins allowing for unchecked viral replication. This hypothesis is in line with the data showing that EBOV and BDBV VP35 can inhibit the IFN induction pathway to the same extent, but in a dose dependent manner.[88] In addition, a higher concentration of viral proteins would mean that there is an increased number of polymerase complexes able to carry out RNA synthesis. This would result in more transcription and replication and production of new virions. As viral gene transcription is carried out specifically by the viral polymerase complex, the next two chapters will examine the BDBV polymerase complex and compare it with that of EBOV.

Chapter 3: Creation and Optimization of a Bundibugyo ebolavirus Minigenome System

INTRODUCTION

Ebolaviruses are classified as Tier 1 Select Agents for study only within a BSL-4 containment laboratory. Not only is the study of ebolaviruses heavily restricted but studies within a BSL-4 laboratory are tedious and time-consuming. It is therefore of interest to have a model system that can be utilized at a lower biosafety level so that (1) more groups can study the virus, (2) the impact of individual mutations can be studied in context of specific activities, such as replication or budding, and (3) screening of therapeutics can occur before testing highly effective candidates against full-length virus.

One model system which has been used extensively to study the replication complex of many viruses is the minigenome system.[101-104] In a minigenome system, only the proteins necessary for viral genome transcription and replication are present along with a 'minigenome'. The simplest minigenome is one which encodes for a reporter molecule such as green fluorescent protein (GFP) or luciferase, which is flanked by upstream and downstream genomic regulatory regions. More complex minigenomes that encode for other viral proteins can also be used. By encoding for viral proteins such as structural proteins and those involved in virion budding, one can study the full replication cycle of a virus without the need for a high containment laboratory. This is because there is no full-length virus capable of replicating and infecting cells.

All non-segmented negative-sense (NNS) RNA viruses utilize a similar polymerase complex for transcription of viral genes and replication of the genome.[44] This

complex consists of a nucleoprotein (N, or NP for filoviruses), a phosphoprotein (P, or VP35 for filoviruses), and an RNA-dependent RNA polymerase (L). In the case of ebolaviruses, a fourth protein, VP30, is also associated with the polymerase complex and acts as a transcriptional activator.[38] The remainder of this chapter will focus on these four proteins and their specific roles for ebolavirus transcription and replication.

The first gene in the ebolavirus genome, NP, is involved in several aspects of the ebolavirus replication cycle, the most well-studied is the encapsulation of the genome RNA. By binding and surrounding the RNA, NP prevents host cell nucleases from degrading the RNA and prevents detection by the host innate immune sensors.[105] NP also encapsulates the viral antigenome, or the RNA intermediate used for genome replication. The NP-RNA interface is in a 1:6 ratio, with six nucleotides bound to every single nucleoprotein.[106] This is similar to the 'rule-of-six' observed with paramyxoviruses, another family within the order *Mononegavirales*, in which each nucleoprotein molecule binds to six nucleotides.[107] In addition to shielding the RNA from detection and degradation, NP may also play a role in the formation of new virions. In a system which produces viral-like particles (VLPs) to study virion release, it was found that while expression of VP40 alone could initiate the release of filamentous VLPs, the presence of NP significantly enhanced the production of VLPs.[37,108] NP also plays a critical role in orchestrating the transcription and replication process. This can be seen by the fact that NP interacts with both the polymerase cofactor VP35 and the transcriptional activator VP30.[40,48] The level of interaction with these two proteins modulates the amount of RNA synthesis as well as whether transcription or replication will be the dominant process.[40,48,60]

Next in the genome is VP35, the ebolavirus phosphoprotein. In addition to acting as the polymerase cofactor VP35 is also involved in subversion of the host innate immune response through interaction with RIG-I in the IFN induction pathway.[84,88] As the polymerase cofactor, VP35 binds both NP and L, acting as a chaperone for the polymerase subunit, L, to interact with viral RNA. As mentioned previously, VP35 contains a binding site for NP, the NP binding peptide (NPBP).[39,40] While bound to VP35, NP is unable to bind to viral RNA and instead, it is hypothesized that, the RNA is now more easily accessible to L. On the other hand, when VP35 and NP are not interacting, NP tightly binds the viral RNA which may be a signal for viral packaging and release.[40,109]

The fifth protein encoded in the ebolavirus genome is the transcriptional activator VP30. VP30 is required for ebolavirus transcription and modulates this process by allowing read-through of a hairpin located in the open reading frame for NP.[110] Removal of this hairpin structure allows for VP30-independent transcription.[110] This RNA hairpin structure is only found upstream of NP and nowhere else in the genome. In addition to guiding transcription, VP30 functions to switch between transcription and replication. This switch occurs based on the phosphorylation status of VP30.[50,60] When in a non- or low-phosphorylation state, VP30 binds strongly to VP35 and transcription is the dominant process.[60] When VP30 is hyper-phosphorylated, the interaction with VP35 is limited and replication becomes the dominant process.[60] The mechanism signaling this switch in phosphorylation state is yet to be determined.

The seventh and last gene of the ebolavirus genome is the large gene, or L, which encodes for the enzymatic subunit of the RNA-dependent RNA polymerase (RdRp). The

polymerase subunit is made up of the proteins VP35 and L, with L being the catalytic subunit.[111] The L protein is made up of five domains which perform all of the functions for transcription and replication of ebolaviruses: RNA-dependent RNA polymerase activity, mRNA capping by a polyribonucleotidyl transferase (PRNTase), and methyltransferase activity.[112,113] The necessity for these domains and their activities is demonstrated by the high homology found between all NNS viruses and mutational analysis of these domains results in a severely limited replicative capacity.[113-115] To carry out the polymerase functions, L interacts with both VP35 and VP30 as well as the viral RNA. VP35 appears to act as a bridge between L and the NP-encapsulated RNA, bringing the catalytic subunit into proximity with the RNA.[116]

A final component that directs the viral transcription and replication process is the untranslated genomic ends. These untranslated regions (UTR) are referred to as the genomic leader (3'-UTR) and trailer (5'-UTR). The RNA sequence and secondary structure of the viral genomic RNA contains important signaling sequences for initiation of transcription and replication.[110,117,118] The leader contains several signaling sequences and structures including a highly conserved initiation site, NP gene start signal, and a sequence of UN_5 repeats.[59,106,117] In contrast to the leader region, the trailer region of ebolavirus genomes is highly variable across species. Much less is known about the trailer although recent data suggests that genome replication is initiated at an internal nucleotide sequence.[119] In addition, binding motifs for host cell proteins have been identified in the trailer region and their roles in regulating replication are under investigation.[114]

In a minigenome system, support plasmids encoding the four proteins of the polymerase complex, NP, VP35, VP30, and L are transfected along with a minigenome encoded plasmid (Figure 3.1).[101,102] The minigenome contains all the necessary signaling sequences for transcription and replication without encoding for any viral proteins, instead, the minigenome contains a gene encoding a reporter, flanked by the leader and trailer. The minigenome is oriented in a 3' → 5' direction to mimic authentic virus. The minigenome system described in this chapter utilizes a T7 polymerase to synthesize the first copy of minigenome RNA. After this, the viral polymerase complex must take over for transcription of the reporter gene and replication of the minigenome. Translation of the reporter mRNA is carried out by host cell machinery as would occur in the context of an infection. The use of a reporter allows for easy quantification of the amount of polymerase activity. Transcription and translation of the reporter gene is carried out in a similar way to how viral proteins would be processed during infection. Therefore, this system can act as a tool for studying the polymerase activity of ebolaviruses.

Minigenome systems are currently available for the ebolaviruses EBOV and RESTV, as well as the related filoviruses MARV and LLOV.[38,57,101,120-122] This chapter describes the design and optimization of a novel minigenome system for BDBV which can be used for investigating the role of individual polymerase complex proteins in transcription (Chapter 4) and as a tool for screening therapeutic compounds (Chapter 5).

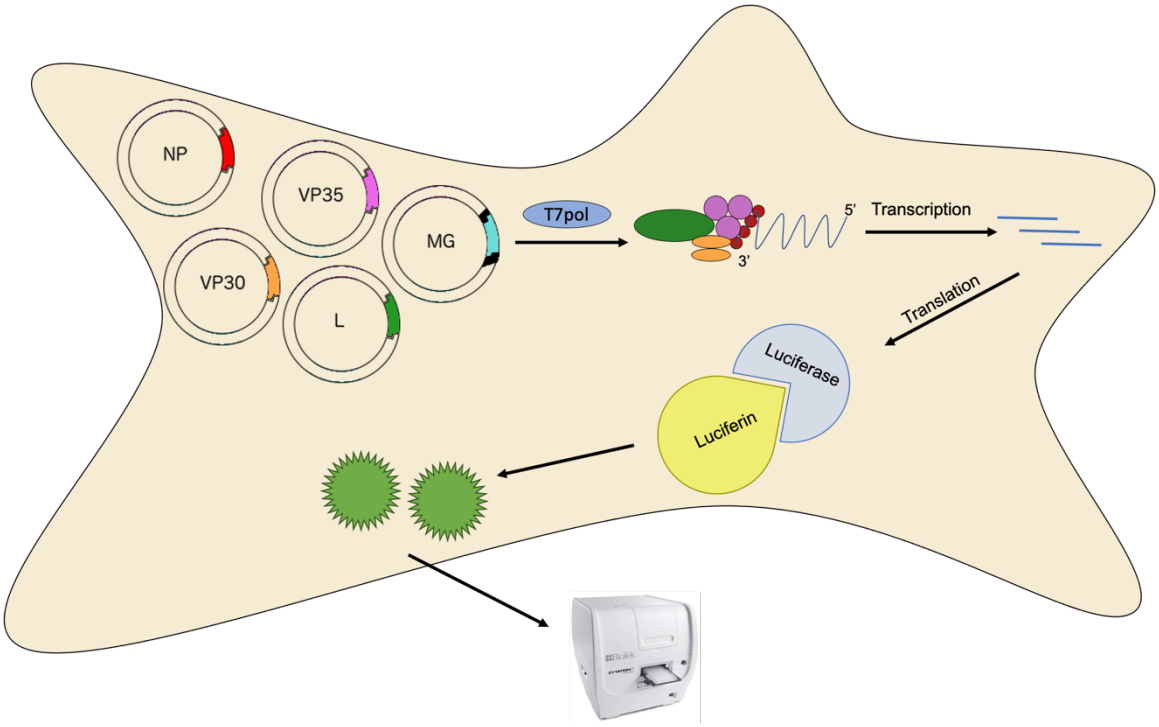

Figure 3.1 Schematic of minigenome assay

Polymerase complex support plasmids NP, VP35, VP30, and L are transfected along with a minigenome (MG) plasmid. A T7 polymerase plasmid is either transfected or stably expressed and transcription of the plasmids is carried out by the T7 polymerase. Viral proteins are translated by the host ribosomes. The minigenome plasmid encoding luciferase is transcribed by the T7 polymerase to produce a negative sense RNA minigenome which is recognized by the viral polymerase complex. After viral transcription of the reporter gene, luciferase is translated by host ribosomes. At the experimental endpoint, cells are lysed, and the luciferase substrate luciferin is added. Enzymatic activity by luciferase is measured as luminescence by spectrometry. Image created by Corri B. Levine using Microsoft PowerPoint.

METHODS

Cell Culture

The baby hamster kidney cell line BSR-T7/5 was used for all transfection experiments. BSR-T7/5 cells stably express the T7 polymerase under positive selection with the antibiotic geneticin (Gibco, Carlsbad, CA) which was added to the medium every other passage.[123] Cells were cultured in complete Dulbecco's modified Eagle medium (cDMEM: 10% FBS + 1% Penicillin/Streptomycin, 1% GlutaMax). Cells were maintained at 37°C and 5% CO_2.

Virus Isolate

A laboratory seed stock of *Bundibugyo ebolavirus* was grown from the serum of a 2007 fatal human case in Uganda (Bundibugyo virus/H. Sapiens-tc-UGA/2007/Bundibugyo-200706291, accession number KU182911) and passaged twice in authenticated Vero E6 cells.[28,76,92] Supernatant was inactivated in TRIzol (Ambion, Carlsbad, CA) before removal from BSL-4 facilities.

Plasmids

The plasmids pTM1_VP30_ZEBOV and p2,0_3E5E_luciferase were a gift from Dr. Elke Muhlberger (Addgene plasmids #69119, 69358).[116] These plasmids were used as the backbone for construction of plasmids encoding BDBV proteins and untranslated regions. The transfection control plasmid pGL4.74[hRluc/TK] (Promega, Madison, WI) encoding Renilla luciferase was used for all luciferase assays.

Cloning

SUPPORT PLASMIDS

Construction of the BDBV support plasmids pTM1_NP_BDBV, pTM1_VP30_BDBV, and pTM1_VP35_BDBV was completed using the backbone of the pTM1_VP30_ZEBOV plasmid after restriction enzyme digestion with EcoRI-HF and PacI (New England Biolabs Inc. (NEB), Ipswich, MA). BDBV RNA was harvested by TRIzol extraction using the Direct-zol RNA miniplus kit (Zymo). Reverse transcription was performed using the SuperScript IV First-Strand Synthesis System (Invitrogen) using a gene-specific forward primer. The gene of interest was then amplified with the Platinum SuperFi PCR Master Mix (Invitrogen) using gene specific primers with the addition of the desired 5' and 3' restriction sites. Following PCR amplification, the product was column purified using the PureLink PCR Purification Kit (Invitrogen), and underwent restriction enzyme digestion with EcoRI-HF and PacI before a second column purification. Ligation of vector and insert was performed using the Fast-Link DNA Ligation Kit (Lucigen, Middlesex, UK). Ligated plasmids were transformed into chemically competent C600 *E. coli* cells (NEB).

The support plasmid pTM1_L_BDBV was constructed using pTM1_VP30_ZEBOV as a backbone after restriction enzyme digestion with AgeI and XhoI (NEB). The L gene was reverse transcribed and amplified in two segments. Reverse transcription was performed using the SuperScript IV First-Strand Synthesis Kit (Invitrogen) using a gene-specific forward primer for each segment and amplification was completed using the Platinum SuperFi PCR Master Mix (Invitrogen). Primers were

designed to encode the end of the gene and an overlapping region complementary to the pTM1 plasmid backbone and reconstructing the restriction sites as per the principles of Gibson cloning.[124] All PCR products were purified using the PureLink PCR Purification Kit (Invitrogen). The final plasmid was ligated using the NEBuilder HiFi DNA Assembly Cloning Kit (NEB) and the ligation mixture was transformed into chemically competent NEB5α *E. coli* cells (NEB). All support plasmids were selected based on ampicillin resistance. Colonies were screened by PCR and restriction digest, and positive clones were confirmed by Sanger sequencing.

MINIGENOME PLASMIDS

The vector backbone for the minigenome plasmids was derived from p2,0_3E5E_luciferase. The restriction enzymes RsrII, NdeI, NotI, and XhoI (NEB) were used to segment the p2,0_3E5E_luciferase plasmid into its component parts: p2,0 vector, leader, trailer, and reporter gene (Figure 3.2, 3E5E). The BDBV leader and trailer regions were constructed as described for L using genome specific forward primers for reverse transcription, addition of an overlapping region to the vector, and reconstruction of restriction sites. The hepatitis delta virus ribozyme self-cleaving site was added to the leader region and the T7 promoter was added to the trailer region during PCR amplification. Construction of the plasmids was completed using NEBuilder HiFi DNA Assembly Cloning Kit (NEB) and the ligation mixture was transformed into chemically competent NEB5α *E. coli* cells (NEB) and selected based on ampicillin resistance. Colonies were screened by PCR and restriction digest, and positive clones were confirmed by Sanger sequencing. The minigenome plasmids consist of the 3'-leader (3) and 5'-trailer

(5) regions of either EBOV (E) or BDBV (B) and are annotated as 3E5E, 3E5B, 3B5E, and 3B5B (Figure 3.2).

Primers used for all cloned plasmids are listed in Table 3.1.

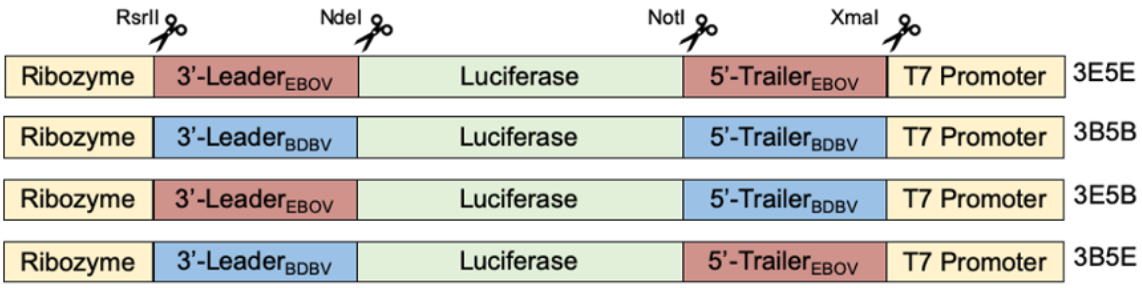

Figure 3.2 Map of minigenome constructs

EBOV (3E5E), BDBV (3B5B) and chimeric minigenomes (3E5B and 3B5E) are represented. Restriction sites for RSRII and NdeI are located outside the leader region, NotI and XmaI are located outside the trailer region. The T7 promoter is located upstream of the 5'-UTR and the Hepatitis delta ribozyme self-cleaving site is located downstream of the 3'-UTR to ensure an exact 3' end. Naming refers to the 3'-leader (3) or 5'-trailer (5) from BDBV (B) or EBOV (E). Image created by Corri B. Levine using Microsoft PowerPoint. Reproduced from Levine, et al 2021 with permission.[125]

Primer Name	Sequence
NP Forward	TCA GAT GAA TTC GCT ACA TTC TCT ATC CAA GAC C
NP Reverse	TGT CCA TTA ATT AAC CAT CAC CTG TGA TGC TGG
VP35 Forward	TTA GCA GAA TTC TAT GAC CTC TAA CAG AGC AAG
VP35 Reverse	TGT ACC TTA ATT AAC CAA CCT TAG ATT TTG AGT CCG AG
VP30 Forward	TTA GGT GAA TTC ATC TTG GGG ATT TCT CTG AAC
VP30 Reverse	AGT CAC TTA ATT AAC CAT CTT ATC TGC GTT GAA TAG GG
L Forward 1	TAG TGG ATC CGC GAA ATG GCA ACT CAA CAT ACA C
L Reverse 1	CCA GGT ATA TTC ACG TAA AAT TTG CGC CAA ATC AAC TGT ACA AGA AAC
L Forward 2	GTT TCT TGT ACA GTT GAT TTG GCG CAA ATT TTA CGT GAA TAT ACC TGG
L Reverse 2	CCG GAT CGT CGA CTT AAT CTC TAA GGG GAT CTT AAG CG
BDBV Leader Forward	GAT GCC CAG GTC GGA CCG CGA GGA GGT GGA GAT GCC ATG CCG ACC CCG GAC ACA CAA AAA G
BDBV Leader Reverse	TTT TGG CGT CTT CCA TAT GCA TTT TGA GGT CTT G
BDBV Trailer Forward	GAT CGC CGT GTA AGC GGC CGC GAT CCC CTT AGA GG
BDBV Trailer Reverse	CAG GGG GAT ATC GAT CCC GGG TAA TAC GAC TCA CTA TAG TGG ACA CAC AAA AAA G

Table 3.1 Primers for Cloning

Underlined sequences correspond to regions in the BDBV genome. *Italicized* sequences correspond to the T7 promoter and hepatitis delta ribozyme sequences located in the minigenome. **Bold** sequences correspond to an overlapping region in the vector required for Gibson assembly. Reproduced from Levine, et al 2021 with permission.[125]

Transfection

BSR-T7/5 cells were plated in 6-well tissue culture treated plates at a density of 4 x 10^5 cells/well as per recommendations for the EBOV minigenome system.[101] When cells reached 70% confluency, they were transfected using Lipofectamine 3000 (Invitrogen), as per the manufacturer's protocol.

Luciferase Assay

Minigenome expression was quantified using the Dual-Luciferase Assay System (Promega). Forty-eight hours after transfection, media was removed, and cell monolayers were washed once with PBS. Cell lysis was completed using passive lysis buffer as per manufacturer's protocol and lysates were collected for downstream analysis. All conditions were tested in triplicate and standardized as relative luminescence units (RLU) calculated as a ratio of Firefly Luciferase to *Renilla* Luciferase.

RESULTS

Generation of a BDBV Replication and Transcription System

In order to study the BDBV polymerase complex in isolation and outside of a high-containment lab, a BDBV minigenome system was created.[125] The genes encoding the polymerase complex proteins NP, VP35, VP30, and L are essential for transcription and replication and therefore essential for minigenome activity. These genes were cloned in the pTM1 vector which contains a T7 RNA polymerase promoter upstream of the gene of interest. To create the minigenome, the UTRs of BDBV were cloned into the p2,0 vector

flanking a luciferase reporter gene (Figure 3.2). This included the leading 460 nucleotides and the trailing 741 nucleotides. Addition of the T7 RNA polymerase promoter and a hepatitis delta ribozyme, a self-cleaving site which ensures an exact 3' end, were added in by PCR amplification. The T7 promotor was directly upstream of the 5'-trailer and the ribozyme was directly downstream of the 3'-leader. The hepatitis delta ribozyme is included to create authentic 3' ends which are necessary for recognition by the viral polymerase complex.[59,106,120] All plasmids were confirmed by Sanger sequencing and no mutations were found. The minigenome construct is identified as 3B5B indicating that the sequences from BDBV (B) are used for the 3'-leader (3) and 5'-trailer (5). In addition to the minigenome 3B5B, two chimeric minigenomes were created using the UTRs from EBOV. These chimeric minigenomes are designated 3E5B, EBOV 3'-leader and BDBV 5'-trailer, and 3B5E, BDBV 3'-leader and EBOV 5'-trailer (Figure 3.2).

Titration of BDBV Minigenome and Support Plasmids

The four proteins of the polymerase complex, NP, VP35, VP30, and L are essential for transcription and replication of the minigenome.[38,122] Titrations were necessary to determine the optimal concentration and ratio of each plasmid to the others. Each support plasmid was titrated from 0 ng to 4 μg, while the concentration of the other three support plasmids and the minigenome encoded plasmid remained constant. Initial plasmid concentrations were chosen based on the published protocol for the EBOV minigenome system.[101] Titrations of the BDBV plasmids resulted in a range of activity indicating an optimal concentration of each plasmid and showing that too little or too much of an individual plasmid renders the system inactive (Figure 3.3). This is consistent with

previous experiments using the MARV, EBOV, and RESTV minigenome systems.[38,57,122] In the case of the minigenome plasmid, increasing concentrations of this plasmid resulted in a linear increase in luciferase activity, as would be expected (Figure 3.3). Removal of any one of the four support plasmids resulted in no detectable luciferase activity indicating that all four proteins are necessary for transcription of the minigenome (Figure 3.3). These studies do not directly measure replication and therefore it is unclear if the BDBV polymerase complex can replicate the minigenome in the absence of VP30 as is the case for EBOV and the related MARV.[38,57,117]

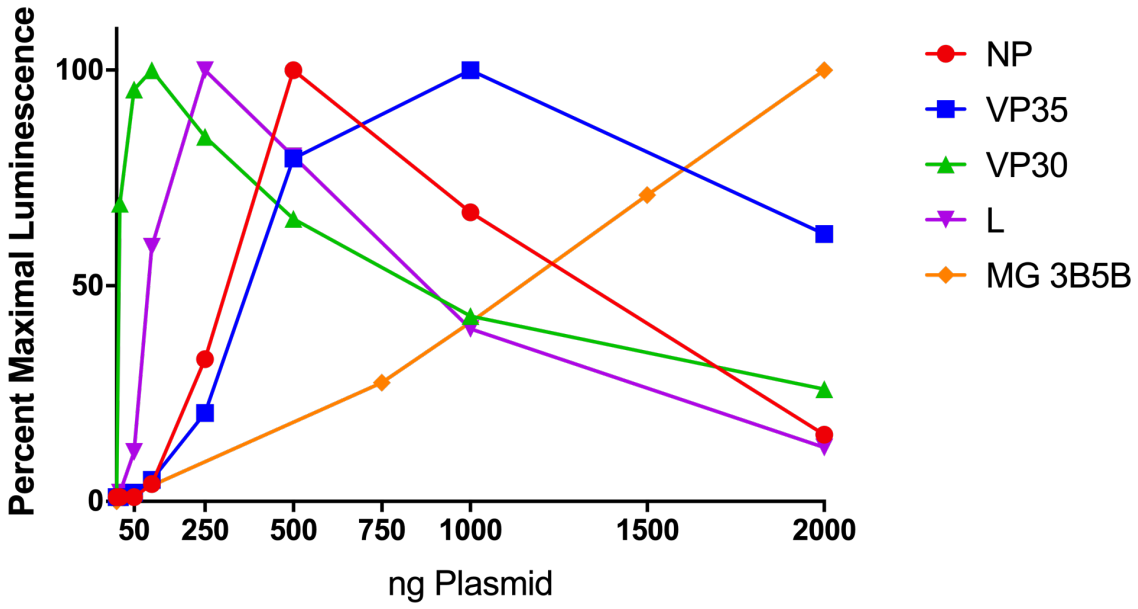

Figure 3.3 Titration of support plasmids and minigenome

BDBV support plasmids NP, VP35, VP30, and L were titrated from 0 ng to 2 µg. Each plasmid was titrated while the concentration of the other four plasmids remained constant. Plasmids that were kept constant were used at the following concentrations: NP 500 ng, VP35 1 µg, VP30 100 ng, L 500 ng, and minigenome 3B5B 2 µg. Each condition was tested in duplicate and is graphed as the mean percent maximal luminescence for each curve. Reproduced from Levine, et al 2021 with permission.[125]

Further testing was completed to define the optimal concentration of each plasmid in the full system using concentrations chosen based on the peak luciferase assay for each plasmid curve (Figure 3.3). Concentrations above and below these peaks were tested in combination to further refine the optimal amount of each plasmid needed for the system (Figure 3.4, not all combinations shown). Based on these titration experiments, the optimized BDBV minigenome system requires: 500 ng NP, 1000 ng VP35, 50 ng VP30, 250 ng L, and 2000 ng minigenome 3B5B.

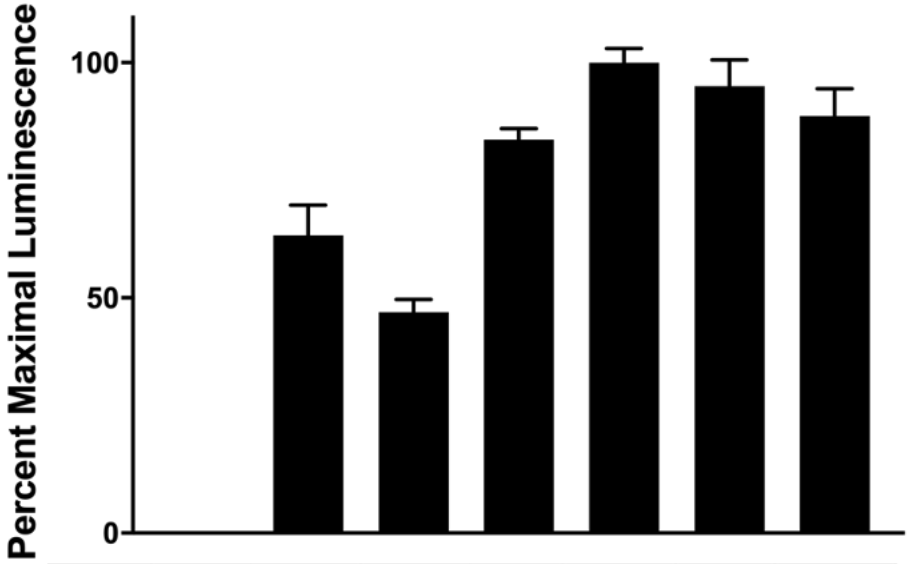

ng plasmid							
NP	500	500	500	500	500	500	500
VP35	1000	500	500	1000	1000	1000	1000
VP30	50	50	100	50	50	50	100
L	0	250	250	250	250	500	250
3B5B	2000	2000	1500	1500	2000	2000	2000

Figure 3.4 Comparison of a narrowed range of plasmid concentrations

A narrowed range of concentrations were tested to determine the optimal input of each support plasmid and the minigenome plasmid. The amount of each plasmid is shown in ng and the minigenome activity from each combination is shown as percent maximal luminescence. Each condition was tested in triplicated and is graphed as mean standard ± deviation. Reproduced from Levine, et al 2021 with permission.[125]

DISCUSSION

This chapter has described the design, creation, and optimization of a novel minigenome system for studying the polymerase complex of the ebolavirus BDBV. This system will aid in future studies aimed at understanding the mechanisms behind differences in pathogenicity between the various ebolavirus species. In addition, this system can be used as a tool to screen therapeutic candidates for inhibition of ebolavirus replication. The BDBV minigenome system described here showed similarity to the EBOV system. The four components of the polymerase complex NP, VP35, VP30, and L were all required for transcription of the minigenome reporter gene, luciferase. Removal of any single plasmid resulted in no detectable signal. It would be of interest to determine if VP30 is only necessary for transcription as is the case with EBOV and RESTV.[38,122]

The overall amount of each plasmid needed for transfection was variable between the EBOV and BDBV systems. Specifically, higher concentrations of VP35 and L were needed in the BDBV system compared to EBOV (2x and 2.5x, respectively) and half as much VP30 was needed. The changes in VP35 and L still maintain a relatively high ratio between these two as is the case for EBOV (5:1 for EBOV, 4:1 for BDBV). It should be noted that in the seminal paper describing the EBOV minigenome, a ratio of 4:1 was found to be optimal.[38] These interpretations should be analyzed with care, though, as transfection concentrations do not necessarily correlate with protein production. In addition, the EBOV minigenome system used here was based on published methods and was not further optimized outside of the previously published parameters. To better understand if there are differences in the concentrations of specific proteins needed for polymerase activity, western blotting or quantitative mass spectrometry should be completed to compare the

amount of protein present after transfection with each plasmid. This would inform whether there truly is a difference in the amount of each protein needed. If different amounts of polymerase complex proteins were needed for each optimized minigenome system, it would be of interest to compare these results to infection with authentic virus as this could point to reasons behind the observed differences in replication efficiency and pathogenicity of these two viruses.

The next two chapters will describe how this novel BDBV minigenome system was used to compare replication complex machinery with the prototypical ebolavirus EBOV (Chapter 4) and to test the inhibitory capacity of several small molecules (Chapter 5).

Chapter 4: Compatibility of the Viral Polymerase Complex Components Between *Bundibugyo* and *Zaire* ebolaviruses

INTRODUCTION

Although closely related, noticeable differences exist in the replication kinetics of EBOV and BDBV as shown in Chapter 2. Previous data suggests that the direct ability of these two viruses to evade the host immune response is not the reason for these differences (Versteeg, unpublished).[88] Instead, variation in the efficiency of the viral polymerase complex may be driving the difference in replication dynamics. To study this, a minigenome system which looks specifically at transcription and replication dynamics was developed for BDBV as described in Chapter 3. It is possible that the BDBV polymerase complex proteins do not carry out transcription and replication as efficiently as other ebolaviruses, specifically EBOV.

Previous research comparing the EBOV polymerase complex with that of RESTV support the idea of that a less efficient polymerase complex may lead to reduced pathogenicity in humans. Overall, sequence similarity between these viruses is 66% for EBOV and BDBV, and 63% for EBOV and RESTV. Similar to what is observed with BDBV, RESTV infection is slower and less abundant that EBOV.[122,126] When the polymerase complex is examined in isolation using a minigenome system, there is a diminished production of the reporter when using the RESTV polymerase complex compared to EBOV. This has been shown in two independent examinations using two different cell lines.[122,126] Further examination looking at the compatibility of the polymerase complex proteins between these two species found that all proteins could be

exchanged with the exception of a complex using EBOV VP35 and RESTV L.[122] Overall, it appeared that RESTV proteins were more likely to be accepted into the EBOV complex while the inverse nearly always resulted in a large decrease in activity. This could point to an increased flexibility in the EBOV polymerase complex to accept mutational changes in these proteins.

When looking across the filovirus genera the compatibility of polymerase complex proteins is much less. Between EBOV and MARV, only VP30 can be exchanged and still result in a functional polymerase complex.[38] This is interesting because VP30 is not an essential polymerase complex protein for MARV transcription like it is for EBOV. The interchangeability of VP30 extends to the third filovirus genus, cuevavirus, and the single member LLOV. LLOV can accept VP30 from RESTV, EBOV, and MARV although minigenome activity is much lower than with LLOV VP30.[120] Other proteins were not exchanged so it is unclear if the polymerase complex of LLOV can function using proteins from the other genera.

To further elucidate the effect of the polymerase complex proteins on replication efficiencies we set out to examine whether BDBV and EBOV polymerase complex proteins could be exchanged and still function to transcribe a minigenome. We hypothesized that the BDBV proteins would have a negative effect when added to the EBOV system and the EBOV proteins would have a positive effect when added to the BDBV system.

METHODS

Minigenome Plasmids

The EBOV minigenome system including the minigenome plasmid and four support plasmids (NP, VP35, VP30, and L) were a gift from Elke Muhlberger (Addgene plasmids #68121, 69119, 69120, 69121, 69358).[116] This system is based on EBOV strain Mayinga. The BDBV minigenome system was cloned an optimized as descripted in Chapter 3.

Transfection

BSR-T7/5 cells were plated in 6-well tissue culture treated plates at a density of 4 x 10^5 cells/well as per recommendations for the EBOV minigenome system.[101] When cells reached 70% confluency, they were transfected using Lipofectamine 3000 (Invitrogen), as per the manufacturer's protocol.

Luciferase Assay

Minigenome expression was quantified using the Dual-Luciferase Assay System (Promega). Forty-eight hours after transfection, media was removed, and cell monolayers were washed once with PBS. Cell lysis was completed using passive lysis buffer as per manufacturer's protocol and lysates were collected for downstream analysis. All conditions were tested in triplicate and standardized as relative luminescence units (RLU) calculated as a ratio of Firefly Luciferase to *Renilla* Luciferase.

Exchange of Plasmids

Support plasmids were exchanged between minigenome systems containing either the EBOV minigenome 3E5E or the BDBV minigenome 3B5B (Figure 3.2). When the minigenome 3E5E was used, the support plasmid concentrations matched that of the complete EBOV system: 500 ng NP, 500 ng VP35, 100 ng VP30, 100 ng L. When the minigenome 3B5B was used, the support plasmid concentrations matched that of the optimized BDBV system: 500 ng NP, 1000 ng VP35, 50 ng VP30, 250 ng L.

Exchange of Minigenomes

Minigenome encoded plasmids were exchanged between minigenome systems containing either all four EBOV support plasmids or all four BDBV support plasmids. Optimal plasmid concentrations were maintained for each species. Minigenomes with species-homologous UTRs as well as chimeric minigenomes containing a UTR from each species were compared. Details of chimeric minigenome construction are described in Chapter 3 and Figure 3.2.

Quantification and Statistical Analysis

All statistical analysis was performed using Prism (v. 9.1.2; GraphPad, San Diego, CA). For the exchange of polymerase complex proteins, each combination was compared to the complete, homologous system. For the comparison of heterologous and chimeric minigenomes, activity was compared to the homologous minigenome (3E5E for EBOV support plasmids, 3B5B for BDBV support plasmids). Analyses were completed using a t-test for comparison of homologous minigenomes, or a one-way ANOVA followed by

Dunnett's method adjusting alpha risk for multiple comparisons with an alpha level set at 0.05 for comparison of polymerase complex protein exchanges and chimeric minigenomes.

RESULTS

Exchange of Polymerase Complex Proteins

To determine if the proteins of the EBOV and BDBV polymerase complexes could interact, all combinations of polymerase complex proteins were examined for the ability to transcribe the minigenome 3B5B or 3E5E (Figure 4.1). VP30 was interchangeable between the systems and there was no significant difference in luciferase activity when this protein was exchanged (Figure 4.1: column #2 v. #5). This interchangeability of VP30 held true for all combinations of the polymerase complex, regardless of the origins of the other proteins (Figure 4.1: columns #3 v. #4, #8 v. #9, #10 v. #13, #12 v. #15, #14 v. #16).

The EBOV system was amenable to substitution of BDBV NP whereby addition of this protein significantly increased minigenome expression 2-fold (Figure 4.1A: column #2 v. #16). This increase in minigenome expression was also seen when both BDBV NP and VP30 were exchanged into the EBOV system (Figure 4.1A: column #14). In contrast, the presence of EBOV NP resulted in a significant decrease in minigenome expression to 27% of maximum when used in the BDBV system (Figure 4.1B: column #2 v. #16). In all instances when BDBV NP was present there was a greater amount of luciferase activity compared to when EBOV NP was used, regardless of the other proteins (Figure 4.1A). This held true for both 3E5E with the optimal concentrations for EBOV and 3B5B with the optimal concentrations for BDBV.

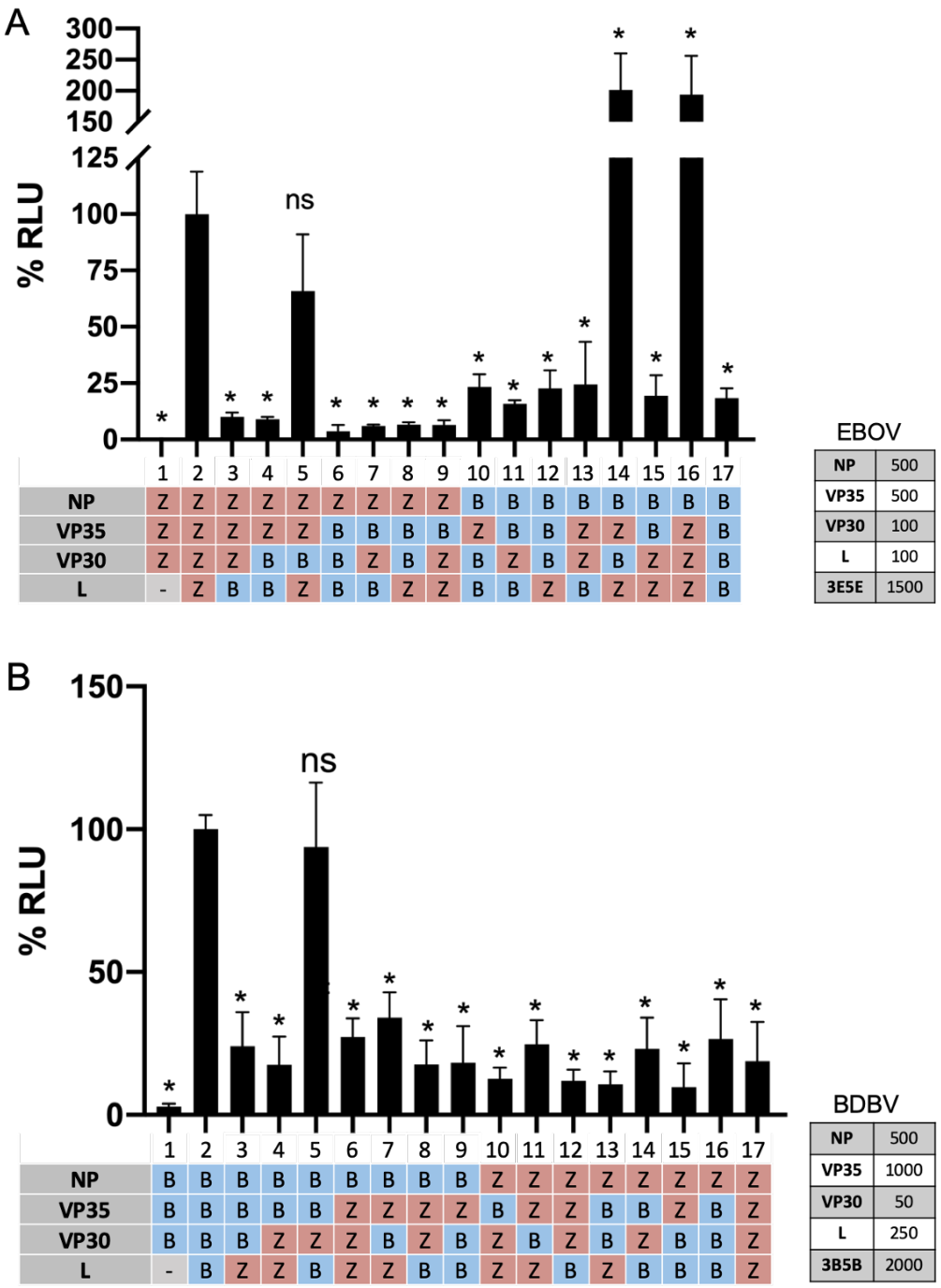

Figure 4.1 Exchange of polymerase complex proteins

Polymerase complex proteins were exchanged in the optimized EBOV (A) or BDBV (B) minigenome system. BDBV (B) and EBOV (Z) plasmids were exchanged at equal concentrations. The combination of plasmids used are shown on the x-axis. Each condition was tested in triplicate and results are shown as mean ± standard deviation. Results are expressed as perfect relative luminescence units (RLU) compared to column #2 which represents 100% activity. ns = non-significant, * $p < 0.0001$ when compared to column #2 by one-way ANOVA with Dunnett's post-hoc analysis. Reproduced from Levine, et al 2021 with permission.[125]

The polymerase unit consisting of EBOV VP35 and L transcribed and replicated the minigenome 3E5E most efficiently (Figure 4.1A: columns #2, #5, #14, #16). When either or both components were substituted by the BDBV protein, a significant reduction in minigenome activity was observed. The 3B5B minigenome, though, was most efficiently transcribed and replicated when the system contained NP, VP35, and L from BDBV (Figure 4.1B: columns #2 & #5). Although all combinations of the polymerase complex proteins had some functionality, most produced less than 40% activity compared to the complete systems, indicating that the compatibility between species is limited to specific proteins and their interactions with the rest of the polymerase complex.

Recognition of Related Minigenomes

Besides the efficiency of the polymerase complex, another mechanism for the observed differences in growth kinetics between EBOV and BDBV could be variations in the transcription and replication signaling components located in the 3'- and 5'- UTR. The ability of the EBOV polymerase complex to transcribe and replicate the minigenome containing the 3'- and 5'-UTRs from BDBV, and vice-versa, were tested. BSR-T7/5 cells were transfected with the complete polymerase complex of either BDBV or EBOV and the heterologous minigenome. Samples were collected 48h post-transfection and luciferase activity was measured. The EBOV polymerase complex was able to transcribe and replicate the minigenome 3B5B but there was a statistically significant decrease in minigenome expression compared to the 3E5E minigenome to 51% maximum activity (Figure 4.2A, $p = 0.0002$). The BDBV polymerase complex was able to transcribe and replicate the minigenome 3E5E but, similarly to EBOV, there was a statistically significant

decrease in minigenome expression compared to the 3B5B minigenome to 40% maximum activity (Figure 4.2B, $p < 0.0001$). These results are in contrast to what was observed when the polymerase complex proteins were exchanged which showed a decrease in minigenome activity to 25% or less compared to the complete system (Figure 4.1A,B column #17). This further emphasizes the need for an optimal ratio of the polymerase complex proteins. These results show that both the EBOV and BDBV polymerase complexes can recognize and transcribe a minigenome from another ebolavirus species, albeit to a lower efficiency.

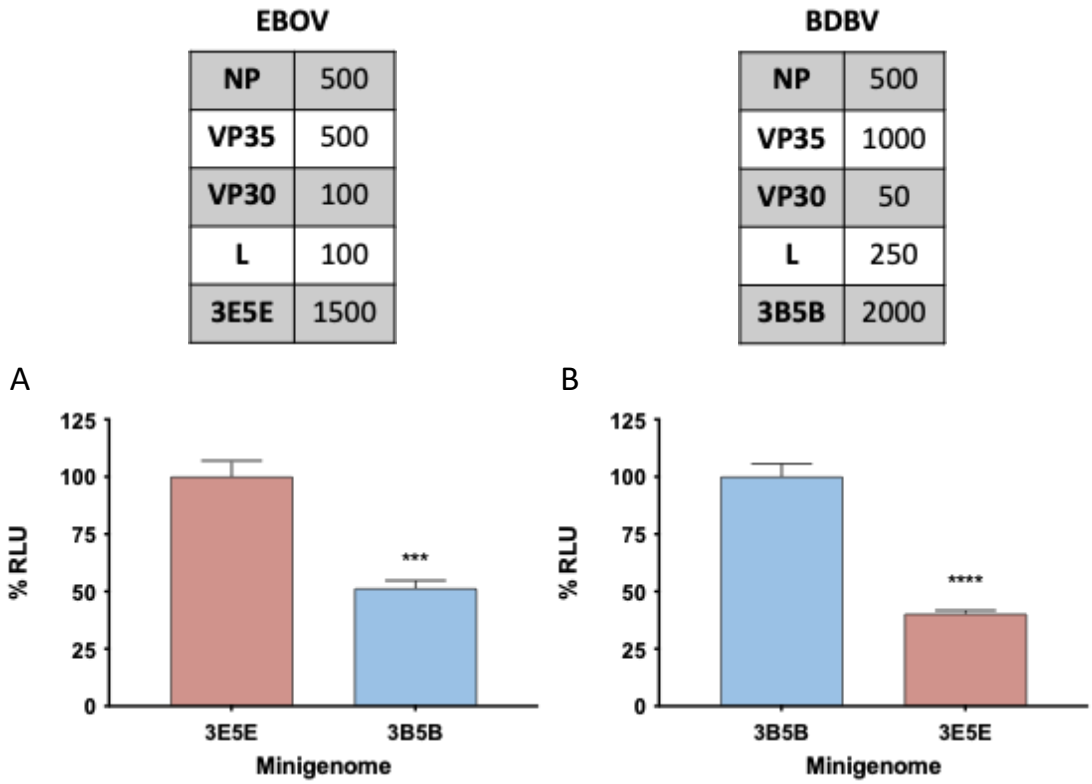

Figure 4.2 Transcription of related minigenomes

Minigenomes 3E5E (red) and 3B5B (blue) were used with the optimized concentrations of support plasmids for the EBOV (A) or BDBV (B) minigenome system. Comparisons were made using a t-test. Each condition was tested in triplicate and is graphed as mean ± standard deviation. Results are expressed as percent relative luminescence units (RLU) compared to the complete system with the homologous minigenome representing 100%. *** $p < 0.001$; **** $p < 0.0001$. Reproduced from Levine, et al 2021 with permission.[125]

Recognition of Chimeric Minigenomes

Based on the results examining replication and transcription of the heterologous minigenome it was of interest to test if the decrease in minigenome reporter activity was due to differences in either the 3'-UTR, the 5'-UTR, or both. The minigenome system allows for manipulation of the genomic ends to study the role of untranslated regions in transcription and replication. Chimeric minigenomes containing the 3'-leader of EBOV and the 5'-trailer of BDBV (3E5B) or the 3'-leader of BDBV and 5'-trailer of EBOV (3B5E) were used (Figure 3.2). The support plasmids were transfected with the optimized concentration for each system along with the minigenome under study. Luciferase activity was measured 48 h post-transfection and compared to the system containing plasmids from a single species.

The EBOV polymerase complex was able to recognize both the 3E5B and 3B5E chimeric minigenomes. The chimera containing the BDBV trailer 3E5B was recognized, but at a significantly reduced level of 54% maximal activity (Figure 4.3A, $p = 0.0002$). Interestingly, the chimera 3B5E, containing the BDBV leader, resulted in a significantly higher level of luciferase activity, 125% maximal activity (Figure 4.3A, $p = 0.0110$). The BDBV polymerase complex was also able to recognize both chimeric minigenomes, although expression was significantly lower than the homologous minigenome. The chimera 3B5E resulted in 77% maximal activity ($p = 0.0053$) and the 3E5B chimera resulted in 57% maximal activity ($p < 0.0001$) (Figure 4.3B). These results point to potential regulatory mechanisms within the leader and trailer regions that can influence genome transcription and replication that are distinct between EBOV and BDBV.

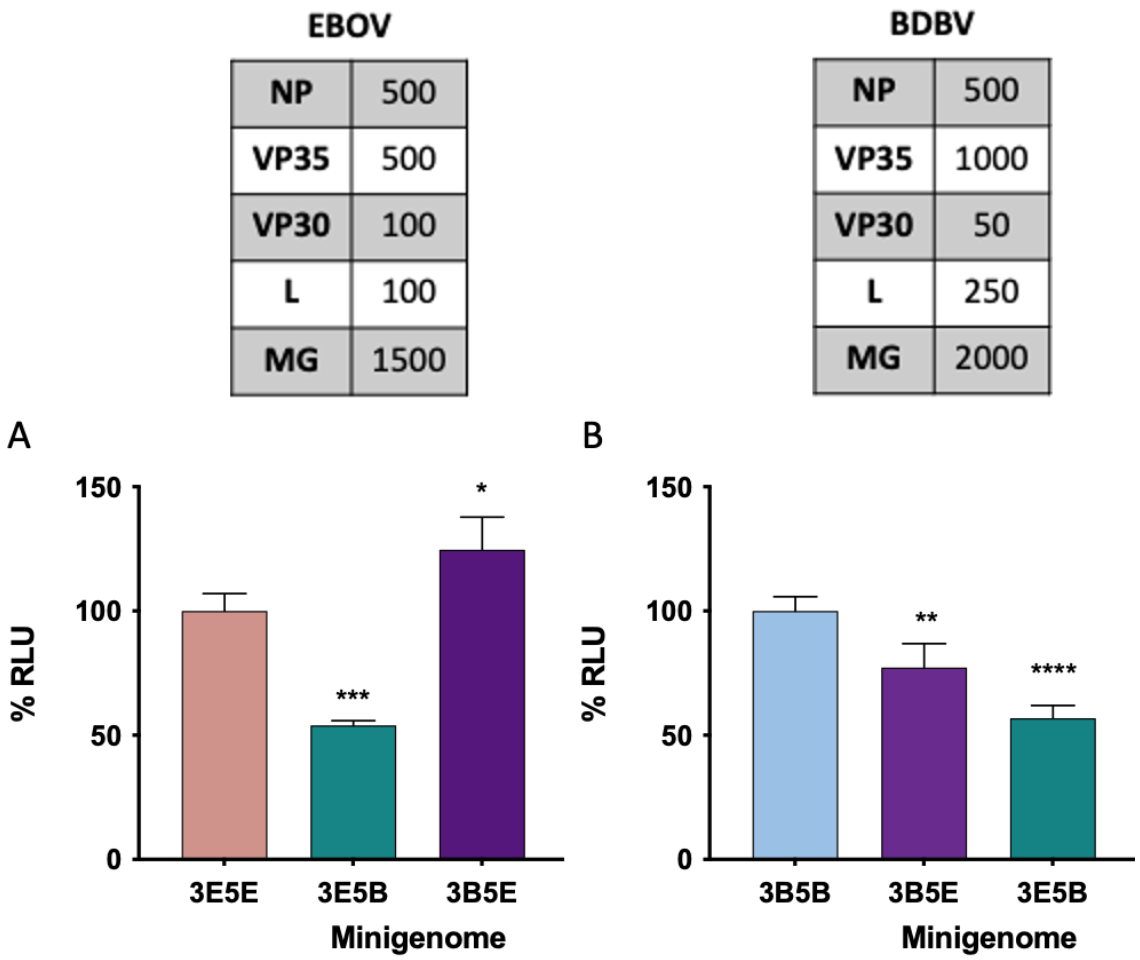

Figure 4.3 Recognition of chimeric minigenomes

Chimeric minigenomes 3E5B (green) and 3B5E (purple) were used with the optimized concentrations of polymerase complex proteins for either EBOV (A) or BDBV (B). Comparisons were made using a one-way ANOVA with Dunnett's post-hoc analysis. Each condition was tested in triplicate and graphed as mean ± standard deviation. Results are expressed as percent relative luminescence units (RLU) compared to the complete system with the homologous minigenome which represents 100%. * $p < 0.05$; ** $p < 0.01$; *** $p < 0.001$; **** $p < 0.0001$. MG = minigenome. Reproduced from Levine, et al 2021 with permission.[125]

Interaction of BDBV NP and Untranslated Regions

NP and the genomic UTRs had differential effects depending on which system they were used. Regardless of the origin of the other polymerase complex proteins, the presence of BDBV NP resulted in an increase in the amount of luciferase activity. The untranslated regions also had a significant effect on minigenome output, with directionality of this impact dependent on which species the other support plasmids came from. Since NP interacts directly with the viral RNA and acts as a 'gate-keeper' for polymerase activity we tested if there would be an interaction effect between these two components. Specifically, would the presence of BDBV NP modify minigenome transcription and replication differently based on the UTR. As expected, the same overall trends were observed for NP and the UTRs (Figure 4.4). That is, the use of BDBV NP increased minigenome activity regardless of the system used, and the impact of the UTRs was the same as observed in Figure 4.1. In the context of the EBOV system, the presence of BDBV NP increased the luciferase activity 2.0 - 2.8 times that of when EBOV NP was used (Figure 4.4A). For the BDBV system, BDBV NP resulted in an increase 1.9 - 6.5 times that of when EBOV NP was used (Figure 4.4B). In the EBOV system, as reported earlier, use of 3B5E resulted in a significant increase in minigenome activity whereas 3E5B and 3B5B resulted in a significant decrease in activity (Figure 4.4A). For the BDBV system, use of both chimeric minigenomes and the 3E5E minigenome resulted in a decrease in activity (Figure 4.4B). Interestingly, there appears to be a synergistic effect between NP and the UTRs, that is, the increase or decrease in minigenome activity cannot be explained by the additive effects of each component when used individually. This interaction is worth further examination in the context of full-length virus.

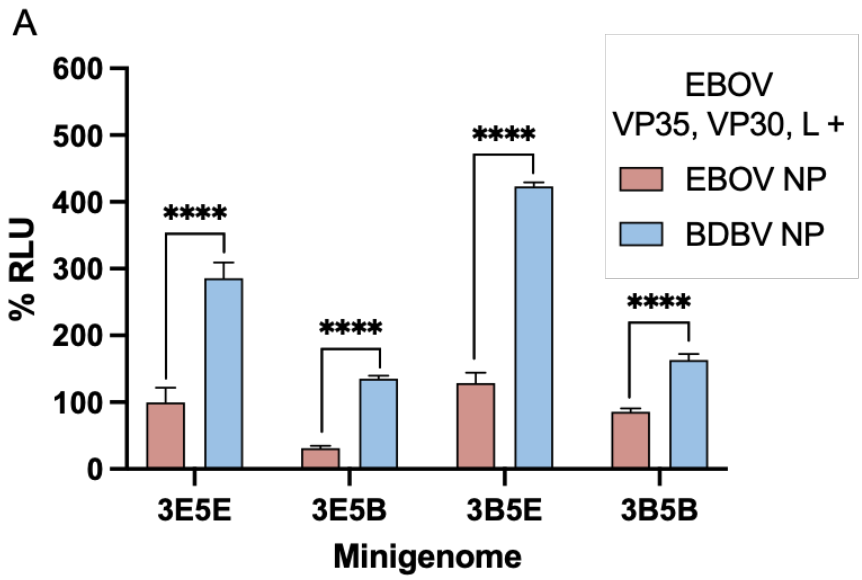

EBOV	
NP	500
VP35	500
VP30	100
L	100
MG	1500

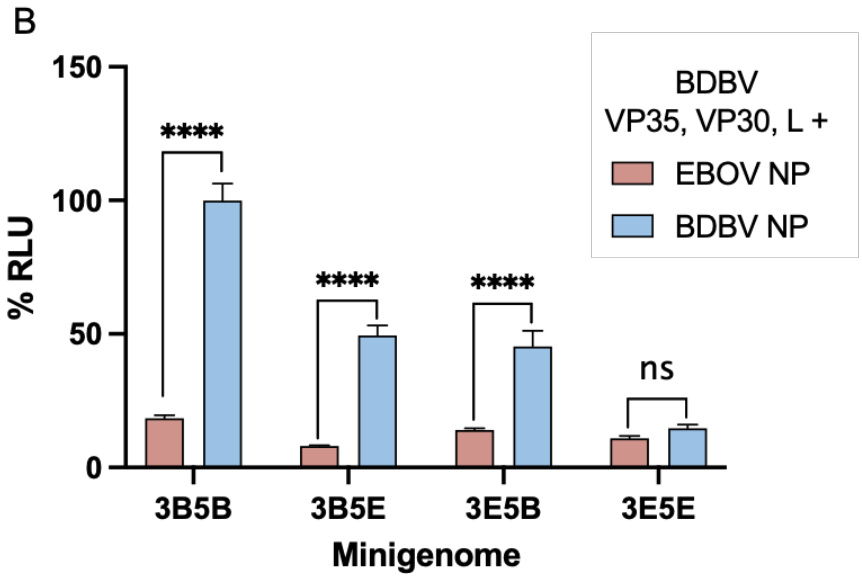

BDBV	
NP	500
VP35	1000
VP30	50
L	250
MG	2000

Figure 4.4 Interaction of NP and genomic leader and trailer regions

The polymerase complex protein NP was exchanged in combination with the homologous and chimeric minigenomes in the context of the (A) EBOV or (B) BDBV minigenome systems. All plasmids were used at the pre-determined optimal concentrations. A t-test was conducted for each minigenome construct and is graphed as mean ± standard deviation. ns = non-significant; **** $p < 0.0001$.

DISCUSSION

There are several possible reasons why viral species may grow differently under similar circumstances: variations in receptor binding affinity, ability to evade detection by immune sensors, or overall capacity to synthesize RNA. In the case of the ebolaviruses EBOV and BDBV, there does not appear to be any major differences in receptor binding or immune evasion mechanisms; however, there does appear to be a difference in replicative capacity. We sought to examine if the proteins that make up the polymerase complex and differences in the untranslated regulatory signals contribute to the overall efficiency of genome transcription and replication. Results from this study indicate that VP30 is interchangeable between the two species, BDBV NP is compatible with the rest of the EBOV polymerase complex, and that both complexes can recognize the leader and trailer regions from the other species.

VP30 has several functions that are key to viral growth including initiating read through at the RNA start/stop stem-loops and mediating the switch from transcription to replication. It is interesting that VP30 was interchangeable between EBOV and BDBV. While a similar effect was seen for the exchange of EBOV and RESTV VP30, the interchangeability was unidirectional: RESTV VP30 resulted in no significant change in the EBOV system, but EBOV VP30 decreased minigenome activity to about 50% in the RESTV system.[122] The VP30 C-terminal domain which interacts with NP is fairly conserved between EBOV and BDBV, while the VP30 binding domain on NP is less well-conserved between species.[48,127] Looking solely at luciferase production we can assume that VP30 from either species is capable of recognizing the RNA secondary structure in the 3'-UTR of both EBOV and BDBV and that VP30 from both species can functionally interact with NP and VP35 from the other species. Since the minigenome system uses luciferase production as a read-out it is difficult to tease apart differences in viral transcription versus replication. To determine if there are differences specifically in replication when VP30 is

exchanged, future experiments can quantify RNA species either by Northern blot, RT-qPCR, or RNA-sequencing.

While VP30 was interchangeable between species, the NP proteins had very specific effects. BDBV NP showed a significant benefit in transcriptional efficiency when used in the EBOV polymerase complex and the use of EBOV NP was detrimental to the transcriptional activity of the BDBV polymerase complex. NP is a central component in viral RNA synthesis as it interacts with the RNA, VP35, and VP30. Any variations between these binding sites (NP-RNA, NP-VP35, or NP-VP30) could have a substantial effect on polymerase activity. Since VP30 was determined to be interchangeable between the two minigenome systems regardless of the origin of the NP plasmid, it is unlikely that the NP-VP30 interaction played a role in the enhanced minigenome activity. There are no differences in the RNA binding site of NP between EBOV and BDBV, although more distant residues could affect this interaction. Therefore, it is plausible that the NP-VP35 interaction is different between EBOV and BDBV and that this interaction resulted in the observed changes in minigenome activity.

The interaction of NP with viral RNA appears to be highly regulated by the interaction of NP with VP35. Specifically, binding of NP to the NPBP of VP35 inhibits NP from binding to RNA.[39,40] This inhibition has an indirect effect in which NPBP bound NP is prevented from oligomerizing and binding RNA.[40] The N- and C-terminal residues (amino acids 20 - 38 and 356 - 381, respectively) involved in NP oligomerization are 100% identical between EBOV and BDBV suggesting both species oligomerize in a similar fashion.[40] The NPBP, however, does show variation between EBOV and BDBV which could result in different binding affinities to NP. It is suggested that there is a yet to be defined process which results in the dissociation of NP from VP35 so that it can oligomerize and associate with viral RNA.[40] Different binding affinities between NP and the NPBP of VP35 could yield a faster/slower dissociation time resulting in changes in polymerase activity. A comparison of binding and minigenome activity in the context of

EBOV shows that mutations resulting in a lower K_D (higher affinity) result in an increase in minigenome activity.[40] Taking this into consideration, a hypothesis that can be drawn from the results in this chapter is that BDBV NP has a high binding affinity to the NPBP of EBOV VP35. This could result in NP persisting in VP35 bound state leaving the RNA accessible for the viral polymerase L and increasing RNA synthesis.

In addition to the polymerase complex proteins, there are several regulatory domains within the untranslated leader and trailer portions of the ebolavirus genomes. As would be expected, both polymerase complexes were able to recognize and transcribe the minigenome from a related ebolavirus species as has been reported for RESTV and EBOV.[122] The RESTV polymerase complex had a reduction to 20% activity when the minigenome 3E5E was used.[122] This result is similar to the findings here where there was a reduction to 40% activity when the 3E5E minigenome was used as a template for the BDBV polymerase complex. In the case of the EBOV polymerase complex, the minigenome 3R5R was transcribed as efficiently as the species homologous minigenome 3E5E.[122] This result is in contrast to what was observed here: there was a 50% reduction in activity when the 3B5B minigenome was used as a template for the EBOV polymerase complex. This result could indicate that either the EBOV polymerase complex was unable to recognize the BDBV leader region as efficiently or there is a signal in the BDBV UTRs resulting in an abatement of transcription and/or replication.

When examining the influence of the leader and trailer regions individually using chimeric minigenomes, there was a clear difference in compatibility for each species. These experiments indicated that the presence of the BDBV 3'-UTR rather than the EBOV 3'-UTR resulted in enhanced transcription by both polymerase complexes. There are several 3'-UTR sequences and structures that are critical for genome transcription (Figure 4.5).[128] The first region is the leading 3 - 4 nucleotides which are unique for each filovirus genera (GCCU for ebolaviruses, UCU for MARV).[120] Neither EBOV nor MARV can recognize the sequence from the other genus.[120] Interestingly, the bat filovirus LLOV is

able to recognize a minigenome containing the leading nucleotides from EBOV but not from MARV.[120] The first 17 nucleotides are identical between EBOV and BDBV and so this region is not expected to play a role in the enhancement of activity seen when the BDBV 3'-UTR was used (Figure 4.5).

The next region that plays a role in transcription initiation is the formation of two RNA hairpin structures. The first hairpin is made up of the first 45 nucleotides and the second, containing the NP gene start signal, is made up of nucleotides 56 - 78 (Figure 4.5). The second hairpin is necessary for VP30 dependent transcription.[106,110] There are several nucleotides which are different between EBOV and BDBV in these two structures, but the majority of these occur within the loops and are unlikely to result in any changes to the hairpin structures. In addition, the NP gene start signal is identical across all known ebolaviruses and varies by one nucleotide from MARV and LLOV.[120]

The final transcriptional signaling element is a series of UN_5 hexamers located just downstream of the NP gene start signal with the first repeat at nucleotide 81-86 (Figure 4.5). Previous work determined that a minimum of three adjacent UN_5 repeats were necessary for efficient transcription and replication and that the presence of more UN_5 hexamers may lead to increased transcription and replication.[106] Whether or not more UN_5 repeats is beneficial is still to be determined. Results from the experiments shown here as well as previous published data suggest that 5 UN_5 repeats appears to result in minigenome activity greater than that of the wildtype EBOV control with eight hexamers.[106] Although other data contrasts this showing that extension of the UN_5 repeats into the preceding hairpin results in increased activity.[129] All of these studies were completed using minigenome systems and so whether or not the number of hexamer repeats will affect full-length viral replication would need to be examined.

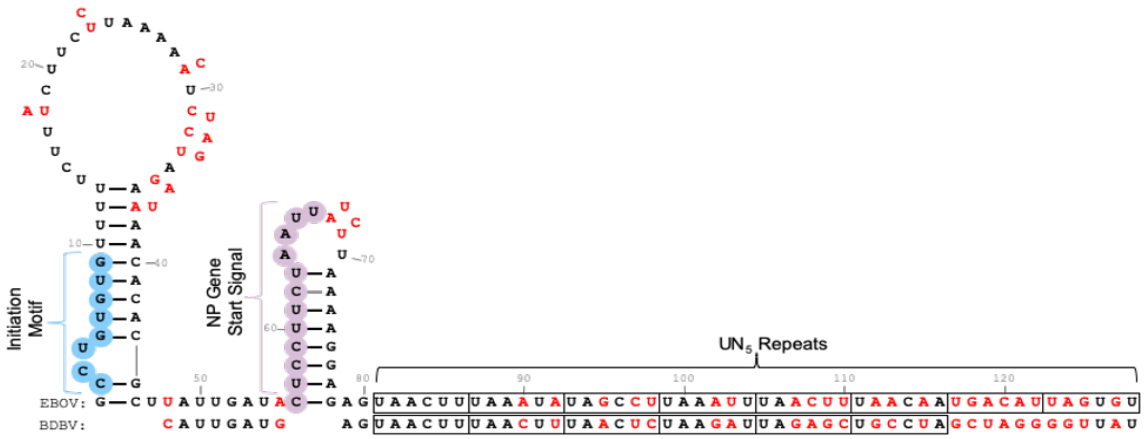

Figure 4.5 EBOV and BDBV 3'-UTR leader

Alignment of the first 128 nucleotides of EBOV and BDBV which contains the transcription signal sequences including the initiation motif (blue), NP gene start signal (purple), and UN_5 promoter repeats (boxed). Nucleotides which are different between species are marked in red. The BDBV nucleotides which differ in the hairpin structure are annotated to the outside of the structure. Image created by Corri B. Levine using VARNA v. 3.9.[128] Reproduced from Levine, et al 2021 with permission.[125]

Another mechanism for the overall reduction in viral replication seen for BDBV compared to EBOV could be due to differences in the 5'-UTR, or trailer region. The minigenomes containing the BDBV 5'-UTR (3B5B and 3E5B) had the greatest reduction in minigenome activity when the EBOV polymerase complex was used (50% maximal activity). Whether this is due to an incompatibility of the EBOV polymerase complex with this region or the presence/absence of an important signaling sequence remains to be determined. It is possible that a positive regulatory signal is lacking in the BDBV trailer resulting in a diminished replicative capacity. The trailer region plays a role in viral genome replication and is quite variable between these two species (Figure 4.6). RNA secondary structure predictions indicate an intricate folding pattern in the EBOV trailer.[130] It is unclear if these RNA structures specifically direct genome replication but based on the vast difference between EBOV and BDBV trailer sequences, it is expected that the folding patterns would be different between the two species. In addition, it is predicted that the trailer region could form a panhandle with the genomic leader region during replication. If this were the case, the structure beyond the first 15 nucleotides would likely be different between EBOV and BDBV due to mismatches introduced in the BDBV genome, both in the leader and trailer regions.

Finally, variations in the trailer region could influence interactions with host cell proteins that are necessary for genome replication. In the EBOV trailer, three 5'-AUUUA-3' motifs have been identified as binding sites for the heat-shock cognate protein family A member 8 (HSPA8).[114] The BDBV trailer contains four AUUUA motifs compared to the three of EBOV, but it is unknown if these motifs are accessible to binding by HSPA8. Characterization of the HSPA8 motif 1 showed that an A→U substitution at the 3' end of this motif resulted in a significant decrease in EBOV minigenome activity.[114] Interestingly, the BDBV sequence corresponding to the EBOV HSP8A motif 1 is off-set by one nucleotide, and contains the A→U nucleotide substitution shown to result in diminished minigenome activity (Figure 4.6). The role of this sequence in BDBV replication can be

studied by introducing a complete motif of AUUUA in the BDBV trailer at nucleotides 18,912 – 18,916 and measuring minigenome activity and viral growth kinetics.

Overall, the data shown in this chapter indicate that there are several compatibilities between the EBOV and BDBV polymerase complexes and untranslated regions, as well as several incompatibilities. We had hypothesized that the BDBV polymerase complex proteins would have a negative effect when used with the EBOV system. This was observed for VP35 and L, but surprisingly an enhancement in activity was seen when BDBV NP was used. In addition, we hypothesized that the EBOV polymerase complex proteins would enhance the BDBV system, but instead we found that NP, VP35, and L from EBOV all decreased the function of the BDBV polymerase complex. Also contrary to our predictions, inclusion of the BDBV leader with the EBOV trailer resulted in increased minigenome production within the EBOV system, while both EBOV UTRs resulted in decreased production in the BDBV system. A better understanding of the features which are unique to BDBV and result in a diminished replicative capacity will inform new therapeutic targets. For example, if the A→U substitution in the HSPA8 motif 1 in the BDBV trailer limits replication, then a drug candidate which blocks these interactions may prevent uncontrolled replication of EBOV. A similar targeted approach could be used to disrupt the interaction of NP and VP35 which appears to have a great effect on the transcriptional and replicative capacities. Future studies should focus on examining the impact of these binding sites and regulatory motifs in context of full-length virus.

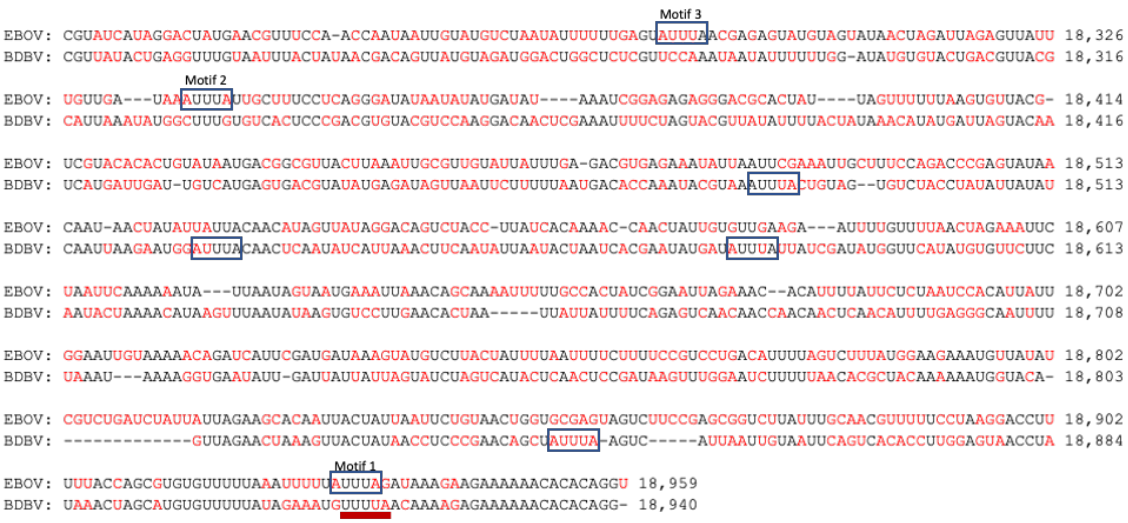

Figure 4.6 Alignment of EBOV and BDBV 5'-UTR trailer

Alignment of the untranslated trailer region of EBOV and BDBV beginning after the L gene stop signal. Nucleotides which are different between species are marked in red. Presumptive HSPA8 motifs are boxed and motifs 1, 2, and 3 are labeled. Underlined sequence shows possible BDBV HSPA8 motif 1 with A→U substitution. Reproduced from Levine, et al 2021 with permission.[125]

Chapter 5: *In Vitro* Efficacy of Small Molecule Inhibitors Against *Bundibugyo* and *Zaire* ebolaviruses

INTRODUCTION

Antiviral therapies have long been sought after as a means of reducing the global burden of viral disease; unfortunately, the concept is simpler than the reality. Antiviral therapies are typically targeted to specific activities involved in viral replication, but many of these activities are carried out by or mimic normal cellular processes. Antiviral drugs can be helicase inhibitors, polymerase inhibitors such as nucleoside analogs, pump inhibitors, and inhibitors of other enzymatic processes.[131] The rapid speed of viral replication also provides an opportunity for select mutations to become dominant, which may result in resistance to the antiviral therapy.[132] To date, the majority of anti-viral therapies are used to combat DNA viruses (herpes simplex, hepatitis B virus, cytomegalovirus) and retroviruses (HIV) as these have a high global burden of disease. Antivirals for RNA virus have been more elusive, but a few are available, mostly for common and widespread infections such as influenza, respiratory syncytial virus, hepatitis C, HIV, and coronaviruses.[131,133-135]

Clinical efforts to find an antiviral small molecule inhibitor for the treatment of high-consequence pathogens such as ebolaviruses has typically been limited to small trials of under 100 subjects, with only a few trials enrolling between 400-600 subjects.[136-140] Because of the highly infectious nature of the disease and the limited number of cases and outbreaks the majority of testing occurs in *in vitro* and *in vivo* models. Thorough pre-clinical testing is necessary so that the top candidates can be at the ready for when cases

emerge, and outbreaks occur. These candidates can move forward as clinical therapeutics through the FDA Animal Rule (21 CFR 314.600-650) in which pre-clinical *in vivo* testing is used to demonstrate efficacy when field trials are not possible or ethical.

Recent work screening libraries of small-molecule inhibitors, some of which include FDA-approved compounds, have provided numerous candidates for anti-EBOV therapy.[121,141-147] As outbreaks of BDBV and EBOV overlap geographically, it is important that the utility of these candidates for treatment of both viruses be examined. Therefore, we selected five candidate molecules from the literature for testing against EBOV and BDBV replication: remdesivir (GS-5734), tenofovir, zidovudine (AZT), cidofovir, and tolcapone. These candidate molecules were selected based on previous reports of anti-EBOV activity and whether the compound had a 50% inhibitory concentration (IC_{50}) that would be biologically relevant based on pharmacokinetic studies. That is, the concentration necessary to inhibit viral replication by 50% must be achievable *in vivo*. Only one of these molecules has been tested in the context of BDBV infection and it was of interest to determine if an effect similar to that seen against EBOV would be observed for the other candidates.

The first candidate, remdesivir, is an adenosine nucleoside analog and has been tested specifically in the treatment of EVD. It selectively inhibits RdRp activity through a mechanism of delayed chain termination.[148,149] In macrophages and liver cells, the IC_{50} against EBOV was 86 nM and 70 nM, respectively.[146,150] Twelve-day treatments by intravenous administration conferred protection when treatment was initiated within three days of infection in a rhesus macaque model of EVD.[149] Safety testing in humans has been shown in the context of both EVD and hospitalized cases of coronavirus disease 2019

(COVID-19).[135,136,151] The major safety concern is in the context of renal impairment, but for Ebola disease the potential benefit of treatment often outweighs the risks. A clinical trial of remdesivir for EVD was carried out in the DRC during a 2018 outbreak and showed a survival benefit similar to that of the antibody therapy ZMapp.[136]

Tenofovir and zidovudine are nucleoside analogs of adenosine and thymidine, respectively, and are FDA approved for the treatment of HIV. These two drugs have been tested using EBOV transcription- and replication-competent VLP (trVLP) systems, which consist of plasmids encoding all of the viral genes along with a minigenome containing a reporter. A combination treatment of tenofovir, zidovudine, and lamivudine significantly reduced luciferase activity from transfected cells, even when administered 24 hours after transfection. Inhibition was also achieved when the drugs were used individually with an IC_{50} = 0.981 μM for tenofovir and IC_{50} = 4.197 μM for zidovudine. When the IC_{50} for each compound was added 24 hours after transfection, the number of copies of both negative-sense and positive-sense RNA, as determined by RT-qPCR, was significantly reduced compared to control.[143] These two drugs, however, have not been tested in the context of a live virus nor have they been tested against BDBV.

Cidofovir is a nucleoside analog of cytidine with FDA approval for the treatment of cytomegalovirus retinitis. It has shown *in vitro* efficacy against other DNA viruses including herpesviruses, adenovirus, and poxvirus, but limited testing has been completed against RNA viruses.[152] *In silico* binding studies indicate that cidofovir is capable of binding in the 2'-O-Methyltransferase domain of EBOV L.[142] *In vitro* analysis shows that cidofovir can inhibit VLP formation in a trVLP system when added up to 24 hours post-transfection.[143] In this system, the IC_{50} was determined to be 7.760 μM with no cytotoxic

activity at this concentration. An orally bioavailable version of cidofovir, Brincidofovir, was tested in four patients with EVD in 2015 but due to the limited number of subjects no conclusive results on efficacy could be determined.[153]

Tolcapone is a catechol-O-methyltransferase inhibitor that is prescribed for the treatment of Parkinson's disease.[154] It has a relatively short half-life and is reversible so the risks of long-term off-target effects are low. Tolcapone was identified to inhibit the interaction between EBOV NP and VP35.[144] This interaction is crucial for EBOV replication and transcription, which cannot occur if these two proteins are blocked from interacting. Tolcapone was found to competitively inhibit the binding of the NPBP on EBOV VP35 to the N-terminal domain of EBOV NP in a dose-dependent manner, but it is unknown if the same binding affinity will occur with other ebolaviruses.[144] Tolcapone was also tested against a recombinant EBOV expressing GFP, and, at a concentration of 10 μM, it significantly inhibited viral replication using an MOI of 0.01 and 2.[144]

This chapter details screening of the five drug candidates using the minigenome systems discussed in Chapter 3 and further testing of the most promising candidate, remdesivir, in BSL-4 against authentic BDBV and EBOV. The experiments here specifically test the utility of a delayed treatment, whereas previous studies have looked primarily at pre-treatment. We hypothesized that the selected small-molecule compounds would have a similar or greater effect against BDBV compared to EBOV in the context of both the minigenome and viral infection because of the delayed growth kinetics of BDBV.

METHODS

Small Molecule Inhibitors

Zidovudine, tenofovir, cidofovir, and tolcapone were manufactured by Selleck Chemicals. Remdesivir was manufactured by MedChem Express. All compounds were reconstituted in dimethyl sulfoxide (DMSO) except for cidofovir which was reconstituted in sterile water, per manufacturer's instructions. Compounds were diluted to the desired concentration in complete medium prior to treatment. A vehicle control (VC) treatment of either DMSO (remdesivir, zidovudine, tenofovir, and tolcapone) or water (cidofovir) was used in every experiment.

Cell Culture

BSR-T7/5 cells were used for minigenome experiments and were maintained in cDMEM (with the addition of the geneticin every other passage to maintain selection of the T7 polymerase. For transfection experiments, cells were plated in 6-well tissue culture treated plates at a density of 4×10^5 cells/well.

The HepG2 liver-derived cell line was used for viral infection assays. HepG2 cells were maintained in complete cEMEM in T-150 flasks at 37°C in 5% CO_2. For experiments, cells were plated on 24-well plates at a density of 5×10^5 cells per well. Once a confluent monolayer was reached, cells were transferred into the BSL-4 for inoculation.

Vero E6 cells were used for titering of all samples. Cells were maintained in cEMEM in T-150 flasks at 37°C in 5% CO_2. Once a confluent monolayer was reached, cells were transferred into the BSL-4 for titrations.

Virus Isolates

A laboratory seed stock of *Zaire ebolavirus* strain Mayinga was grown from the serum of a fatal human case in 1976 in the Democratic Republic of the Congo (Zaire ebolavirus/H.sapiens-tc/COD/1976/Yambuku-Mayinga, accession number NC_002549) and passaged twice in authenticated Vero E6 cells.[90,91] This strain was used to best translate results from the minigenome experiments as the EBOV minigenome system was built using the EBOV strain Mayinga sequence.

A laboratory seed stock of *Bundibugyo ebolavirus* was grown from the serum of a 2007 fatal human case in Uganda (Bundibugyo virus/H. Sapiens-tc-UGA/2007/Bundibugyo-200706291, accession number KU182911) and passaged twice in authenticated Vero E6 cells.[28,76,92]

Toxicity Testing

Metabolic activity was assessed in both BSR-T7/5 cells and HepG2 cells to determine cytotoxicity of remdesivir. For both cell lines, 5 x 10^4 cells were plated per well in a 96-well plate. A 2-fold dilution series from 100 μM to 0.4 μM was added to wells 24 h after plating. An MTT cell proliferation assay (Promega) was carried out 48 h after treatment for BSR-T7/5 cells and 120 h after treatment for HepG2 cells, to match incubation times from the minigenome and full-length virus inhibition assays. DMSO was used as a VC and set to represent 100% viability.

Drug Treatment using Minigenome

Minigenome assays were carried out as described in Chapter 3. Briefly, 6-well plates were seeded with BSR-T7/5 cells and transfected with plasmids encoding the NP, VP35, VP30, and L proteins of either EBOV or BDBV and the corresponding minigenome construct. As a negative control, one set of wells was transfected without the L plasmid. Compounds were tested using a 2-fold dilution series from 0.4 μM - 100 μM. Media only and VC wells were used for each compound tested with the VC well representing 0% inhibition. Compounds were added to wells either 1-, 12-, or 24-hours post-transfection (hpt). Samples from all conditions were collected in passive lysis buffer 48 hpt for analysis by luciferase assay as described in Chapter 3.

Drug Treatment using Live Virus

HepG2 cells were plated as described in Chapter 2 and transferred to the BSL-4 for infection. A multiplicity of infection (MOI) of 0.1 was used for measuring growth kinetics in the presence of remdesivir. This MOI was chosen to ensure multiple rounds of infection as would be observed *in vivo*. To inoculate, media was removed from all wells and 150 μL of inoculum in serum free media was added to each well. Plates were incubated at 37°C in 5% CO_2 for 1 h with gentle rocking every 15 m. After 1 h, wells were washed five times with PBS to ensure removal of unattached virions. After the final wash, 500 μL complete media with the appropriate concentration of remdesivir was added. To determine the 90% inhibitory concentration (IC_{90}), remdesivir was diluted 2-fold using a range of 0.98nm - 1 μM. To measure viral growth in the context of a single treatment, supernatant was collected at the final timepoint of 120 hpi. To measure growth kinetics in the context of continuous

treatment, 100 μL supernatant was removed at 1, 24, 48, 72, 96, and 120 hpi and replaced with a 5X solution of fresh drug to maintain the desired concentration.

RESULTS

Toxicity Testing

Toxicity testing was completed to determine any cytotoxic effects remdesivir may have in the cell types tested (BSR-T7/5 and HepG2). To match experiments measuring inhibition of the minigenome system or authentic virus, a single dose was added to each well 24 h after plating. An MTT assay which measures cellular metabolic activity was carried out 48 h after treatment for the BSR-T7/5 cells and 120 h after treatment for the HepG2 cells. In the BSR-T7/5 cells, a reduction in metabolic activity to 88% of VC was only observed at the highest concentration of 100 μM (Figure 5.1A). For the HepG2 cells, there was a reduction in metabolic activity when remdesivir concentrations were greater than 3.13 μM, with a reduction in metabolic activity to 70%, 56%, and 40% of VC for 12.5 μM, 25 μM, and 50 μM, respectively (Figure 5.1B).

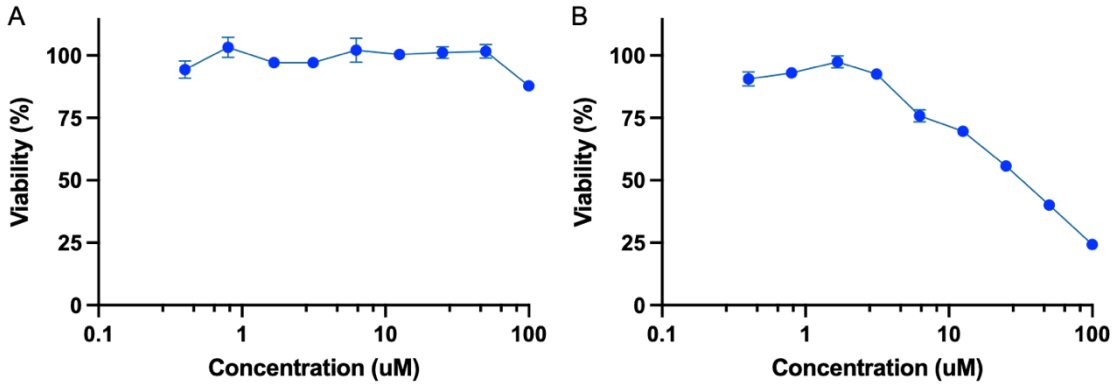

Figure 5.1 Cell viability with remdesivir treatment

Cell viability was determined by measuring metabolic activity in (A) BSR-T7/5 cells after 48 h and (B) HepG2 cells after 120 h. DMSO was used as VC and set to represent 100% viability.

Inhibitory Effects of Select Small Molecules on Minigenome Activity

The purpose of the following studies was to specifically test the effects of post-transfection treatment and determine if delayed treatment would still have an inhibitory effect on minigenome transcription and replication. Using the EBOV and BDBV minigenomes described in Chapter 3, zidovudine (AZT), tenofovir, cidofovir, tolcapone, and remdesivir were tested for the ability to inhibit polymerase complex activity. An upper concentration limit of 100 μM was chosen, and serial 2-fold dilutions were used to generate an inhibition curve. Three timepoints were chosen for the initiation of treatment in the minigenome system: 1, 12, and 24 hpt. These timepoints were chosen to gauge inhibition of first round transcription (1 hpt), early transcription (12 hpt), and late transcription and replication (24 hpt). Zidovudine, tenofovir, cidofovir, and tolcapone all showed no inhibitory effect on minigenome activity regardless of the concentration used or the timing of treatment when compared to vehicle control (Figure 5.2A-L).

Interestingly, there was a spike in measured luciferase activity at the lowest concentrations of zidovudine and tenofovir and across all concentrations for tolcapone. This was not seen with cidofovir. Zidovudine, tenofovir, and tolcapone were solubilized in DMSO whereas cidofovir was solubilized in water. It is possible that the DMSO VC had a cytotoxic effect resulting in the appearance of increased activity for the lower doses that don't contain as much DMSO. The final concentration of DMSO for the VC wells was 1% for zidovudine and tenofovir and 2% for tolcapone.

Remdesivir was the one compound which showed both a time and concentration dependent inhibitory effect on minigenome activity for both EBOV and BDBV (Figure 5.2M-O). The effect of remdesivir when initiated at a later timepoint post-transfection

showed that the BDBV minigenome system was more susceptible than EBOV. Inhibition curves were uniform between species when treatment was administered 1 hpt (Figure 5.2M). When treatment was delayed to 12 hpt (Figure 5.2N) and 24 hpt (Figure 5.2O), a clear separation of the inhibition curves could be seen between species, especially in context of 24 hpt delayed treatment. Remdesivir was just as effective at inhibiting BDBV minigenome activity when treatment was delayed while only higher concentrations inhibited EBOV minigenome activity. As with some of the other compounds tested, there appeared to be an increase in minigenome activity when lower concentrations were used, and the final concentration of DMSO for the VC well was 2%. Interestingly, with the 12 and 24 hpt treatments, this spike in activity with low concentrations was only observed for the EBOV minigenome system and all concentrations had at least some inhibitory effect on the BDBV minigenome system. Based on these results it was decided to test the efficacy of a delayed treatment with remdesivir in the context of viral infection.

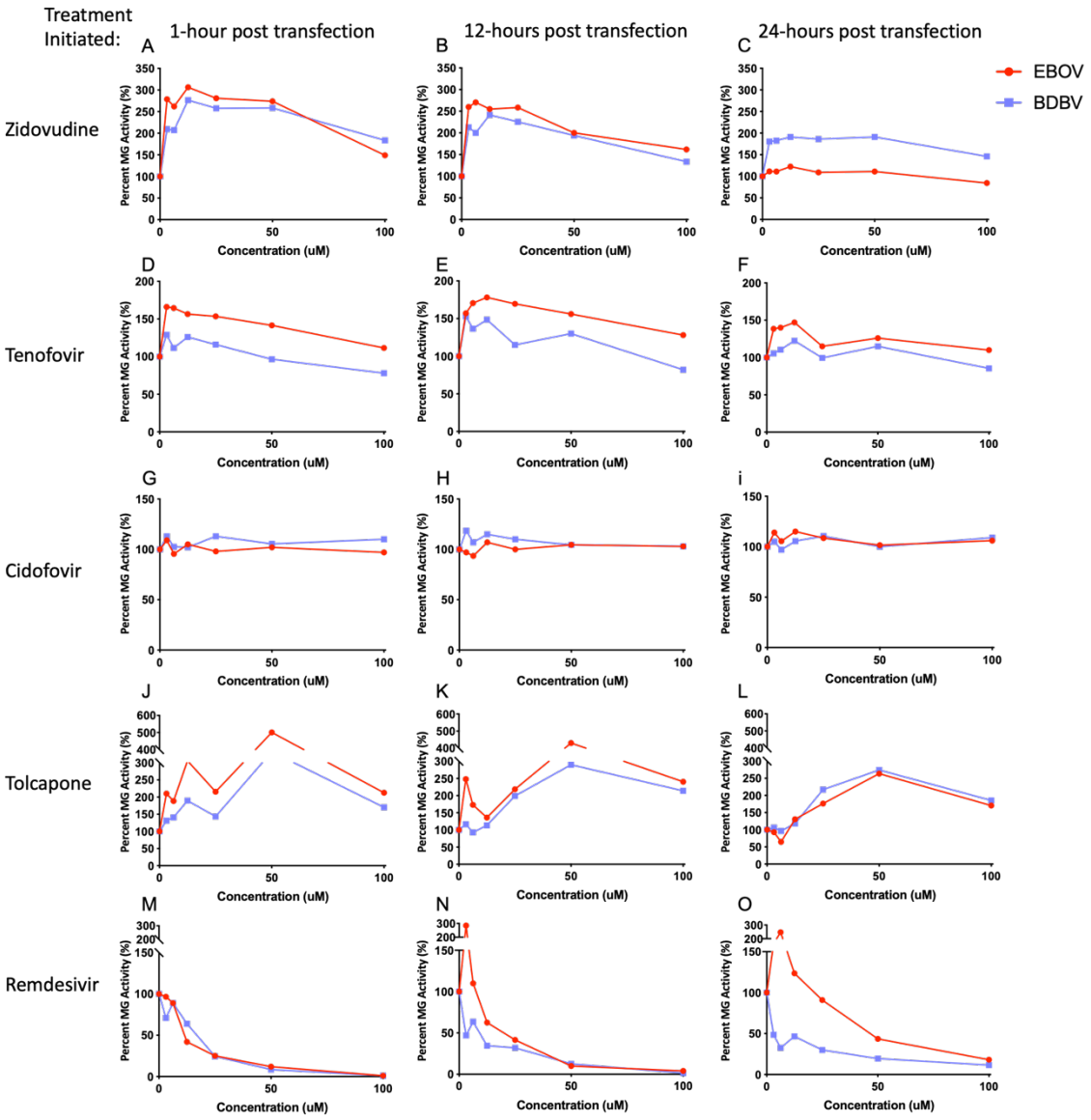

Figure 5.2 Small molecule inhibition of EBOV and BDBV minigenome systems

Minigenome activity for EBOV (red) and BDBV (blue) was assessed after treatment with small molecule inhibitors zidovudine (A-C), tenofovir (D-F), cidofovir (G-I), tolcapone (J-L), and remdesivir (M-O). Compounds were added either 1-, 12-, or 24-hours post-transfection and luciferase activity was measured 48 h post-transfection. A vehicle only control was set to represent 100% minigenome activity.

Single Treatment Effect on Viral Replication

It was of interest to compare the results in the minigenome system in the context of viral infection to determine if the minigenome system offers an approximation of *in vitro* effectivity. To do so, three concentrations which showed a range of inhibition in both minigenome systems across treatment timepoints were chosen for testing: 12.5 μM, 25 μM, and 50 μM. Treatment timepoints were selected to match those from the minigenome: 1 hpi to inhibit the first round of transcription, 24 hpi to inhibit the early increase of transcription, and 48 hpi to inhibit late transcription and genome replication. As with the minigenome experiments, a single dose of remdesivir was given at the specified timepoint post-infection. Five days post-infection, samples were collected for endpoint titering.

It was found that all concentrations of remdesivir completely inhibited both EBOV and BDBV viral growth below the lower limit of detection (LLOD) when a single treatment was initiated 1 hpi (Figure 5.3). When treatment was delayed to either 24 or 48 hpi, no inhibition was observed for either virus (Figure 5.3). This contrasts with the results obtained in the minigenome system where all concentrations of remdesivir had a least some inhibitory effect on BDBV minigenome activity and concentrations of 50 μM and 100 μM inhibited EBOV minigenome activity even when administered 24 hpt. These results indicate that a single dose of remdesivir, above 10 μM, is ineffective at inhibiting ongoing viral transcription and replication *in vitro*.

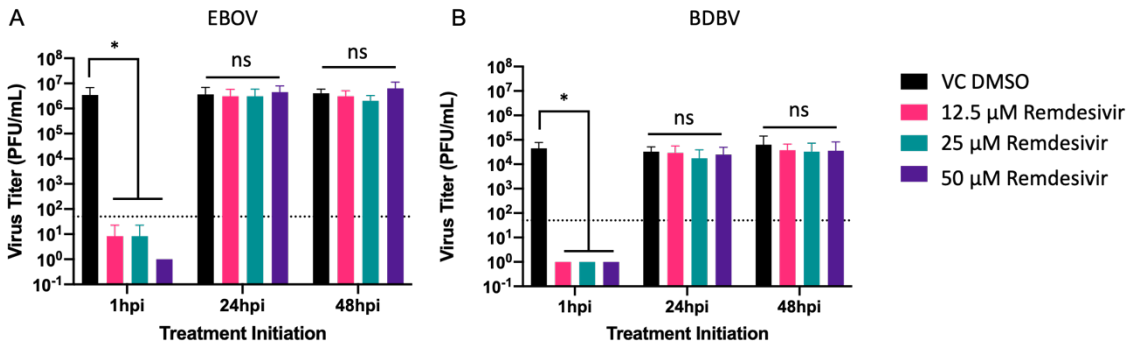

Figure 5.3 Inhibition of EBOV and BDBV infection using a single dose of remdesivir

A single treatment of remdesivir using a concentration of 12.5, 25, or 50 µM was added to wells 1-, 24-, or 48-hpi. Supernatant was collected 120 hpi, clarified and titered to determine treatment effects. Endpoint titers were compared to the DMSO VC by multiple t-tests. ns = not significant; * $p < 0.05$.

Titration of Remdesivir against Full-Length Virus

Since the three concentrations chosen from the minigenome experiment were all fully effective in inhibiting viral growth when administered 1 hpi, it was of interest to determine the lowest dose that would be effective at this time point. To do so, a titration curve was completed for both EBOV and BDBV with samples collected 120 hpi (Figure 5.4A). Remdesivir was titrated from 1 μM down to 0.98 nM and the IC_{90} was calculated using the final dose response curve (Figure 5.4B). Based on this experiment, viral growth inhibition was observed at all concentrations greater than 3.91 nM. The IC_{90} was determined to be 109.6 nM for BDBV and 284.1 nM for EBOV, that is, at these concentrations 90% of viral growth was inhibited. These concentrations were used for further testing of a delayed treatment with continuous drug replacement.

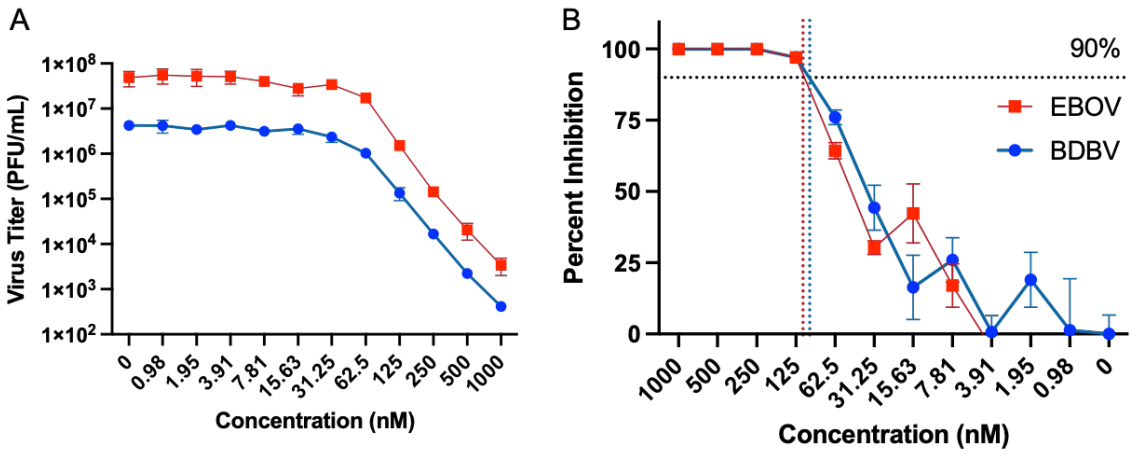

Figure 5.4 Titration of remdesivir in context of viral infection

A 2-fold dilution series was tested for inhibitory effects against viral infection with EBOV (red) or BDBV (blue) with a single remdesivir treatment initiated 1 hpi. (A) Viral titers as determined by plaque assay. (B) Inhibitory effect with VC treatment representing no inhibition. Titers are graphed as mean ± standard deviation. Inhibition curve is graphed as mean ± SEM. Reproduced from Levine, et al 2021 with permission.[125]

Continuous Treatment Effect on Viral Replication & Growth

As a substantial amount of viral transcription occurs within the first 24 hours after infection, it is not surprising that a concentration which worked when administered 1 hpi would not be as efficient when delayed. In order to inhibit this sustained transcription and replication, we tested if continuous replacement of remdesivir would have an observable effect. A previous study indicated that the intracellular half-life of the active metabolite of remdesivir is 14 – 24 h.[149] Therefore, drug was replenished every 24 h to maintain a consistent concentration of the active metabolite within cells. Samples were collected immediately before treatment every 24 h. When cells were treated with the IC_{90}, there was no difference compared to vehicle control at any timepoint sampled (Figure 5.5). These results show that substantial viral replication occurs within the first 24 h of infection that cannot be inhibited by concentrations that prove effective when started at 1 hpi.

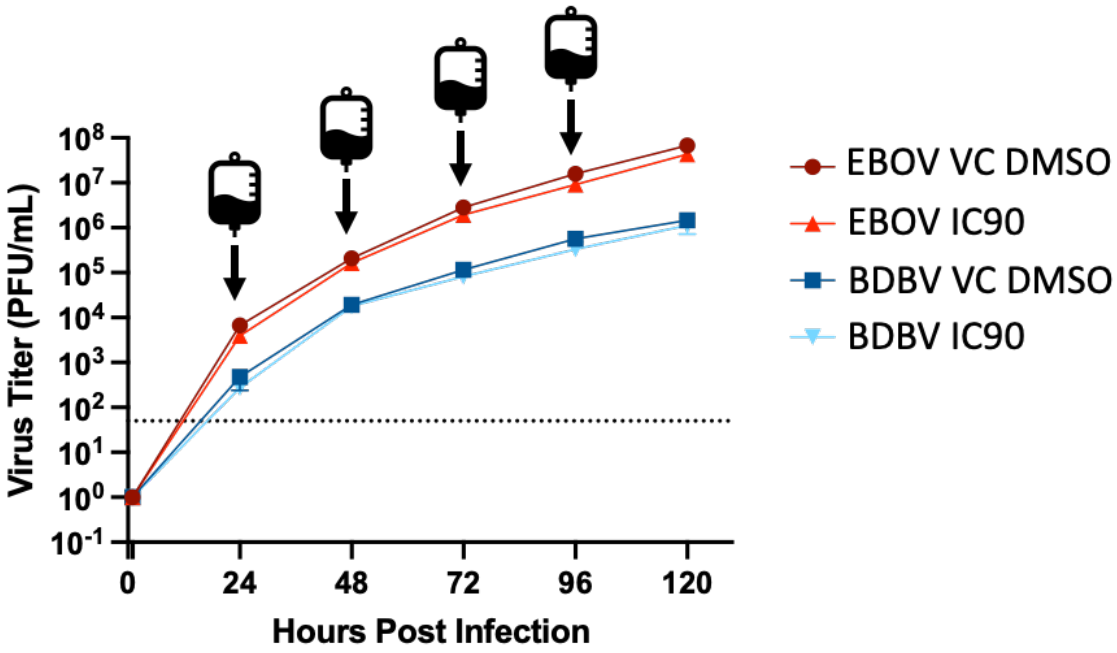

Figure 5.5 Delayed continuous treatment with IC90 of remdesivir

Remdesivir was used at the IC_{90} for each virus: 285 nM for EBOV (red) and 110 nM for BDBV (blue) Remdesivir treatment was initiated 24 hpi and fresh compound was replenished every 24 h as indicated by the symbol. Titers are shown as mean ± SEM. Reproduced from Levine, et al 2021 with permission.[125]

We next tested if a higher concentration of remdesivir replenished every 24 h could inhibit viral growth if treatment was delayed. To test this, a continuous treatment scheme was tested using remdesivir at concentrations of 12.5 μM, 25 μM, and 50 μM. A significant effect was seen at all timepoints 48 h after treatment was started for both EBOV and BDBV (Figure 5.6, 12.5 μM shown). There was minimal variation between the three concentrations suggesting that a saturating dose had been met. While there was a cytotoxic effect observed by MTT assay at these concentrations, this does not negate the effects of remdesivir on viral growth and replication at these concentrations. If the toxicity of remdesivir was the reason for reduced titers, then a difference would be expected between the three concentrations. Instead, the effect on viral titers were indistinguishable suggesting a direct effect on viral growth at concentrations above the saturating dose. The greatest effect was seen for BDBV when treatment was initiated 24 hpi. By 5 dpi, viral titers were reduced nearly to the LLOD (Figure 5.6A). A slight decrease in titer was also observed for BDBV when treatment was delayed 48 hpi but the same stark reduction was not visible at 120 hpi (Figure 5.6B). It is expected that for both the 24 and 48 hpi delayed treatment, BDBV titers would drop below the LLOD if the experiment were carried out past 120 hpi. For infection with EBOV, when treatment was delayed 24 hpi there was a significant reduction in viral titers compared to vehicle control. In contrast to BDBV, the EBOV titers plateaued rather than decreased over time (Figure 5.6C). When treatment was delayed 48 hpi in the context of EBOV infection, titers were reduced a maximum of 1 log by the final collection timepoint of 120 hpi (Figure 5.6D). Based on these results, delayed treatment is more effective in the context of BDBV infection than EBOV infection, and in both cases the dose must be substantially higher than what would be effective at 1 hpi.

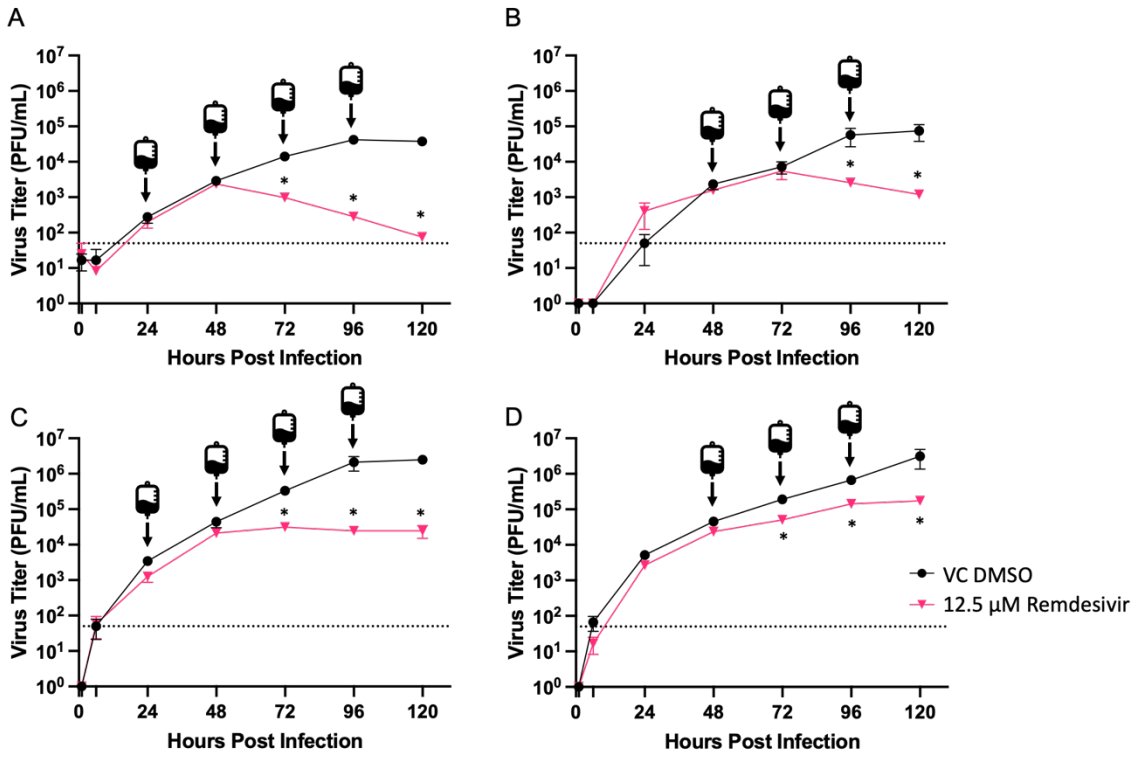

Figure 5.6 Delayed continuous treatment with a high concentration of remdesivir

A concentration of 12.5 mM was used to test a delayed, continuous treatment against infection with BDBV (A,B) and EBOV (C,D). Remdesivir treatment was initiated 24 hpi (A,C) or 48 hpi (B,D) and replenished every 24 h as indicated by the symbol. Titers are shown as mean ± SEM. * $p < 0.05$ as determined by one-way ANOVA.

DISCUSSION

Finding suitable drug candidates for the treatment of high-consequence pathogens is a complicated process and requires careful planning before testing can occur with authentic virus. Tools, such as minigenome systems, which can be safely used outside of a high-containment facility provide a means to screen and select for promising candidates for more intricate testing in BSL-4. Remdesivir had previously shown benefit *in vitro* against both EBOV and BDBV and *in vivo* against EBOV. The experiments shown here built on this previous data to test the efficacy of a delayed remdesivir treatment. Remdesivir showed a modest effect against EBOV in both the minigenome system and against viral infection, while the effects against BDBV were much more pronounced. Based on the results of experiments in Chapter 2, it was expected that BDBV would be more sensitive to remdesivir than EBOV due to the delayed growth kinetics. This was observed in the minigenome system where a treatment delayed 24 hpt still inhibited BDBV minigenome activity.

Previous studies have utilized a pre-treatment scheme or a treatment delay of 1 or 2 h, therefore we sought to test a longer delay of 24 or 48 hpi. The reason for this is to mimic what would be expected clinically, as treatment is usually not sought until substantial viral replication has already taken place. It was encouraging to see a significant decrease in EBOV titers even when treatment was delayed 24 h, although the titers appeared to plateau rather than decrease. A similar, but less substantial drop in EBOV titers was also observed when treatment was delayed 48 h. This result may point to a reason behind the limited efficacy of remdesivir against EVD in clinical trials, especially in patients with a high viral load. The results presented here suggest that once a certain titer

is reached, remdesivir treatment can only control further transcription/replication and that ongoing replication continues unabated. This theory was further examined when looking at remdesivir treatment in the context of BDBV infection which grows slower and reaches lower titers. Delayed treatment initiated either 24 or 48 hpi resulted in not only a significant decrease in viral titers but a continuous decrease over time. At the time of treatment initiation, BDBV was consistently a log lower than EBOV. Based on this data, the *in vitro* threshold for effect is at approximately 10^4 PFU/mL. Future studies should investigate what this threshold would be in context of infection in an NHP model as well as in a clinical setting.

The effects of remdesivir observed in the minigenome system, coupled with the greater efficacy against BDBV infection, may offer clarification on the mechanism of remdesivir in inhibiting ebolavirus growth. As transcription is the primary viral process occurring in the minigenome system and the major process occurring early after infection, it is likely that remdesivir has the greatest impact in inhibiting transcription. This inhibition would have a large, cascading effect on the rest of the viral lifecycle: inhibition of transcription prevents production of proteins to assemble new polymerase complexes which results in further reduction in transcription and genome replication. The result would be a decrease in the production and release of new virions and infection of other cells would be slowed or halted. This appears to be the case with BDBV as seen by the gradual reduction in viral titer over time after remdesivir treatment is initiated. In the case of EBOV, it can be postulated that the assembly of new polymerase complexes and viral replication had already reached steady-state levels by 24 hpi and so, while the addition of

remdesivir inhibited transcription by newly formed polymerase complexes, those already performing genome replication continued without inhibition.

The results of this study point to a mechanism for the effectiveness of remdesivir early after infection. This mechanism is in the inhibition of viral transcription, thereby limiting further viral replication and virion production. Remdesivir may still be a viable treatment option for clinical cases of BDBV infection which has a slower growth rate *in vitro* and may therefore have a more limited growth capacity *in vivo*. In addition, the effect of remdesivir in moderating further EBOV growth may prove beneficial in the context of combination therapies. That is, while other therapeutics such as antibody therapies can prevent new virions from infecting cells, remdesivir can act on already infected cells and limit the production of new virions. This should be further investigated in *in vivo* models as has been done for the related MARV and should be considered for future clinical trials during ebolavirus outbreaks.[155]

Chapter 6: Discussion – Mechanism for Delayed Viral Growth Kinetics and Use of Remdesivir (GS-5734) in the treatment of Ebola disease

Role of the Polymerase Complex in Ebolavirus Growth Kinetics

Filoviruses are known to cause severe and oftentimes fatal disease, but the spectrum of disease varies across the *Ebolavirus* genus; even within the outbreak causing species of EBOV, SUDV, and BDBV there is variability ranging from upwards of 90% lethality down to 25% lethality. The exact mechanism behind such a difference is still unknown; although, several hypotheses have been presented including differences in health care infrastructure, immune evasion capabilities, and molecular variations in viral growth. In regard to healthcare infrastructure, East and Central African countries showed no significant differences in CFR between outbreaks, meaning this is unlikely to be the sole reason between the species-specific CFRs.[22] In addition, *in vivo* experiments using NHPs have shown a similar pattern of decreased lethality when comparing infections with EBOV to infections with BDBV.[77,78,97] This is further examined in *in vitro* experiments showing decreased viral titers and slower growth kinetics for BDBV compared to EBOV.[94] Previous studies have examined the possibility that BDBV has a diminished ability to block the host innate immune response. These studies were unable to show any difference in inhibitory capacity between the immune antagonist proteins of both species.[88] Additionally, in cell lines with the innate immune signaling molecules RIG-I or STAT-2 knocked out, there was no difference in viral growth indicating that subversion of the immune response may not be the reason behind differences in viral growth (Versteeg, unpublished).

Instead, it is possible that the observed differences are due to a diminished replicative capacity of BDBV. A less efficient polymerase complex would result in less transcription and replication of viral genes and genome. Any effects on transcription would have a cascading effect on the rest of the viral lifecycle including genome replication and

immune evasion. For instance, if the immune antagonists VP35 and VP24 were produced at lower levels, there is a higher chance of infection being detected by immune sensors. Along a similar line, the switch to genome replication is thought to occur only after a threshold is met for production of viral proteins. The longer it takes for proteins to be transcribed and translated, the longer it takes for genome replication and virion release. In turn, this delay in replication allows the host time to detect an infection and mount a robust response. While EBOV appears to grow quite rapidly and speed past these defenses, the slower growth of BDBV results in an infection that can be better controlled by the host. This dissertation addresses the hypothesis that molecular variations in the polymerase complex between the ebolaviruses EBOV and BDBV affect the replicative capacity. Specifically. that the polymerase complex of BDBV functions less efficiently than that of EBOV.

Throughout this dissertation, EBOV and BDBV have been directly compared when looking at growth kinetics, synthesis of vRNA and mRNA, and susceptibility to inhibition by nucleoside analogs. In all cases, EBOV was more productive than BDBV. While the rate of production of infectious virions was similar between species, the rate of vRNA and mRNA production was increased for EBOV. In addition, more copies of EBOV VP35 and L mRNA were produced per genome compared to BDBV. As these two proteins are essential for viral RNA synthesis it is possible that increased concentrations of these proteins would further increase production of viral transcripts and vRNA. To further examine this process, a minigenome system was developed for BDBV so that the polymerase complexes could be studied in isolation. The BDBV minigenome system adds to the platforms available for studying ebolaviruses outside of a high containment laboratory.

Using the newly designed BDBV minigenome system along with a previously established EBOV minigenome system, it was possible to directly compare the output of luciferase between the two polymerase complexes. Use of the EBOV polymerase

consistently produced more luciferase compared to BDBV even at optimized plasmid concentrations. This builds upon the data presented showing an increased production of transcripts and genome copies. In addition, the minigenome systems allowed us to mix-and-match the proteins of the polymerase complex to determine the effects on RNA synthesis. We had hypothesized that BDBV proteins would reduce the amount of the minigenome reporter, luciferase that would be produced. Instead, it was found that when the BDBV NP was used with EBOV VP35 and L there was an increase in minigenome transcription. One possible mechanism for this result is a difference in binding affinities between EBOV and BDBV NP and the polymerase cofactor VP35. In this scenario, BDBV NP would have a greater binding affinity for EBOV VP35 resulting in the viral RNA being more accessible to the enzymatic subunit, L. This would allow for increased RNA synthesis and perhaps more rapid RNA synthesis. The exchange of VP35, L, or both had a detrimental effect on minigenome activity for both the EBOV and BDBV system. This is likely due to a less than optimal ratio of the various polymerase complex proteins as well as an incompatibility with the regulatory leader and trailer regions.

Although replication was not directly measured in these experiments, it is interesting to note the variation in minigenome expression when different trailer sequences were utilized. Whenever the BDBV trailer was used as a template for the EBOV polymerase complex, there was a reduction in minigenome output. This could indicate a mechanism by which replication of BDBV genomes is hindered. This would account for the different rate of genome production observed in the course of viral infection. This could be investigated by quantifying the number of antigenome copies for homologous and chimeric minigenomes.

Based on the results showing slower growth and transcription for BDBV compared to EBOV, it was expected that BDBV would be more susceptible to inhibition by a nucleoside analog. Of all compounds tested, only remdesivir proved effective at limiting BDBV minigenome activity. Not only was remdesivir effective at limiting minigenome

transcription, but the effect was still observed when treatment was delayed, which was not seen with the EBOV polymerase complex. These results were confirmed in the context of viral infection with treatment delayed up to 48 hpi. Remdesivir was most effective when administered shortly after infection (1 hpi) a time when viral gene transcription is the predominant process; therefore, the utility of remdesivir appears to be in the ability to prevent transcription.

As explained earlier, any effect on transcription would create a domino effect in which further transcription and replication would be hindered due to insufficient quantities of polymerase complex proteins (Figure 6.1A). This is shown by the reduction in viable virus when treatment is initiated before, during, or shortly after infection (Figure 6.1B).[149] The results examining the effects of delayed remdesivir treatment on viral infection further support the earlier conclusion that transcription efficiency is varied between EBOV and BDBV. When a single treatment was used 24 hpi there was no effect on endpoint titers. At this point in infection, it would be expected that new polymerase complexes have been assembled and a greater amount of transcription is taking place. To overcome this, a continued, high-dose treatment regimen would be necessary to inhibit all transcriptional activity as was the case for BDBV, but not EBOV (Figure 6.1C,D). The EBOV polymerase complexes appears to have high RNA synthesis activity that had increased beyond that which could be inhibited by remdesivir and therefore the effects were minimal (Figure 6.1C). The BDBV polymerase complex, in contrast, which has less active transcription taking place, could be inhibited by remdesivir thus reducing further viral growth (Figure 6.1D).

The studies presented here have some limitations which should be considered. First, all studies were completed *in vitro* and do not account for other disease processes which occur during infection with either EBOV or BDBV such as immune cell activation, complete innate immune response, and cytokine release. These other processes may also play a role in the observed delayed and limited growth of BDBV compared to EBOV. In

addition, care should be taken when translating results from *in vitro* drug studies to *in vivo* experiments. Careful observation of drug toxicity should be monitored when testing higher concentrations or new formulations. Some cytotoxicity was observed in the studies presented here using high concentrations (>10 μM) of remdesivir in the HepG2 cell culture. Finally, experiments using the minigenome system presented here look at only a single portion of viral replication. It is therefore necessary to confirm results in the context of full-length replicating virus. While minigenome systems are an excellent tool for examining the effects of mutations and mapping functional domains, these will not always translate to a relevant effect in full-length virus.

In summary, the mechanism for delayed growth kinetics of BDBV compared to EBOV appears to lie in the efficiency of the polymerase complex. Transcription of BDBV viral mRNA is diminished compared to that of EBOV resulting in a lower concentration of key viral proteins. This results in fewer new polymerase complexes to carry out secondary transcription and replication, as well as delayed packaging and release until sufficient viral matrix proteins are produced. Further, there may be a reduced capacity to inhibit innate immune sensors as these proteins are produced in lower concentrations.

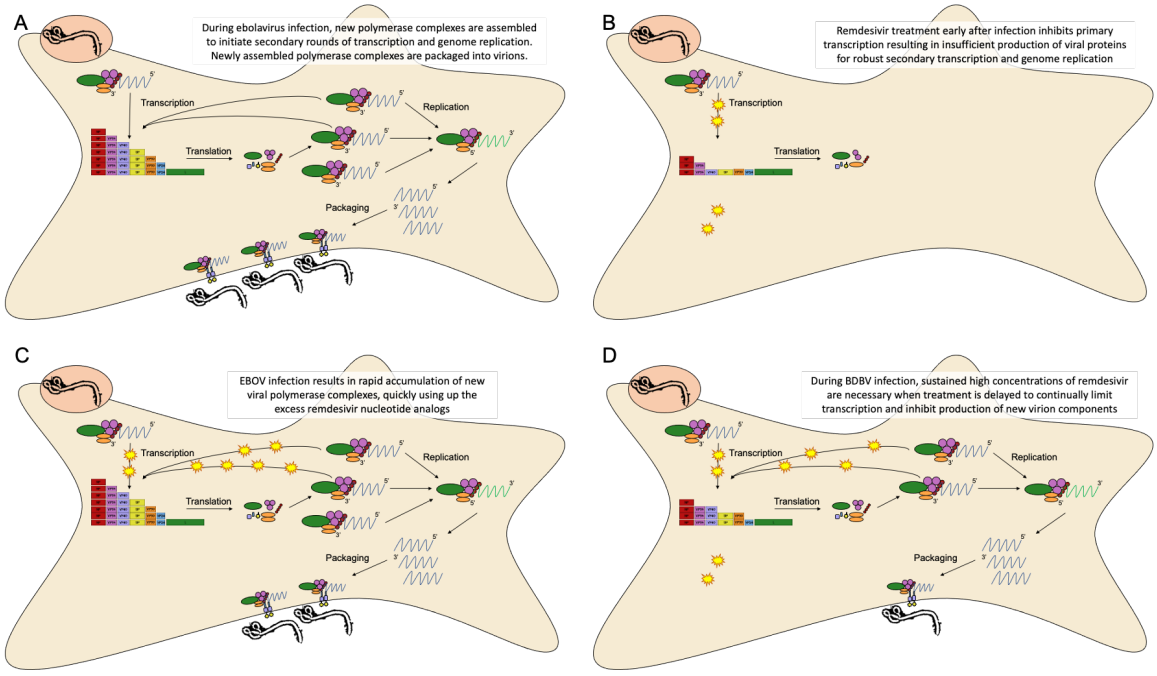

Figure 6.1 Remdesivir inhibition of ebolavirus RNA synthesis and viral propagation

(A) Upon release into the cytoplasm, the pre-packaged ebolavirus polymerase complex beings a primary round of gene transcription and production of additional polymerase complexes. These new complexes carry out secondary transcription and replication of the viral genome through an antigenomic intermediate. As viral matrix proteins are produced assembly and budding of new virions occurs. (B) When the nucleoside analog remdesivir (✸) is added shortly after infection primary transcription is inhibited and no new virions are produced. (C, D) Once secondary transcription and genome replication an increased concentration of remdesivir is necessary to have an effect. In the case of EBOV (C) where transcription is abundant and rapid, the polymerase complexes quickly use up the remdesivir resulting in minimal changes in virus production. During BDBV infection (D) where less transcription occurs, a sustained high concentration of remdesivir can inhibit transcription and suppresses viral growth. Image created by Corri B. Levine using Microsoft PowerPoint.

SUGGESTIONS FOR USE OF REMDESIVIR IN THE TREATMENT OF EBOLA DISEASE

In the wake of the 2014 - 2016 West African EVD outbreak, the WHO assembled a priority list of therapeutics to be tested in the face of future ebolavirus outbreaks. In 2018, an EBOV outbreak emerged in the DRC and a 4-arm clinical trial was initiated, the PALM trial, which consisted of three antibody therapies and one small molecule inhibitor remdesivir.[136] At an interim data analysis, it was shown that two of the antibody therapies (mAb114 and REGN-EB3) performed superiorly to the ZMapp antibody cocktail and remdesivir alone. Although mAb114 and REGN-EB3 outperformed remdesivir, remdesivir treatment still provided benefit with a mortality rate of 53% overall and 29% in those with a low viral load as indicated by a Ct > 22.0. This is still a reduction compared to historical data indicating an average mortality rate of 76% for EBOV (CI: 63-87%).[21]

While remdesivir did not perform as well as expected in the PALM trial, the results should not preclude the use of remdesivir for treatment of ebolavirus infections in the future, especially in the case of infection with other ebolavirus species. BDBV, as shown in this dissertation, has slower and delayed growth kinetics compared to EBOV. This difference in replicative capacities translated to a higher susceptibility to treatment with remdesivir. Not only did BDBV have a lower IC_{90} compared to EBOV, but a strong inhibitory effect was observed even when treatment was delayed 24 or 48 hpi. These results suggest that remdesivir may provide greater therapeutic benefit when used in cases of BDBV infection than have been documented for EBOV infections. It is therefore important to not yet rule out the use of remdesivir in the treatment of BDBV infections.

Based on the results of the PALM trial and the data presented in this dissertation, it is clear there is greater benefit when treatment is initiated early, before substantial viral replication occurs. This translates to providing therapy as soon as possible after symptom onset or a known exposure occurs. In the case of post-exposure prophylaxis, the standard ten-day series of remdesivir infusions is likely not feasible, but a single or shortened course may be beneficial. This is similar to the use of antibody therapies or convalescent plasma as post-exposure prophylaxis. *In vitro* data from this dissertation and previous studies indicate that a single treatment initiated just before or shortly after cellular infection can inhibit the first round of viral transcription thereby inhibiting the creation of new virions and preventing subsequent rounds of infection.[149] The utility of a single, high-dose treatment would need to be explored further in *in vivo* models. The only immediate post-exposure treatment data published to date utilized a treatment of of 3 mg/kg for 10 days in a rhesus macaque model, a dose which the authors state was suboptimal.[149] It would be interesting to examine post-exposure prophylaxis using a more optimal dose for NHPs (10 mg/kg) and a shortened treatment regimen.

Another option is to increase the dose of remdesivir if treatment were to be delayed. This was necessary in the experiments presented here, where higher *in vitro* concentrations were needed when treatment was delayed either 24 or 48 hpi. This is likely due to the increased amount of transcription and replication occurring over the course of infection. A higher, saturating dose of remdesivir would be necessary to prevent ongoing transcription. Future *in vivo* and clinical trials should examine the efficacy of extending the duration of the loading dose (10 mg/kg for NHPs, 200 mg/kg for humans) especially in those with high viral load. Care should be taken to monitor for any signs of toxicity, especially

hepatotoxicity, if doses were to be increased especially since filoviruses cause extensive liver damage. This would require a discussion about the risks of using a higher dose compared to discontinuing treatment.

Finally, combination therapy using an antiviral and an antibody or antibody cocktail will likely prove to be the most beneficial treatment for ebolavirus infections. The mechanisms of action for these two types of therapeutics are in targeting vastly different aspects of the viral lifecycle. As demonstrated previously and further highlighted within this dissertation, the small molecule antiviral remdesivir inhibits the polymerase complex from elongation of viral RNA, primarily by limiting the production of mRNA encoding viral genes.[148,156] The inhibition of transcription and replication limits the production of new virions which can continue the infection and replication cycle, an important target in order to maintain control of an infection. Antibody therapy, in contrast, prevents new infections and targets infected cells. Therefore, combination therapy that targets multiple parts of the viral life cycle may be the key for successful treatment of ebolavirus infections, and has been shown to be efficacious against the related MARV in an NHP model.[155] As the only non-biologic to show clinical efficacy against ebolavirus infection, remdesivir will continue to be a valuable option for therapy. Modified treatment schemes and treatment of less pathogenic ebolaviruses may be more efficacious than what has been previously tested.

References

1 Ebola haemorrhagic fever in Sudan, 1976. Report of a WHO/International Study Team. *Bull World Health Organ* **56**, 247-270 (1978).

2 Ebola haemorrhagic fever in Zaire, 1976. *Bull World Health Organ* **56**, 271-293 (1978).

3 Kuhn, J. H. *et al.* Proposal for a revised taxonomy of the family Filoviridae: classification, names of taxa and viruses, and virus abbreviations. *Arch Virol* **155**, 2083-2103, doi:10.1007/s00705-010-0814-x (2010).

4 Control, C. f. D. *Ebola Virus Disease Distribution Map: Cases of Ebola Virus Disease in Africa Since 1976*, <https://www.cdc.gov/vhf/ebola/history/distribution-map.html> (2021).

5 Leroy, E. M. *et al.* Fruit bats as reservoirs of Ebola virus. *Nature* **438**, 575-576, doi:10.1038/438575a (2005).

6 Pourrut, X. *et al.* The natural history of Ebola virus in Africa. *Microbes Infect* **7**, 1005-1014, doi:10.1016/j.micinf.2005.04.006 (2005).

7 Goldstein, T. *et al.* The discovery of Bombali virus adds further support for bats as hosts of ebolaviruses. *Nat Microbiol* **3**, 1084-1089, doi:10.1038/s41564-018-0227-2 (2018).

8 Forbes, K. M. *et al.* Bombali Virus in Mops condylurus Bat, Kenya. *Emerg Infect Dis* **25**, 955-957, doi:10.3201/eid2505.181666 (2019).

9 Towner, J. S. *et al.* Isolation of genetically diverse Marburg viruses from Egyptian fruit bats. *PLoS Pathog* **5**, e1000536, doi:10.1371/journal.ppat.1000536 (2009).

10 Le Guenno, B. *et al.* Isolation and partial characterisation of a new strain of Ebola virus. *Lancet* **345**, 1271-1274, doi:10.1016/s0140-6736(95)90925-7 (1995).

11 Hayes, C. G. *et al.* Outbreak of fatal illness among captive macaques in the Philippines caused by an Ebola-related filovirus. *Am J Trop Med Hyg* **46**, 664-671, doi:10.4269/ajtmh.1992.46.664 (1992).

12 Jahrling, P. B. *et al.* Preliminary report: isolation of Ebola virus from monkeys imported to USA. *Lancet* **335**, 502-505, doi:10.1016/0140-6736(90)90737-p (1990).

13 Miranda, M. E. *et al.* Seroepidemiological study of filovirus related to Ebola in the Philippines. *Lancet* **337**, 425-426, doi:10.1016/0140-6736(91)91199-5 (1991).

14 Vol. 39 *Morbidity Mortality Weekly Report* (ed Centers for Disease Control) 221 (1990).

15 Emanuel, J., Marzi, A. & Feldmann, H. Filoviruses: Ecology, Molecular Biology, and Evolution. *Adv Virus Res* **100**, 189-221, doi:10.1016/bs.aivir.2017.12.002 (2018).

16 Dowell, S. F. *et al.* Transmission of Ebola hemorrhagic fever: a study of risk factors in family members, Kikwit, Democratic Republic of the Congo, 1995. Commission de Lutte contre les Epidemies a Kikwit. *J Infect Dis* **179 Suppl 1**, S87-91, doi:10.1086/514284 (1999).

17 Jacob, S. T. *et al.* Ebola virus disease. *Nat Rev Dis Primers* **6**, 13, doi:10.1038/s41572-020-0147-3 (2020).
18 Francesconi, P. *et al.* Ebola hemorrhagic fever transmission and risk factors of contacts, Uganda. *Emerg Infect Dis* **9**, 1430-1437, doi:10.3201/eid0911.030339 (2003).
19 Chowell, G., Hengartner, N. W., Castillo-Chavez, C., Fenimore, P. W. & Hyman, J. M. The basic reproductive number of Ebola and the effects of public health measures: the cases of Congo and Uganda. *J Theor Biol* **229**, 119-126, doi:10.1016/j.jtbi.2004.03.006 (2004).
20 Munster, V. J. *et al.* Outbreaks in a Rapidly Changing Central Africa - Lessons from Ebola. *N Engl J Med* **379**, 1198-1201, doi:10.1056/NEJMp1807691 (2018).
21 Lefebvre, A. *et al.* Case fatality rates of Ebola virus diseases: a meta-analysis of World Health Organization data. *Med Mal Infect* **44**, 412-416, doi:10.1016/j.medmal.2014.08.005 (2014).
22 Kawuki, J., Musa, T. H. & Yu, X. Impact of recurrent outbreaks of Ebola virus disease in Africa: a meta-analysis of case fatality rates. *Public Health* **195**, 89-97, doi:10.1016/j.puhe.2021.03.027 (2021).
23 Parra, J. M., Salmeron, O. J. & Velasco, M. The first case of Ebola virus disease acquired outside Africa. *N Engl J Med* **371**, 2439-2440, doi:10.1056/NEJMc1412662 (2014).
24 Liddell, A. M. *et al.* Characteristics and Clinical Management of a Cluster of 3 Patients With Ebola Virus Disease, Including the First Domestically Acquired Cases in the United States. *Ann Intern Med* **163**, 81-90, doi:10.7326/M15-0530 (2015).
25 Languon, S. & Quaye, O. Filovirus Disease Outbreaks: A Chronological Overview. *Virology (Auckl)* **10**, 1178122X19849927, doi:10.1177/1178122X19849927 (2019).
26 Alsop, Z. Ebola outbreak in Uganda "atypical", say experts. *Lancet* **370**, 2085, doi:10.1016/s0140-6736(07)61880-7 (2007).
27 Wamala, J. F. *et al.* Ebola hemorrhagic fever associated with novel virus strain, Uganda, 2007-2008. *Emerg Infect Dis* **16**, 1087-1092, doi:10.3201/eid1607.091525 (2010).
28 Towner, J. S. *et al.* Newly Discovered Ebola Virus Associated with Hemorrhagic Fever Outbreak in Uganda. *PLoS Pathogens* **4**, e1000212, doi:10.1371/journal.ppat.1000212 (2008).
29 Roddy, P. *et al.* Clinical manifestations and case management of Ebola haemorrhagic fever caused by a newly identified virus strain, Bundibugyo, Uganda, 2007-2008. *PLoS One* **7**, e52986, doi:10.1371/journal.pone.0052986 (2012).
30 MacNeil, A. *et al.* Proportion of Deaths and Clinical Features in Bundibugyo Ebola Virus Infection, Uganda. *Emerging Infectious Diseases* **16**, 1969-1972, doi:10.3201/eid1612.100627 (2010).
31 Kratz, T. *et al.* Ebola Virus Disease Outbreak in Isiro, Democratic Republic of the Congo, 2012: Signs and Symptoms, Management and Outcomes. **10**, e0129333, doi:10.1371/journal.pone.0129333 (2015).

32 Congo, M. o. D. R. o. t. *Declaration of the end of the Ebola Haemorrhagic Fever epidemic in the Haut-Uélé Ouest Health District, Orientale Province, DR CONGO*, <https://reliefweb.int/report/democratic-republic-congo/d%C3%A9claration-de-la-fin-de-l%E2%80%99%C3%A9pid%C3%A9mie-de-fi%C3%A8vre-h%C3%A9morragique-%C3%A0-virus> (2012).
33 Kuhn, J. H. *et al.* ICTV Virus Taxonomy Profile: Filoviridae. *J Gen Virol* **100**, 911-912, doi:10.1099/jgv.0.001252 (2019).
34 Feldmann, H., Sprecher, A. & Geisbert, T. W. Ebola. *N Engl J Med* **382**, 1832-1842, doi:10.1056/NEJMra1901594 (2020).
35 de La Vega, M. A., Wong, G., Kobinger, G. P. & Qiu, X. The multiple roles of sGP in Ebola pathogenesis. *Viral Immunol* **28**, 3-9, doi:10.1089/vim.2014.0068 (2015).
36 Basler, C. F. Molecular pathogenesis of viral hemorrhagic fever. *Semin Immunopathol* **39**, 551-561, doi:10.1007/s00281-017-0637-x (2017).
37 Licata, J. M., Johnson, R. F., Han, Z. & Harty, R. N. Contribution of ebola virus glycoprotein, nucleoprotein, and VP24 to budding of VP40 virus-like particles. *J Virol* **78**, 7344-7351, doi:10.1128/JVI.78.14.7344-7351.2004 (2004).
38 Muhlberger, E., Weik, M., Volchkov, V. E., Klenk, H. D. & Becker, S. Comparison of the transcription and replication strategies of marburg virus and Ebola virus by using artificial replication systems. *J Virol* **73**, 2333-2342 (1999).
39 Leung, D. W. *et al.* An Intrinsically Disordered Peptide from Ebola Virus VP35 Controls Viral RNA Synthesis by Modulating Nucleoprotein-RNA Interactions. *Cell Rep* **11**, 376-389, doi:10.1016/j.celrep.2015.03.034 (2015).
40 Kirchdoerfer, R. N., Abelson, D. M., Li, S., Wood, M. R. & Saphire, E. O. Assembly of the Ebola Virus Nucleoprotein from a Chaperoned VP35 Complex. *Cell Rep* **12**, 140-149, doi:10.1016/j.celrep.2015.06.003 (2015).
41 Green, T. J. *et al.* Common mechanism for RNA encapsidation by negative-strand RNA viruses. *J Virol* **88**, 3766-3775, doi:10.1128/JVI.03483-13 (2014).
42 Sun, Y., Guo, Y. & Lou, Z. A versatile building block: the structures and functions of negative-sense single-stranded RNA virus nucleocapsid proteins. *Protein Cell* **3**, 893-902, doi:10.1007/s13238-012-2087-5 (2012).
43 Wan, W. *et al.* Structure and assembly of the Ebola virus nucleocapsid. *Nature* **551**, 394-397, doi:10.1038/nature24490 (2017).
44 Jamin, M. & Yabukarski, F. Nonsegmented Negative-Sense RNA Viruses-Structural Data Bring New Insights Into Nucleocapsid Assembly. *Adv Virus Res* **97**, 143-185, doi:10.1016/bs.aivir.2016.09.001 (2017).
45 Prins, K. C. *et al.* Basic residues within the ebolavirus VP35 protein are required for its viral polymerase cofactor function. *J Virol* **84**, 10581-10591, doi:10.1128/JVI.00925-10 (2010).
46 Zhu, L. *et al.* Ebola virus replication is regulated by the phosphorylation of viral protein VP35. *Biochem Biophys Res Commun* **521**, 687-692, doi:10.1016/j.bbrc.2019.10.147 (2020).
47 Xu, W. *et al.* Ebola virus VP30 and nucleoprotein interactions modulate viral RNA synthesis. *Nat Commun* **8**, 15576, doi:10.1038/ncomms15576 (2017).

48 Kirchdoerfer, R. N., Moyer, C. L., Abelson, D. M. & Saphire, E. O. The Ebola Virus VP30-NP Interaction Is a Regulator of Viral RNA Synthesis. *PLoS Pathog* **12**, e1005937, doi:10.1371/journal.ppat.1005937 (2016).
49 Biedenkopf, N., Schlereth, J., Grunweller, A., Becker, S. & Hartmann, R. K. RNA Binding of Ebola Virus VP30 Is Essential for Activating Viral Transcription. *J Virol* **90**, 7481-7496, doi:10.1128/JVI.00271-16 (2016).
50 Biedenkopf, N., Lier, C. & Becker, S. Dynamic Phosphorylation of VP30 Is Essential for Ebola Virus Life Cycle. *J Virol* **90**, 4914-4925, doi:10.1128/JVI.03257-15 (2016).
51 Cantoni, D. & Rossman, J. S. Ebolaviruses: New roles for old proteins. *PLoS Negl Trop Dis* **12**, e0006349, doi:10.1371/journal.pntd.0006349 (2018).
52 Geisbert, T. W. *et al.* Pathogenesis of Ebola hemorrhagic fever in cynomolgus macaques: evidence that dendritic cells are early and sustained targets of infection. *Am J Pathol* **163**, 2347-2370, doi:10.1016/S0002-9440(10)63591-2 (2003).
53 Aleksandrowicz, P. *et al.* Ebola virus enters host cells by macropinocytosis and clathrin-mediated endocytosis. *J Infect Dis* **204 Suppl 3**, S957-967, doi:10.1093/infdis/jir326 (2011).
54 Yu, D. S. *et al.* The lifecycle of the Ebola virus in host cells. *Oncotarget* **8**, 55750-55759, doi:10.18632/oncotarget.18498 (2017).
55 Cote, M. *et al.* Small molecule inhibitors reveal Niemann-Pick C1 is essential for Ebola virus infection. *Nature* **477**, 344-348, doi:10.1038/nature10380 (2011).
56 Carette, J. E. *et al.* Ebola virus entry requires the cholesterol transporter Niemann-Pick C1. *Nature* **477**, 340-343, doi:10.1038/nature10348 (2011).
57 Muhlberger, E., Lotfering, B., Klenk, H. D. & Becker, S. Three of the four nucleocapsid proteins of Marburg virus, NP, VP35, and L, are sufficient to mediate replication and transcription of Marburg virus-specific monocistronic minigenomes. *J Virol* **72**, 8756-8764 (1998).
58 Shabman, R. S. *et al.* Deep sequencing identifies noncanonical editing of Ebola and Marburg virus RNAs in infected cells. *mBio* **5**, e02011, doi:10.1128/mBio.02011-14 (2014).
59 Hume, A. J. & Muhlberger, E. Distinct Genome Replication and Transcription Strategies within the Growing Filovirus Family. *J Mol Biol* **431**, 4290-4320, doi:10.1016/j.jmb.2019.06.029 (2019).
60 Biedenkopf, N., Hartlieb, B., Hoenen, T. & Becker, S. Phosphorylation of Ebola virus VP30 influences the composition of the viral nucleocapsid complex: impact on viral transcription and replication. *J Biol Chem* **288**, 11165-11174, doi:10.1074/jbc.M113.461285 (2013).
61 Velasquez, G. E. *et al.* Time From Infection to Disease and Infectiousness for Ebola Virus Disease, a Systematic Review. *Clin Infect Dis* **61**, 1135-1140, doi:10.1093/cid/civ531 (2015).
62 Bwaka, M. A. *et al.* Ebola hemorrhagic fever in Kikwit, Democratic Republic of the Congo: clinical observations in 103 patients. *J Infect Dis* **179 Suppl 1**, S1-7, doi:10.1086/514308 (1999).
63 Okware, S. I. *et al.* An outbreak of Ebola in Uganda. *Trop Med Int Health* **7**, 1068-1075, doi:10.1046/j.1365-3156.2002.00944.x (2002).

64 McElroy, A. K. *et al.* Ebola hemorrhagic Fever: novel biomarker correlates of clinical outcome. *J Infect Dis* **210**, 558-566, doi:10.1093/infdis/jiu088 (2014).
65 Leligdowicz, A. *et al.* Ebola virus disease and critical illness. *Crit Care* **20**, 217, doi:10.1186/s13054-016-1325-2 (2016).
66 Kortepeter, M. G., Bausch, D. G. & Bray, M. Basic clinical and laboratory features of filoviral hemorrhagic fever. *J Infect Dis* **204 Suppl 3**, S810-816, doi:10.1093/infdis/jir299 (2011).
67 Sagui, E. *et al.* Severe Ebola Virus Infection With Encephalopathy: Evidence for Direct Virus Involvement. *Clin Infect Dis* **61**, 1627-1628, doi:10.1093/cid/civ606 (2015).
68 de Greslan, T. *et al.* Ebola Virus-Related Encephalitis. *Clin Infect Dis* **63**, 1076-1078, doi:10.1093/cid/ciw469 (2016).
69 Fitzpatrick, G. *et al.* The Contribution of Ebola Viral Load at Admission and Other Patient Characteristics to Mortality in a Medecins Sans Frontieres Ebola Case Management Centre, Kailahun, Sierra Leone, June-October 2014. *J Infect Dis* **212**, 1752-1758, doi:10.1093/infdis/jiv304 (2015).
70 Rollin, P. E., Bausch, D. G. & Sanchez, A. Blood chemistry measurements and D-Dimer levels associated with fatal and nonfatal outcomes in humans infected with Sudan Ebola virus. *J Infect Dis* **196 Suppl 2**, S364-371, doi:10.1086/520613 (2007).
71 Rowe, A. K. *et al.* Clinical, virologic, and immunologic follow-up of convalescent Ebola hemorrhagic fever patients and their household contacts, Kikwit, Democratic Republic of the Congo. Commission de Lutte contre les Epidemies a Kikwit. *J Infect Dis* **179 Suppl 1**, S28-35, doi:10.1086/514318 (1999).
72 Jacobs, M. *et al.* Late Ebola virus relapse causing meningoencephalitis: a case report. *Lancet* **388**, 498-503, doi:10.1016/S0140-6736(16)30386-5 (2016).
73 Diallo, B. *et al.* Resurgence of Ebola Virus Disease in Guinea Linked to a Survivor With Virus Persistence in Seminal Fluid for More Than 500 Days. *Clin Infect Dis* **63**, 1353-1356, doi:10.1093/cid/ciw601 (2016).
74 Mate, S. E. *et al.* Molecular Evidence of Sexual Transmission of Ebola Virus. *N Engl J Med* **373**, 2448-2454, doi:10.1056/NEJMoa1509773 (2015).
75 Falzarano, D. *et al.* Single Immunization With a Monovalent Vesicular Stomatitis Virus-Based Vaccine Protects Nonhuman Primates Against Heterologous Challenge With Bundibugyo ebolavirus. **204**, S1082-S1089, doi:10.1093/infdis/jir350 (2011).
76 Gilchuk, P. *et al.* Efficacy of Human Monoclonal Antibody Monotherapy Against Bundibugyo Virus Infection in Nonhuman Primates. *The Journal of Infectious Diseases* **218**, S565-S573, doi:10.1093/infdis/jiy295 (2018).
77 Hensley, L. E. *et al.* Demonstration of cross-protective vaccine immunity against an emerging pathogenic Ebolavirus Species. *PLoS Pathog* **6**, e1000904, doi:10.1371/journal.ppat.1000904 (2010).
78 Mire, C. E. *et al.* Vesicular Stomatitis Virus-Based Vaccines Protect Nonhuman Primates against Bundibugyo ebolavirus. **7**, e2600, doi:10.1371/journal.pntd.0002600 (2013).

79 Gupta, M., Macneil, A., Reed, Z. D., Rollin, P. E. & Spiropoulou, C. F. Serology and cytokine profiles in patients infected with the newly discovered Bundibugyo ebolavirus. *Virology* **423**, 119-124, doi:10.1016/j.virol.2011.11.027 (2012).
80 Leung, D. W. *et al.* Structural basis for dsRNA recognition and interferon antagonism by Ebola VP35. *Nat Struct Mol Biol* **17**, 165-172, doi:10.1038/nsmb.1765 (2010).
81 Prins, K. C. *et al.* Mutations abrogating VP35 interaction with double-stranded RNA render Ebola virus avirulent in guinea pigs. *J Virol* **84**, 3004-3015, doi:10.1128/JVI.02459-09 (2010).
82 Basler, C. F. *et al.* The Ebola virus VP35 protein functions as a type I IFN antagonist. *Proc Natl Acad Sci U S A* **97**, 12289-12294, doi:10.1073/pnas.220398297 (2000).
83 Edwards, M. R. *et al.* Differential Regulation of Interferon Responses by Ebola and Marburg Virus VP35 Proteins. *Cell Rep* **14**, 1632-1640, doi:10.1016/j.celrep.2016.01.049 (2016).
84 Luthra, P. *et al.* Mutual antagonism between the Ebola virus VP35 protein and the RIG-I activator PACT determines infection outcome. *Cell Host Microbe* **14**, 74-84, doi:10.1016/j.chom.2013.06.010 (2013).
85 Prins, K. C., Cardenas, W. B. & Basler, C. F. Ebola virus protein VP35 impairs the function of interferon regulatory factor-activating kinases IKKepsilon and TBK-1. *J Virol* **83**, 3069-3077, doi:10.1128/JVI.01875-08 (2009).
86 Reid, S. P. *et al.* Ebola virus VP24 binds karyopherin alpha1 and blocks STAT1 nuclear accumulation. *J Virol* **80**, 5156-5167, doi:10.1128/JVI.02349-05 (2006).
87 Mateo, M. *et al.* VP24 is a molecular determinant of Ebola virus virulence in guinea pigs. *J Infect Dis* **204 Suppl 3**, S1011-1020, doi:10.1093/infdis/jir338 (2011).
88 Dilley, K. A. *et al.* The Ebola virus VP35 protein binds viral immunostimulatory and host RNAs identified through deep sequencing. *PLoS One* **12**, e0178717, doi:10.1371/journal.pone.0178717 (2017).
89 Daigneault, M., Preston, J. A., Marriott, H. M., Whyte, M. K. B. & Dockrell, D. H. The Identification of Markers of Macrophage Differentiation in PMA-Stimulated THP-1 Cells and Monocyte-Derived Macrophages. *PLoS ONE* **5**, e8668, doi:10.1371/journal.pone.0008668 (2010).
90 Marzi, A. *et al.* Delayed Disease Progression in Cynomolgus Macaques Infected with Ebola Virus Makona Strain. *Emerg Infect Dis* **21**, 1777-1783, doi:10.3201/eid2110.150259 (2015).
91 Feldmann, H. & Geisbert, T. W. Ebola haemorrhagic fever. *Lancet* **377**, 849-862, doi:10.1016/S0140-6736(10)60667-8 (2011).
92 Mire, C. E. *et al.* Vesicular Stomatitis Virus-Based Vaccines Protect Nonhuman Primates againstBundibugyo ebolavirus. **7**, e2600, doi:10.1371/journal.pntd.0002600 (2013).
93 Mire, C. E. *et al.* Single injection recombinant vesicular stomatitis virus vaccines protect ferrets against lethal Nipah virus disease. *Virol J* **10**, 353, doi:10.1186/1743-422X-10-353 (2013).
94 Gupta, M., Goldsmith, C. S., Metcalfe, M. G., Spipopoulou, C. F. & Rollin, P. E. Reduced virus replication, proinflammatory cytokine production, and delayed

macrophage cell death in human PBMCs infected with the newly discovered Bundibugyo ebolavirus relative to Zaire ebolavirus. **402**, 203-208, doi:10.1016/j.virol.2010.03.024 (2010).
95 Cross, R. W. *et al.* The Domestic Ferret (Mustela putorius furo) as a Lethal Infection Model for 3 Species of Ebolavirus. *J Infect Dis* **214**, 565-569, doi:10.1093/infdis/jiw209 (2016).
96 Kozak, R. *et al.* Ferrets Infected with Bundibugyo Virus or Ebola Virus Recapitulate Important Aspects of Human Filovirus Disease. *J Virol* **90**, 9209-9223, doi:10.1128/JVI.01033-16 (2016).
97 Brannan, J. M. *et al.* Post-exposure immunotherapy for two ebolaviruses and Marburg virus in nonhuman primates. *Nat Commun* **10**, 105, doi:10.1038/s41467-018-08040-w (2019).
98 Smither, S. J. *et al.* An Investigation of the Effect of Transfected Defective, Ebola Virus Genomes on Ebola Replication. *Front Cell Infect Microbiol* **10**, 159, doi:10.3389/fcimb.2020.00159 (2020).
99 Calain, P., Monroe, M. C. & Nichol, S. T. Ebola virus defective interfering particles and persistent infection. *Virology* **262**, 114-128, doi:10.1006/viro.1999.9915 (1999).
100 Liao, L. E. *et al.* Quantification of Ebola virus replication kinetics in vitro. *PLOS Computational Biology* **16**, e1008375, doi:10.1371/journal.pcbi.1008375 (2020).
101 Cressey, T., Brauburger, K. & Muhlberger, E. Modeling Ebola Virus Genome Replication and Transcription with Minigenome Systems. *Methods Mol Biol* **1628**, 79-92, doi:10.1007/978-1-4939-7116-9_6 (2017).
102 Hoenen, T. Minigenome Systems for Filoviruses. *Methods Mol Biol* **1604**, 237-245, doi:10.1007/978-1-4939-6981-4_18 (2018).
103 Hannemann, H. Viral replicons as valuable tools for drug discovery. *Drug Discov Today* **25**, 1026-1033, doi:10.1016/j.drudis.2020.03.010 (2020).
104 Te Velthuis, A. J. W., Long, J. S. & Barclay, W. S. Assays to Measure the Activity of Influenza Virus Polymerase. *Methods Mol Biol* **1836**, 343-374, doi:10.1007/978-1-4939-8678-1_17 (2018).
105 Sugita, Y., Matsunami, H., Kawaoka, Y., Noda, T. & Wolf, M. Cryo-EM structure of the Ebola virus nucleoprotein-RNA complex at 3.6 A resolution. *Nature* **563**, 137-140, doi:10.1038/s41586-018-0630-0 (2018).
106 Weik, M., Enterlein, S., Schlenz, K. & Muhlberger, E. The Ebola virus genomic replication promoter is bipartite and follows the rule of six. *J Virol* **79**, 10660-10671, doi:10.1128/JVI.79.16.10660-10671.2005 (2005).
107 le Mercier, P. & Kolakofsky, D. Bipartite promoters and RNA editing of paramyxoviruses and filoviruses. *RNA* **25**, 279-285, doi:10.1261/rna.068825.118 (2019).
108 Noda, T. *et al.* Ebola virus VP40 drives the formation of virus-like filamentous particles along with GP. *J Virol* **76**, 4855-4865, doi:10.1128/jvi.76.10.4855-4865.2002 (2002).
109 Lin, A. E. *et al.* Reporter Assays for Ebola Virus Nucleoprotein Oligomerization, Virion-Like Particle Budding, and Minigenome Activity Reveal the Importance of Nucleoprotein Amino Acid Position 111. *Viruses* **12**, doi:10.3390/v12010105 (2020).

110 Weik, M., Modrof, J., Klenk, H. D., Becker, S. & Muhlberger, E. Ebola virus VP30-mediated transcription is regulated by RNA secondary structure formation. *J Virol* **76**, 8532-8539, doi:10.1128/jvi.76.17.8532-8539.2002 (2002).
111 Tchesnokov, E. P., Raeisimakiani, P., Ngure, M., Marchant, D. & Gotte, M. Recombinant RNA-Dependent RNA Polymerase Complex of Ebola Virus. *Sci Rep* **8**, 3970, doi:10.1038/s41598-018-22328-3 (2018).
112 Liang, B. *et al.* Structure of the L Protein of Vesicular Stomatitis Virus from Electron Cryomicroscopy. *Cell* **162**, 314-327, doi:10.1016/j.cell.2015.06.018 (2015).
113 Valle, C. *et al.* The C-Terminal Domain of the Sudan Ebolavirus L Protein Is Essential for RNA Binding and Methylation. *J Virol* **94**, doi:10.1128/JVI.00520-20 (2020).
114 Volchkov, V. E. *et al.* Characterization of the L gene and 5' trailer region of Ebola virus. *J Gen Virol* **80 (Pt 2)**, 355-362, doi:10.1099/0022-1317-80-2-355 (1999).
115 Poch, O., Blumberg, B. M., Bougueleret, L. & Tordo, N. Sequence comparison of five polymerases (L proteins) of unsegmented negative-strand RNA viruses: theoretical assignment of functional domains. *J Gen Virol* **71 (Pt 5)**, 1153-1162, doi:10.1099/0022-1317-71-5-1153 (1990).
116 Trunschke, M. *et al.* The L-VP35 and L-L interaction domains reside in the amino terminus of the Ebola virus L protein and are potential targets for antivirals. *Virology* **441**, 135-145, doi:10.1016/j.virol.2013.03.013 (2013).
117 Muhlberger, E. Filovirus replication and transcription. *Future Virol* **2**, 205-215, doi:10.2217/17460794.2.2.205 (2007).
118 Bach, S. *et al.* Regulation of VP30-Dependent Transcription by RNA Sequence and Structure in the Genomic Ebola Virus Promoter. *J Virol*, doi:10.1128/JVI.02215-20 (2020).
119 Deflube, L. R. *et al.* Ebolavirus polymerase uses an unconventional genome replication mechanism. *Proc Natl Acad Sci U S A* **116**, 8535-8543, doi:10.1073/pnas.1815745116 (2019).
120 Manhart, W. A. *et al.* A Chimeric Lloviu Virus Minigenome System Reveals that the Bat-Derived Filovirus Replicates More Similarly to Ebolaviruses than Marburgviruses. *Cell Rep* **24**, 2573-2580 e2574, doi:10.1016/j.celrep.2018.08.008 (2018).
121 Nelson, E. V. *et al.* An RNA polymerase II-driven Ebola virus minigenome system as an advanced tool for antiviral drug screening. *Antiviral Res* **146**, 21-27, doi:10.1016/j.antiviral.2017.08.005 (2017).
122 Boehmann, Y., Enterlein, S., Randolf, A. & Muhlberger, E. A reconstituted replication and transcription system for Ebola virus Reston and comparison with Ebola virus Zaire. *Virology* **332**, 406-417, doi:10.1016/j.virol.2004.11.018 (2005).
123 Buchholz, U. J., Finke, S. & Conzelmann, K. K. Generation of bovine respiratory syncytial virus (BRSV) from cDNA: BRSV NS2 is not essential for virus replication in tissue culture, and the human RSV leader region acts as a functional BRSV genome promoter. *J Virol* **73**, 251-259 (1999).
124 Gibson, D. G. *et al.* Enzymatic assembly of DNA molecules up to several hundred kilobases. *Nat Methods* **6**, 343-345, doi:10.1038/nmeth.1318 (2009).

125 Levine, C. B., Mire, C. E. & Geisbert, T. W. Comparison of Zaire and Bundibugyo Ebolavirus Polymerase Complexes and Susceptibility to Antivirals through a Newly Developed Bundibugyo Minigenome System. *J Virol* **95**, e0064321, doi:10.1128/JVI.00643-21 (2021).
126 Bodmer, B. S. *et al.* Differences in Viral RNA Synthesis but Not Budding or Entry Contribute to the In Vitro Attenuation of Reston Virus Compared to Ebola Virus. *Microorganisms* **8**, doi:10.3390/microorganisms8081215 (2020).
127 Hartlieb, B., Muziol, T., Weissenhorn, W. & Becker, S. Crystal structure of the C-terminal domain of Ebola virus VP30 reveals a role in transcription and nucleocapsid association. *Proc Natl Acad Sci U S A* **104**, 624-629, doi:10.1073/pnas.0606730104 (2007).
128 Darty, K., Denise, A. & Ponty, Y. VARNA: Interactive drawing and editing of the RNA secondary structure. *Bioinformatics* **25**, 1974-1975, doi:10.1093/bioinformatics/btp250 (2009).
129 Bach, S., Biedenkopf, N., Grunweller, A., Becker, S. & Hartmann, R. K. Hexamer phasing governs transcription initiation in the 3'-leader of Ebola virus. *RNA* **26**, 439-453, doi:10.1261/rna.073718.119 (2020).
130 Sztuba-Solinska, J. *et al.* A small stem-loop structure of the Ebola virus trailer is essential for replication and interacts with heat-shock protein A8. *Nucleic Acids Res* **44**, 9831-9846, doi:10.1093/nar/gkw825 (2016).
131 Leyssen, P., De Clercq, E. & Neyts, J. Molecular strategies to inhibit the replication of RNA viruses. *Antiviral Res* **78**, 9-25, doi:10.1016/j.antiviral.2008.01.004 (2008).
132 Richman, D. D. Antiviral drug resistance. *Antiviral Res* **71**, 117-121, doi:10.1016/j.antiviral.2006.03.004 (2006).
133 Baumert, T. F., Berg, T., Lim, J. K. & Nelson, D. R. Status of Direct-Acting Antiviral Therapy for Hepatitis C Virus Infection and Remaining Challenges. *Gastroenterology* **156**, 431-445, doi:10.1053/j.gastro.2018.10.024 (2019).
134 Arts, E. J. & Hazuda, D. J. HIV-1 antiretroviral drug therapy. *Cold Spring Harb Perspect Med* **2**, a007161, doi:10.1101/cshperspect.a007161 (2012).
135 Beigel, J. H. *et al.* Remdesivir for the Treatment of Covid-19 - Final Report. *N Engl J Med*, doi:10.1056/NEJMoa2007764 (2020).
136 Mulangu, S. *et al.* A Randomized, Controlled Trial of Ebola Virus Disease Therapeutics. *N Engl J Med* **381**, 2293-2303, doi:10.1056/NEJMoa1910993 (2019).
137 Lee, J. S. *et al.* Anti-Ebola therapy for patients with Ebola virus disease: a systematic review. *BMC Infect Dis* **19**, 376, doi:10.1186/s12879-019-3980-9 (2019).
138 Dodd, L. E. *et al.* A meta-analysis of clinical studies conducted during the West Africa Ebola virus disease outbreak confirms the need for randomized control groups. *Sci Transl Med* **11**, doi:10.1126/scitranslmed.aaw1049 (2019).
139 Davey, R. T. *et al.* A Randomized, Controlled Trial of ZMapp for Ebola Virus Infection. *N Engl J Med* **375**, 1448-1456, doi:10.1056/NEJMoa1604330 (2016).
140 Sissoko, D. *et al.* Experimental Treatment with Favipiravir for Ebola Virus Disease (the JIKI Trial): A Historically Controlled, Single-Arm Proof-of-Concept

Trial in Guinea. *PLoS Med* **13**, e1001967, doi:10.1371/journal.pmed.1001967 (2016).
141 Edwards, M. R. *et al.* High-Throughput Minigenome System for Identifying Small-Molecule Inhibitors of Ebola Virus Replication. *ACS Infect Dis* **1**, 380-387, doi:10.1021/acsinfecdis.5b00053 (2015).
142 Zhao, Z., Martin, C., Fan, R., Bourne, P. E. & Xie, L. Drug repurposing to target Ebola virus replication and virulence using structural systems pharmacology. *BMC Bioinformatics* **17**, 90, doi:10.1186/s12859-016-0941-9 (2016).
143 McCarthy, S. D. S. *et al.* A Rapid Screening Assay Identifies Monotherapy with Interferon-ß and Combination Therapies with Nucleoside Analogs as Effective Inhibitors of Ebola Virus. **10**, e0004364, doi:10.1371/journal.pntd.0004364 (2016).
144 Liu, G. *et al.* A Sensitive in Vitro High-Throughput Screen To Identify Pan-filoviral Replication Inhibitors Targeting the VP35-NP Interface. *ACS Infect Dis* **3**, 190-198, doi:10.1021/acsinfecdis.6b00209 (2017).
145 Brown, C. S. *et al.* In silico derived small molecules bind the filovirus VP35 protein and inhibit its polymerase cofactor activity. *J Mol Biol* **426**, 2045-2058, doi:10.1016/j.jmb.2014.01.010 (2014).
146 Warren, T. K. *et al.* Antiviral activity of a small-molecule inhibitor of filovirus infection. *Antimicrob Agents Chemother* **54**, 2152-2159, doi:10.1128/AAC.01315-09 (2010).
147 Panchal, R. G. *et al.* Identification of an antioxidant small-molecule with broad-spectrum antiviral activity. *Antiviral Res* **93**, 23-29, doi:10.1016/j.antiviral.2011.10.011 (2012).
148 Tchesnokov, E. P., Feng, J. Y., Porter, D. P. & Gotte, M. Mechanism of Inhibition of Ebola Virus RNA-Dependent RNA Polymerase by Remdesivir. *Viruses* **11**, doi:10.3390/v11040326 (2019).
149 Warren, T. K. *et al.* Therapeutic efficacy of the small molecule GS-5734 against Ebola virus in rhesus monkeys. *Nature* **531**, 381-385, doi:10.1038/nature17180 (2016).
150 Siegel, D. *et al.* Discovery and Synthesis of a Phosphoramidate Prodrug of a Pyrrolo[2,1-f][triazin-4-amino] Adenine C-Nucleoside (GS-5734) for the Treatment of Ebola and Emerging Viruses. *J Med Chem* **60**, 1648-1661, doi:10.1021/acs.jmedchem.6b01594 (2017).
151 Wang, Y. *et al.* Remdesivir in adults with severe COVID-19: a randomised, double-blind, placebo-controlled, multicentre trial. *The Lancet*, doi:10.1016/s0140-6736(20)31022-9 (2020).
152 Chemaly, R. F., Hill, J. A., Voigt, S. & Peggs, K. S. In vitro comparison of currently available and investigational antiviral agents against pathogenic human double-stranded DNA viruses: A systematic literature review. *Antiviral Res* **163**, 50-58, doi:10.1016/j.antiviral.2019.01.008 (2019).
153 Dunning, J. *et al.* Experimental Treatment of Ebola Virus Disease with Brincidofovir. *PLoS One* **11**, e0162199, doi:10.1371/journal.pone.0162199 (2016).

154 Kurth, M. C. & Adler, C. H. COMT inhibition: a new treatment strategy for Parkinson's disease. *Neurology* **50**, S3-14, doi:10.1212/wnl.50.5_suppl_5.s3 (1998).
155 Cross, R. W. *et al.* Combination therapy protects macaques against advanced Marburg virus disease. *Nat Commun* **12**, 1891, doi:10.1038/s41467-021-22132-0 (2021).
156 Wang, J. *et al.* Mechanism of Inhibition of the Reproduction of SARS-CoV-2 and Ebola Viruses by Remdesivir. *Biochemistry*, doi:10.1021/acs.biochem.1c00292 (2021).

VITA

Corri Beth Levine was born on May 22, 1989, in Rochester, NY to Nancy and Stephen Levine. She married Ben Perry on August 2, 2015. Corri and Ben's family happily includes two exotic parrots: Jordan and Bentley. She inherited her love for animals and learning from her father and her passion for helping others from her mother. Throughout her education, Corri constantly pursued extra math and science courses as well as any experience she could gain in veterinary medicine. From a young age she competed in equestrian competitions and continued to do so in high school with her pony Tradewins "Windy". In high school, Corri joined the Pittsford women's rowing team and competed at various regattas. Corri graduated from Honeoye Falls-Lima high school in 2007.

After high school, Corri attended Cornell University. While at Cornell, Corri was a four-year member of the men's heavyweight rowing team serving as a coxswain in 2007-2008 for the first freshman crew and from 2008-2011 for the junior varsity crew. In 2010, Corri steered her crew to a silver medal finish at the EARC Sprints Championship. Corri was awarded the Ackerman Award for leadership, camaraderie, and competitiveness. In addition to athletics, Corri took on two research positions during her time at Cornell. She worked part-time as a laboratory assistant for the Center for Materials Research where she learned how to use an electron microscope. Corri also worked as a research assistant for nearly two years in the laboratory of Dr. Joseph Wakshlag studying animal physiology, nutrition, and metabolism. Her work during her

undergraduate studies led to two co-author publications. In 2011, Corri graduated with her B.S. in animal science with a minor in microbiology.

After graduation, Corri spent two months in Jerusalem, Israel studying Judaism at Neve Yerushalayim. In addition, she interned at Terem Emergency Health Center collecting medical data looking at cellulitis therapies and rates of readmission. Upon return to the U.S., Corri continued her research career as a laboratory technician at the University of Rochester Center for Translation Neuromedicine under Dr. Steven Goldman. In this position she contributed on several research projects studying myelination disorders, one of which led to a co-author publication in Cell: Stem Cell. In 2013, Corri returned to Cornell University to work again for Dr. Wakshlag and complete her master's degree in Veterinary Medicine. Her master's thesis, titled "The effects of select plant extracts on canine neoplastic cell growth and signaling" was done in conjunction with Royal Canin with the goal of producing a cancer therapeutic pet food, and led to two first author publications. In addition to her thesis work, Corri worked as a laboratory technician II for both Drs. Wakshlag and Angela-McCleary Wheeler. In this position she managed and performed experiments for several research projects leading to nine co-author publications. Corri graduated from Cornell with an M.S. in 2016.

Corri began her doctorate training in the summer of 2016 when she matriculated as a Ph.D. student at the University of Texas Medical Branch in the Human Pathophysiology and Translational Medicine program. In addition to doctoral work, Corri pursued an M.P.H. in epidemiology which she completed in May 2021. During her doctorate studies, Corri took an active role in the university's biocontainment and

pandemic preparedness efforts under Dr. Susan McLellan. While the COVID-19 pandemic disrupted many activities on campus, Corri took full advantage of the chance to be on the frontlines of cutting-edge clinical research and public health outreach. Corri worked on the NIAID-sponsored Adaptive COVID-19 Treatment Trials which led to the classification of remdesivir as standard of care for treating COVID-19 patients. In addition, Corri took a lead in establishing the university's first biorepository for clinical infectious disease samples. Outside of her studies, Corri was a highly active volunteer with the Galveston County Health District's Medical Reserve Corps, participating in their contact tracing program and working several COVID-19 vaccination clinics. Corri plans to pursue a career where she can join her passion for studying infectious disease and contributing to the betterment of public health.

EDUCATION

B.S., May 2011, Cornell University, Ithaca, New York

M.S., May 2016, Cornell University, Ithaca, New York

M.P.H., May 2021, The University of Texas Medical Branch, Galveston, Texas

PUBLICATIONS

Levine, CB, Mire CE, Geisbert TW. Comparison of Zaire and Bundibugyo ebolavirus polymerase complexes and susceptibility to antivirals through a newly developed Bundibugyo minigenome system. *J Virol.* 2021; JVI0064321. doi: 10.1128/JVI.00643-21.

Schein CH, **Levine CB**, McLellan SLF, Negi SS, Braun W, Dreskin SC, Anaya ES, Schmidt J. Synthetic proteins for COVID-19 diagnostics. *Peptides*. 2021;143:170583. Doi: 10.1016/j.peptides.2021.170583.

Woolsey C, Borisevich V, Prasad AN, Agans KN, Deer DJ, Dobias NS, Heymann JC, Foster SL, **Levine CB**, Medina L, Melody K, Geisbert JB, Fenton KA, Geisbert TW, Cross RW. Establishment of an African green monkey model for COVID-19 and protection against re-infection. *Nat Immunol*. 2021;22(1):86-98. Doi: 10.1038/s41590-020-00835-8.

Baldanza VE, Rogic A, Yan W, **Levine CB**, Levine RA, Miller AD, McCleary-Wheeler AL. Evaluation of canonical Hedgehog signaling pathway inhibition in canine osteosarcoma. *PLoS One*. 2020;15(4). doi: 10.1371/journal.pone.0231762.

Levine CB*, Ansar M*, Dimet A*, Miller A, Moon J, Rice C, Schaeffer A, Andersson J, Ekpo-Otu S, McGrath E, Sarraj H. Student Evaluation of Interprofessional Experiences Between Medical and Graduate Biomedical Students. *J of Res in Interprofessional Practice and Education*. 2019;*9*(1). doi: 10.22230/jripe.2019v9n1a274.

Levine CB, Bayle J, Biourge V, Wakshlag JJ. Cellular effects of a turmeric root and rosemary leaf extract on canine neoplastic cell lines. *BMC Vet Res*. 2017;13(1):388. doi:10.1186/s12917-017-1302-2.

Rizzo VL, **Levine CB**, Wakshlag JJ. The effects of sulforaphane on canine osteosarcoma proliferation and invasion. *Vet Comp Oncol*. 2017;15(3):718-730. doi:10.1111/vco.12212.

Escaffre O, Saito TB, Juelich TL, Ikegami T, Smith JK, Perez DD, Atkins C, **Levine CB**, Huante MB, Nusbaum RJ, Endsley JJ, Freiberg AN, Rockx Barry. Contribution of Human Lung Parenchyma and Leukocyte Influx to Oxidative Stress and Immune System-Mediated Pathology following Nipah Virus Infection. Perlman S, ed. *J Virol*. 2017;91(15):e00275–17. doi:10.1128/JVI.00275-17.

Levine CB, Bayle J, Biourge V, Wakshlag JJ. Effects and synergy of feed ingredients on canine neoplastic cell proliferation. *BMC Vet Res*. 2016;12(1):159. doi:10.1186/s12917-016-0774-9.

Loftus JP, Cavatorta D, Bushey JJ, **Levine CB**, Sevier CS, Wakshlag JJ. The 5-lipoxygenase inhibitor tepoxalin induces oxidative damage and altered PTEN status prior to apoptosis in canine osteosarcoma cell lines. *Vet Comp Oncol*. 2016;14(2):e17-e30. doi:10.1111/vco.12094.

Bell MA, **Levine CB**, Downey RL, et al. Influence of endurance and sprinting exercise on plasma adiponectin, leptin and irisin concentrations in racing Greyhounds and sled dogs. *Aust Vet J*. 2016;94(5):154-159. doi:10.1111/avj.12436.

Brunke MW, Frye CW, **Levine CB**, Hansen C, Wakshlag JJ. Insulin-Like Growth Factor-1 and Selected Insulin-Like Growth Factor Binding Protein Concentrations during an Ultramarathon Sled Dog Race. *Scientific World Journal*. 2016;2016(2):5686372-5686375. doi:10.1155/2016/5686372.

Pfeil von DJF, Cummings BP, Loftus JP, **Levine CB**, Mann S, Downey RL, Griffitts C, Wakshlag JJ. Evaluation of plasma inflammatory cytokine concentrations in racing sled dogs. *Can Vet J*. 2015;56(12):1252-1256.

Frank L, Mann S, **Levine CB**, Cummings BP, Wakshlag JJ. Increasing body condition score is positively associated interleukin-6 and monocyte chemoattractant protein-1 in Labrador retrievers. *Vet Immunol Immunopathol*. 2015;167(3-4):104-109. doi:10.1016/j.vetimm.2015.07.010.

Spoo JW, Downey RL, Griffitts C, Horst RJ, **Levine CB**, Childs RM, Wakshlag JJ. Plasma vitamin D metabolites and C-reactive protein in stage-stop racing endurance sled dogs. *J Vet Intern Med*. 2015;29(2):519-525. doi:10.1111/jvim.12546.

Bell MJ, Donaldson EM, Mann S, Gillette RL, **Levine CB**, Wakshlag JJ. The Effects of Exercise on Serum Chemistry, Non-Esterified Fatty Acid, Insulin and Glucagon Dynamics during a 400 Meter Sprint in Racing Greyhounds. *Open Journal of Veterinary Medicine*. 2015;05(06):142-151. doi:10.4236/ojvm.2015.56020.

Huntingford JL, **Levine CB**, Mustacich DJ, Corrigan D, Downey RL, Wakshlag JJ. The Effects of Low Intensity Endurance Activity on Various Physiological Parameters and Exercise Induced Oxidative Stress in Dogs. *Open Journal of Veterinary Medicine*. 2014;04(07):134-144. doi:10.4236/ojvm.2014.47016.

Wang S, Bates J, Li X, Schanz S, Chandler-Militello D, **Levine C**, Maherali N, Studer L, Hochedlinger K, Windrem M, Goldman SA. Human iPSC-derived oligodendrocyte progenitor cells can myelinate and rescue a mouse model of congenital hypomyelination. *Cell Stem Cell*. 2013;12(2):252-264. doi:10.1016/j.stem.2012.12.002.

Wakshlag JJ, Struble AM, **Levine CB**, Bushey JJ, Laflamme DP, Long GM. The effects of weight loss on adipokines and markers of inflammation in dogs. *Br J Nutr*. 2011;106 Suppl 1(S1):S11-S14. doi:10.1017/S0007114511000560.

Permanent address: 301 University Blvd, Galveston, TX 77555

This dissertation was typed by Corri Levine